Neuronal cell lipidomics and role of cholesterol in α-synuclein binding and aggregation

Martin Jakubec

Thesis for the Degree of Philosophiae Doctor (PhD)
University of Bergen, Norway
2019

UNIVERSITY OF BERGEN

Neuronal cell lipidomics and role of cholesterol in α-synuclein binding and aggregation

Martin Jakubec

Thesis for the Degree of Philosophiae Doctor (PhD)
at the University of Bergen

Date of defence: 22.03.2019

© Copyright Martin Jakubec

The material in this publication is covered by the provisions of the Copyright Act.

Year: 2019

Title: Neuronal cell lipidomics and role of cholesterol in α-synuclein binding and aggregation

Name: Martin Jakubec

Print: Skipnes Kommunikasjon / University of Bergen

The oldest and strongest emotion of mankind is fear, and the oldest and strongest kind of fear is fear of the unknown.

- **H. P. Lovecraft**

We can take these Deadites!

We can take ’em!

With ***science***!

- **Ash, Evil Dead 3**

Scientific environment

The work presented in this dissertation was carried out at the Faculty of Mathematics and Natural Sciences at The Department of Molecular Biology between November 2015 and December 2017 and at the Department of Biological Sciences between January 2018 and January 2019. The whole period was supervised by Professor Øyvind Halskau and a period between November 2015 and September 2017 was co-supervised by Dr. Samuel Furse, primarily on lipidomics. The project was funded by The Norwegian Research Council (grant to Halskau, NFR240063) and partially supported by The Meltzer Research Foundation (grant to Jakubec) and The Norwegian NMR Platform, NNP (infrastructure grant 226244/F50). The thesis training section was supported by The Norwegian Biochemical Society and by The Molecular and Computational Biology, BioStruct and BioCat research schools (various travel grants to Jakubec).

Acknowledgments

This dissertation would not have been possible without the support of many individuals, for which I am grateful.

I want to express my sincere gratitude to my supervisor, Professor Øyvind Halskau. Your dedication, enthusiasm and guidance have been solid support which allows for my impressive professional growth. I learned so much in the last three years! Even through hard-times of Department merging and exciting times of your family growth, you been available for me whenever I needed help or advice, thank you for that.

I would also like to thank my co-supervisor Dr. Samuel Furse. You have been an indispensable guide through the harsh environment of international science and you helped me to discover the exciting and mesmerizing field of lipid science. Also, thank you for all squash seasons we had together.

My thanks also belong to all past and present lab members who help me with the project. In particular, I thank Morten Govasli for all bits of advice regarding protein expression and purification, Fedor Kryuchkov for personal MS lessons**,** Diana Turcu for help with various instruments, Jarle Underhaug and Jose Carlos Reyes Guerrero for help with NMR, Espen Bariås and Vinnit George for help with lab work and of course Øyvind Strømland for various science improving tips. I would also like to thank my colleagues Maxim Bril'kov and Kirill Jefimov for amazing mountain hikes and all the gym lessons. I promise I will exercise more often!

Special thank also goes, for my wife. Iveta, thank you for providing me with a place which I can call home, anywhere in the world. Everything that I have achieved would not be possible without your love and support.

Martin Jakubec

Bergen, January 24th, 2019

Table of Contents

List of publications

Paper I — Cholesterol is a strong promotor of an α-Synuclein membrane binding mode that accelerates oligomerization

Jakubec M., Furse S., Bariås E., Govasli M. L., George V., Turcu D., Morozova-Roche L., Halskau Ø.

Manuscript, 2019

Paper II — Evidence that *Listeria innocua* modulates its membrane's stored curvature elastic stress, but not fluidity, through the cell cycle

Furse S., **Jakubec M,** Rise F., Williams H.E., Rees C.E.D., Halskau Ø.

Scientific reports, **7,** 8012, 2017

Paper III — Fast and quantitative phospholipidomic analysis of SH-SY5Y neuroblastoma cell cultures using LC-MS/MS and 31P NMR

Jakubec M., Bariås E., Kryuchkov F., Hjørnevik L. V., Halskau Ø.

Manuscript, 2019

Contribution to the following article, not included in thesis, was also made

Paper IV — Detection of misfolded protein aggregates from a clinical perspective

Strømland Ø*., **Jakubec M.*,** Furse S., Halskau Ø.

J. Clin Transl Res, **2(1),** 11-26, 2016 (Review)

* Shared first authorship

Selected abbreviations

27-OHC – 27-hydroxycholesterol

AD – Alzheimer's disease

AFM – atomic force microscopy

EGCG - epigallocatechin gallate

FA – fatty acid

GluCer – glycosylceramide

GM1 – monosialganglioside

IDP – intrinsically disorder proteins

NAC – amyloid binding central domain

PA – glycerophosphates

PC – phosphatidylcholine

PD - Parkinson's disease

PE – phosphatidylethanolamine

PG – phosphatidylglycerol

PI – phosphatidylinositol

PrP – prion protein

PS – phosphatidylserine

ROS – reactive oxygen species

SM – sphingomyelin

SMALN – SMA lipid nanodiscs

ThT – thioflavin T

TPE-TPP - tetraphenylethene tethered with triphenylphosphonium

Abstract

α-Synuclein is an intrinsically disordered protein whose fold and multimeric state is strongly affected by its environment. The monomers of α-synuclein are enriched in the presynaptic terminals of dopaminergic neurons and seem to have a role in synaptic vesicles recycling and transmitter release. Specific cellular conditions can promote α-synuclein oligomerization which, in the end, results in neuronal death. Lipids seem to be one of these conditions as they are involved in both the native and pathogenic role of α-synuclein. This thesis aims to explore α-synuclein:lipid interaction and how binding to certain lipids may trigger or suppress oligomerization. Furthermore, it aims to establish and use lipidomic techniques for improving the state of knowledge of the lipid environment that might affect α-synuclein function and dysfunction.

In Paper I we investigated how cholesterol, the most abundant lipid in mammals, affect α-synuclein affinity towards the lipid bilayer and its oligomerization properties. For this work we tested and optimized the preparation of SMA lipid nanodiscs containing cholesterol. Then, we used these nanodiscs to investigate lipid-mediated changes in fibrillation. We also determined individual amino acid affinities towards the lipid bilayer within the α-synuclein primary sequence. The results suggest the existence of two binding modes: the N-terminal and NAC binding mode. The N-terminal mode seems to be preferred in the presence of anionic lipids (like PG), and this binding leads to a delay in fibrillation onset. The NAC-binding mode seems to be promoted in the presence of lipid bilayers containing cholesterol and speed up α-synuclein oligomerization significantly.

In Paper II, we focused on lipidomics methods. We established and optimized a method for lipid isolation, followed by phospholipid identification and quantification using ^{31}P NMR. These methods were first tested on populations of a prokaryotic organism, *L. innocua,* which were arrested at the C/D boundary of its cell cycle. We discovered that *L. innocua* modulates its lipid composition, and both cardiolipin and phosphatidylethanolamine fall significantly between the B period and the C/D boundary. When we investigated how these lipid changes could affect the physical properties models of the cell membrane, we observed that the decrease of PE content

seems to be compensated for by an increase of PG. In the absence of other factors, this would result in decreasing stored curvature stress, while maintaining membrane fluidity.

In Paper III, we used methods established in Paper II for the lipidomic analysis of the SH-SY5Y cell line, which is a commonly used neuronal cell model for Parkinson's disease research. We also developed an automated script for analysis of the fatty acid chain distribution of phospholipids by LC-MS/MS. We observed several deviations of lipid content from commonly used lipid models and lipid content of brain matter. The most interesting ones are a high content of PC, low content of SM and PS and absence of longer fatty acid chains, including 22:6 PS.

1 Introduction

Proteins are essential to cellular metabolism and, together with the plasma membrane, they form the framework on which cells are built. To fulfil their functions, most proteins must fold into a particular three-dimensional architecture, which is determined mainly by their amino acid sequence. However, there is the group of proteins which lacks this predefined structure coded by amino-acids and is mostly intrinsically disordered. Many of these proteins play an essential role in neurodegeneration, like Aβ in Alzheimer's disease, the prion protein (PrP) in Creutzfeldt-Jakob and Kuru-Kuru diseases, or α-synuclein in Parkinson's disease. These diseases are also often referred to as misfolding or amyloid forming diseases, to highlight the role of misfolded and aggregated protein in their aetiology. Amyloid is a plaque consisting of misfolded protein, lipids and other biomolecules appearing in tissue affected by neurodegeneration. As the research progress, there is an increasing awareness that the cell lipid environments play a crucial role in the progress of these diseases. The lipids seem to be important in all stages of a neurodegenerative amyloid disease, from driving the misfolding and aggregation of proteins, to explain cytotoxic mechanisms where protein oligomers interact with and adversely affect cell membranes, and to participation in cell-to-cell amyloid seed transfer.

1.1 Common features of amyloid fibrils forming proteins

Between its synthesis on the ribosome and final degradation through proteolysis, there is a wide range of states that a protein can adopt through co-and-post translational modification, compartmentalization, and interactions with partners. Usually, the functional state of protein starts with a monomer fold which is achieved by intramolecular interaction within the protein itself (see Figure 1). The resulting tertiary units can further assemble into the higher-order functional quaternary structure. In many cases, there is a close relationship between the tertiary and quaternary structural level and the protein function. In the last two decades, however, it has become increasingly recognized that many fully functional proteins do not have well-defined tertiary folds. These proteins, often referred to as intrinsically disordered proteins (IDPs), adopts a multitude of different conformational states within physiological conditions [1,2]. The

amyloid-forming proteins are overrepresented in IDPs group and are very non-typical in their folding behaviour. These proteins are notable for their folding instability, or more precisely their folding promiscuity, which is driven by their ability to easily form intermolecular contact with another monomer of itself or other IDPs. This intermolecular interaction could lead to a mainly hydrophobically driven chain-reaction leading the formation of nonstructured, amorphous deposits or oligomers which then form β-sheet structured aggregates and later amyloid fibrils deposits. These large aggregates, both amorphous and structured, are linked with human diseases, and their accumulation can (with notable exceptions) be correlated with the pathological progress of amyloid diseases.

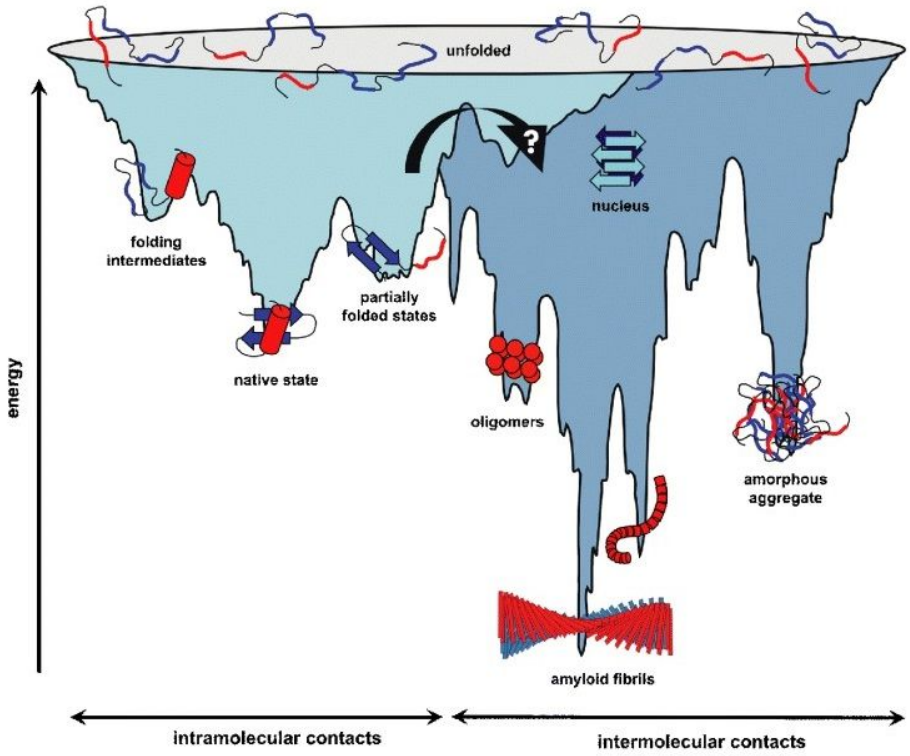

Figure 1: Energy landscape of possible protein folding pathways. Intramolecular contacts lead to a locally stable functional fold which is localized higher on energy plane. Amyloid-forming proteins can reach the more energy stable state of amyloid fibrils, usually with the help of seeding nuclei. One of the possible agents influencing this behavior of amyloid-forming proteins (black arrow) is the lipid environment. The figure was replicated with permission from [3].

There are currently known 37 peptides which are associated with the formation of amyloid deposits (see review [4] for full list). Seven of these proteins are form amyloid deposits in the central nervous system in humans and correlate with neurodegenerative diseases. An overview of these peptides is in Table 1. These neurodegenerative peptides share some similar features like small size and being intrinsically disordered. However, there are no other similarities in the sequence, structure or function.

Table 1: Overview of seven neurodegenerative amyloid-forming proteins and peptides with examples of associated diseases (based on [4]).

Peptide/ protein name	Number of residues (protein length)	Associated diseases	Ref.
amyloid-β-peptide	40-42	Alzheimer disease Hereditary cerebral haemorrhage with amyloidosis	[5,6]
α-synuclein	140	Parkinson disease Dementia with Lewy bodies Multiple system atrophy	[7–9]
Prion protein	208	Creutzfeldt-Jakob disease Fatal Insomnia Gerstmann-Sträussler-Scheinker disease Huntington disease-like 1 Spongiform encephalopathy New variant Creutzfeldt-Jakob disease Kuru	[10–12]
Microtubule-associated protein tau	352-441	Pick disease Progressive supranuclear palsy Corticobasal degeneration Frontotemporal lobar neurodegeneration Hallervorden-Spatz disease	[13–15]
Huntingtin exon 1	103-187	Huntington's disease	[16]
ABri peptide	34	Familial British dementia	[17]
ADan peptide	34	Familial Danish dementia	[18]

The progress of neurodegenerative amyloid diseases differs, based on which region of the brain is affected by cell loss and based on in which region of a brain the amyloid plaques will occur later in progress of a disease. However, there are common features shared by all neurodegenerative amyloid proteins: (i) the ability to oligomerize from

seeds, (ii) form amyloid fibrils with similar structure, (iii) propagate through organism, and (iv) to interact with lipids.

1.1.1 The oligomerization and seeding properties of amyloid-forming proteins

The amyloid-forming proteins generally have similar aggregation pathways [19–21]. These pathways represent a conversion process of normally soluble protein into an insoluble, aggregated state, which involves nucleation and growth steps. As presented in Figure 1, this aggregation process is part of the protein misfolding process involving alterations in protein secondary and tertiary structure [1]. When the quantity of obtained fibrils is measured, for example by ThT dye, the sigmoidal kinetics with three distinct phases can be observed [22] (Figure 2A). These phases are generally described as a lag phase, an exponential (elongation) phase and an equilibrium (saturation) phase. In the lag phase, the most population of protein is in monomeric form; however, there is an ongoing nucleation process. This oligomerization process is in reversible equilibrium, and there is a balance between the assembly and disassembly of oligomers (Figure 2B). The next step, nucleation, is fast autocatalytic surface growth, where the equilibrium is shifted towards fibrils growth. The assembly process is considerably faster as the stability of fibrils is much higher and the concentration of monomers is decreasing rapidly. The process ends with saturation, where the monomer population is almost depleted, and the assembly and disassembly of fibrils are, again, in a balance. The progress of this aggregation can be described by The Finke-Watzky two-step nucleation kinetic model [21] (Figure 2C).

There are some notable known exceptions to this general model. In some cases, it has been found that monomers can convert rapidly into unstructured aggregates which are not able to support the growth of organized fibrils. Still, it is possible that later these aggregates undergo a structural reorganization to generate nucleation seed which eventually leads to the formation of fibrils [23]. Moreover, during aggregation, the oligomers can follow an alternate pathway which does not lead to final amyloid conformation. This off-pathway oligomerization usually leads to non-toxic aggregates [23].

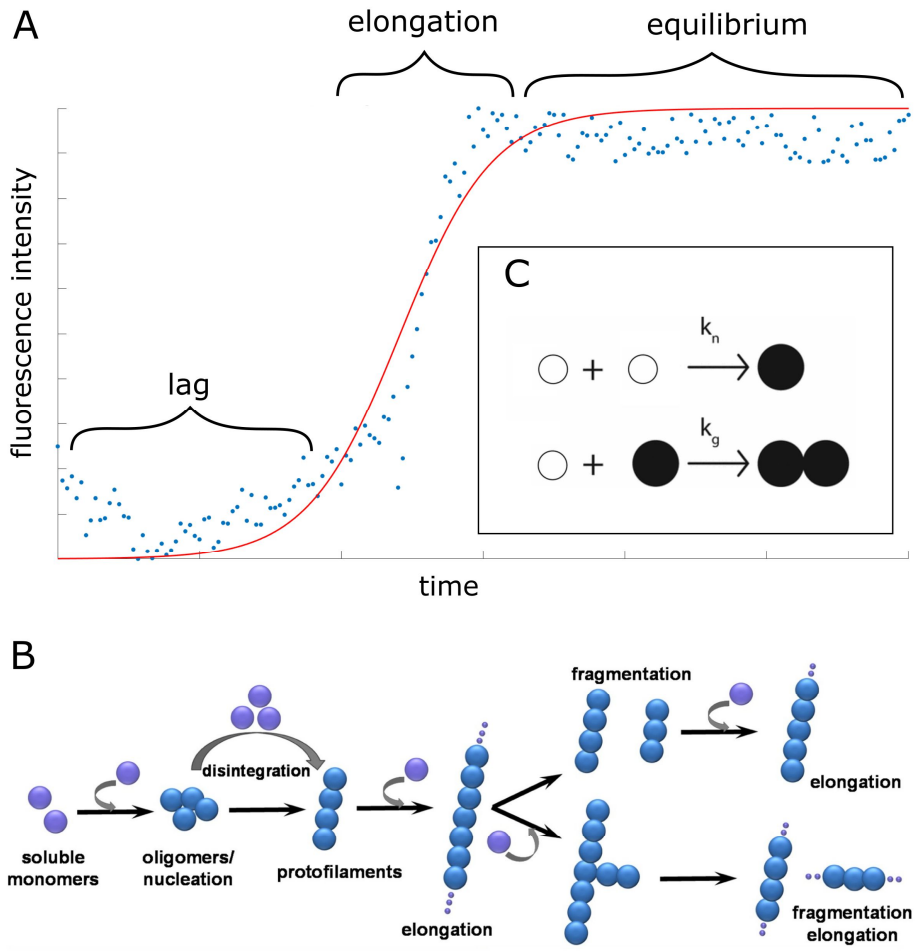

Figure 2: The oligomerization and fibrillation process of amyloid-forming proteins. (A) Generic example of the fibrillation process monitored by ThT fluorescence. There are three distinct observable phases: (i) a lag phase, where the population of protein is mostly monomeric, and where no observable change in fluorescence can be observed. However, in this phase, there is already appearance of a minor oligomeric population. (ii) An elongation phase, where the oligomers are rapidly converted into protofilaments which are then elongated by monomers. (iii) An equilibrium phase, where the elongation and dissociation of fibrils are in equilibrium and the population of monomers is almost completely depleted. (B) Schematic overview of the oligomerization processes. This figure panel was replicated with permission from [24]. (C) The Finke-Watzky two-step nucleation model, used to describe these processes mathematically, is based on two different conversion speeds. The conversion speed from monomer (○, white circle) to oligomer (●, black circle) is different from the conversion speed of monomer assisted by oligomer; $k_n \neq k_g$. This figure panel was replicated with permission from [25].

1.1.2 The amyloid fibril structure

There are three features universally accepted as shared properties of amyloid structures: a fibrillary morphology, a cross-β structure and an ability to be stained selectively by specific dyes. Amyloid fibrils are several micrometers long thread-like structures with typical diameters of 7-13 nm and various lengths up to several μm. They are composed of 2-8 protofilaments whose turns could either twist around each or be associated laterally as flat ribbons [26,27]. The fibrils possess so-called cross-β-architecture which refers to laminated β-sheets running along the fibril composed of β-strand which are perpendicular to the axis of the fibril [28,29]. These structures can be monitored by binding of dyes such as thioflavin-T (ThT), Congo red or their derivatives. The amyloid specific dyes bind along surface side-chains grooves running parallel to a fibril's axis. There is interesting morphological and structural similarity of the fibrils formed by different polypeptides chains. This can be explained by the dominance of main chain interactions, and it seems that amino-acid side chains are playing an only minor role in assembly of fibrils [30].

The amyloid form is more stable than the native state of the intrinsically disordered protein. In organisms, this is a molecular state that leads to irreversible fibril formation and later formation of deposits and plaques. Amyloid fibrils have very high hydrophobicity — this leads to their interaction with other components of the cell, like other hydrophobic protein and lipids and to the formation of insoluble extracellular plaques and intracellular bodies [20]. Composition and localization of these plaques and bodies vary for different amyloid-forming proteins and different diseases. For example, α-synuclein can form intracellular particles in two different cell types with entirely different neurodegenerative progress. First types are Lewy bodies, intracellular particles in dopaminergic neurons of s*ubstantia nigra* observed the in Parkinson's disease (PD) patients [31]. Second types are glial cytoplasmic inclusion, formed in oligodendroglia, usually not localized to the specific region of the brain [32].

The remarkable stability of amyloid fibrils become apparent when one considers sterilization techniques for working with infectious prions. Typical sterilization technique for instruments that come into contact with brain matter of New variant

Creutzfeldt-Jakob patients is the combination of chemical cleaning and pressurised steam sterilization at 136°C for at least 18 min [33]. This stability can be explained by the arrangement of hydrogen bonds in the amyloid architecture of the β-sheet and by the presence of multiple closely interacting sheets. The tight packing of the β-sheets in fibrils leads to stable fibrils with lengths in order of microns and tensile strength approaching the steal [34]. In nature, the amyloid structures are also used by bacteria to form a scaffold for biofilm formation [35]. The amyloid structures have also been used in the biotechnology field and led, for example, to the exciting design of nanowires [36], metal filters [37] or self-assembly scaffolds for wound healing [38].

1.1.3 Prion-like propagation in an organism

The prion protein (PrP) is, so far, the only neurodegenerative amyloidogenic protein that has conclusively been shown to have infectious properties. This infectious exogenous prion particles can aggregate with benign PrP molecules present in the organism and impose their anomalous structure on them [12,39,40]. The prion particles act as a seeding agent that can start the chain reaction of PrP misfolding and aggregation. This seeding acceleration is the same which can be observed during fibrillation of all the other amyloidogenic proteins, and which can be described by The Finke-Watzky two-step nucleation model [21]. This led to the theory that other neurodegenerative amyloid proteins are using similar prion-like propagation technique via seeds to spread through the organism. The prion-like propagation was indeed observed for several amyloidogenic proteins including Aβ, tau, and α-synuclein.

The experiments showed that Aβ-amyloid rich extract from Alzheimer's disease patients or from mice overexpressing Aβ precursor protein could induce early cerebral Aβ-amyloid angiopathy in mice models [41,42]. The induction of Aβ deposits is dependent both on the concentration of Aβ seed injected into the organism and on the production of human sequence Aβ in a host brain. The injection of control brain homogenate, without aggregated Aβ, do not induce amyloid deposit formation in the brain of tested mice. Also, selective denaturation of Aβ seeds completely negates the ability of brain sample to seed Aβ aggregation [42]. Prion-like propagation of Aβ oligomers through brain was also observed, injection of Aβ-rich extract into on

neocortex region eventually lead to deposit formation in axonally coupled regions, neocortex and allocortex, similar to the progress of Alzheimer's disease [43,44]. The extract was injected directly into the brain through the nose, so these reports serve more as a proof of prion-like propagation of Aβ in the organism than proof of possible infections properties of Aβ peptide.

Very similar results have been observed using tau oligomers — the injection of brain extract containing aggregated tau into the brain of mouse induced the formation of tau lesions which propagates from the injection site to axonally connected areas [45]. However, unlike Aβ, the same effect could be observed in non-transgenic mice (not overexpressing tau), suggesting that endogenous tau is amyloidogenic at physiological concentrations and the simple addition of exogenous seeds is enough to start aggregation pathway [46,47].

Another amyloid protein with experimental evidence indicating its prion-like propagation is α-synuclein; this case will be discussed more in depth later. Briefly, the first sign of prion behavior in α-synuclein was observed when grafted neuron cells containing endogenous α-synuclein seeds led to the development of Lewy bodies from 11 to 16 years after the surgery in humans [48,49]. The same effect (but in the much shorter timeline) has been observed in several *in vitro* [50–52] and animals studies [53–55]. Consistent with prion-like behavior, α-synuclein seeds has been showed to generate lesions in both transgenic [54,55] (overexpressing α-synuclein) and wild-type mice [56,57]. The α-synuclein seeds are also used in the design of new early PD diagnosis. In this test cerebrospinal fluid from the patient is mixed with synthetic monomers of α-synuclein and early fibrillation, monitored by ThT, indicates positive synucleopathies even in the non-symptomatic stage of disease [58].

1.1.4 Sensitivity to lipid environment

Another common feature for all neurodegenerative amyloid proteins is their ability to interact with the lipid environment. There are two roles of lipid environment in amyloid proteins pathogenesis. The first role of the lipids is to regulate the fold and aggregation of amyloid-forming proteins. The second role is in amyloid-driven membrane degradation. The amyloid oligomers can have a pathological effect on physical

membrane properties, including their integrity which can ultimately lead to cell death. Following are examples of amyloid-forming proteins interacting with lipids. The α-synuclein and lipid interactions are described in detail in different section (1.5 α-Synuclein interaction with lipids).

The oligomeric aggregates of Aβ have been identified to be cytotoxic via membrane disruption, which suggests a direct interaction of cytotoxic Aβ species with a lipid membrane [59]. This interaction seems to be highly promoted by anionic lipid headgroups, like phosphatidylglycerol (PG) or phosphatidylserine (PS) [60,61]. It has also been observed that gangliosides affect Aβ aggregation. Monosialganglioside (GM1) has been shown to promote the generation of more toxic Aβ species when present in a specific lipid:protein ratios [62,63] and in the presence of lipid-raft membrane models [64,65]. It also seems that cholesterol affects the progress of AD, not by interacting with Aβ directly but by affecting the processing of Aβ precursor protein, which leads to the increased generation of Aβ fragments (reviewed in [66]). The mechanism of Aβ toxicity seems to be dysregulation of Ca^{2+} homeostasis by ion channel-like pore formation [67]. However, the annular amyloid pore has been observed only *in vitro* and is disputed by many researchers. Other possible suggested pathological processes include membrane thinning or leakage through transmembrane aggregates (reviewed in [68]). Nevertheless, the dysregulation of Ca^{2+} homeostasis has been consistent in the pathology of AD, but the mechanism of this regulation disorder and the role of lipids in them is still unknown.

The prion protein is attached to the membrane in mammalian neuronal cells via a glycosylphosphatidylinositol anchor [69]. This anchor is necessary for its localization in cell and prion-induced neurotoxicity [70,71]. The toxicity of PrP aggregates has been correlated with their ability to disrupt and interact with lipid membranes and to affect the ionic homeostasis in the cell [72–75]. The disruption of the membrane by prion protein aggregates could be caused by membrane thinning [72,76] or by the formation of ion pore channels [73]. The prion proteins (both native and pathological forms) has also been found to be associated with lipid rafts containing both cholesterol and sphingolipids [77–79], and both of these components seem to be essential for the

endocytosis of PrP in epithelial cells [80]. Moreover, it has been observed that early association of PrP with lipid rafts stabilizes its conformation in the non-pathological state in the early secretory pathways [81].

There are also reports of *in vitro* tau oligomers and lipid bilayer interaction. The oligomers of tau can disturb a lipid packing and compromise membrane structural integrity of anionic lipid vesicles; however, there is no-observed interaction with zwitterionic lipids [82,83].

1.2 α-Synuclein

Parkinson's disease (PD) is the second most common neurodegenerative disorder after Alzheimer's disease [8]. It was first characterized more than 200 years ago by James Parkinson as "Shaking Palsy" [84]. However, it was not until 1997 that connection between PD and α-synuclein was established [9,85]. Polymeropoulos *et al.* [85] reported that mutation A53T in SNCA, the α-synuclein gene, was found to be present in three Greek families suffering from PD. Simultaneously Spillantini *et al.* [9] reported the presence of α-synuclein in Lewy bodies and Lewy neurites of idiopathic PD and dementia with Lewy bodies (DLB) patients. Later it has been discovered that true culprits are the oligomers of α-synuclein which are causing the death of dopaminergic neurons in *substantia nigra* [86]. After more than 20 years of intensive research, there is an abundance of information about α-synuclein. However, we still don't have a complete picture of the role of α-synuclein in healthy cells, its pathological transition, and neurotoxicity mechanism.

Part of the problem is the complexity of PD. For now, it is impossible to predict if the person will acquire PD with 100% accuracy. Still, there are several known elements which, to some degree, increase the possibility to acquire PD. These so-called risk factors are usually cumulative and if several of them are present the onset of PD can be observed in younger age. The risk factors can be gene mutations (such as SNCA or GBA), chronical inflammation or a sedentary lifestyle (for the full list see review [87]). However, the most of PD cases are still idiopathic (i.e., the cause is unknown) as we still don't see a complete picture of how risk factors in some cases evolve into a full manifestation of the disease and not in the others. The key is presumably in processes

which takes place at the molecular level and which involve complex lipid environment. Indeed, part of the problem seems to be the effect of lipid environment on the protein and difficulty to study this protein/lipid interaction.

α-Synuclein is a very conservative protein with high sequence similarity in all vertebrae. However, some differences between species can be observed. A most notable one is that several other mammals, including long-living elephants, have threonine on position 53 in their wild-type variant of α-synuclein [88]. This substitution is same like pathological mutation A53T seen in humans. It is not clear why we cannot see similar oligomerization in this non-human α-synuclein molecules. Most probably this is due to other single amino-acid differences between molecules, including other substitutions (G68E and V95G), which together lowers affinity of α-synuclein to anionic vesicles [88]. Nevertheless, the following text is focused only on the human sequence of α-synuclein.

1.2.1 Localization and physiological function of α-synuclein

α-Synuclein is abundantly expressed in the brain, and it is highly enriched in the nervous system [89]. However, some levels of α-synuclein expression have also been detected in cerebrospinal fluid (CSF), muscle, kidney, liver, lung, heart, testis, blood vessels, blood plasma, platelets, lymphocytes and red blood cell [89–98].

In the neural cells, α-synuclein is predominantly located in the presynaptic terminal of neurons [99,100]. Still, it seems that it does not play an influential role in synapse development as it is one of the last presynaptic proteins to become enriched in synaptic terminals [101]. Localization to the presynaptic terminal could also be explained by the high affinity of α-synuclein towards synaptic vesicle membranes lipids [102,103], or by its interaction with the SNARE protein synaptobrevin-2 [104,105]. The physiological role of α-synuclein in the presynaptic terminal is not yet fully understood. However, it seems that the presence of α-synuclein has a direct effect on synaptic plasticity by regulating vesicle packaging and trafficking [106–108]. α-Synuclein seems to regulate the number of synaptic vesicles docked at the synapse during neurotransmitter release [109], the duration of vesicle fusion with the plasma membrane [110] and the assembly of synaptic vesicles [111–113].

There are multiple reports that α-synuclein also localizes and binds to mitochondria [114–118]. However, this binding is associated more with the pathological effects of α-synuclein oligomers, than with physiological role of monomer. Overexpression of α-synuclein can lead to fragmentation of mitochondria, disruption of mitochondrial membrane integrity and the increased production of reactive oxygen species (ROS) [119–121]. Furthermore, *in vitro,* it was observed that the oligomers of α-synuclein could disrupt membranes containing mitochondrial phospholipid cardiolipin [121].

α-Synuclein localization in the nucleus has been observed since its discovery, hence its name [102]. However, since then the reports of its nuclear localization has been inconsistent [122–125]. Only phosphorylated α-synuclein at Ser-129 was reported to be highly enriched in the nucleus of cultured neurons as well as in cortical neurons of transgenic mice that overexpress α-synuclein [126,127]. It has been showed that α-synuclein can inhibit histone acetylation [128] and that histone deacetylase inhibitors, or knockdown of histone deacetylase – Sirtuin-2, rescue the neurotoxicity of α-synuclein both in cell cultures and in *Drosophila* models [128,129]. Nevertheless, the physiological role of phosphorylated α-synuclein in the nucleus is not known.

There are also reports of α-synuclein association with Golgi complex [130], endoplasmic reticulum (ER) [131,132] and with multiple cytoskeletal components *in vitro* [133–135]. However, all of these association are cytotoxic and most probably doesn't play any role in the healthy neuronal cell.

1.2.3 The structure of α-synuclein

α-Synuclein is a small, acidic, 140 amino acid long protein with a molecular weight of 14 kDa (Figure 3). It is composed of three identified domains: the N-terminal lipid-binding domain (1-60), the amyloid-binding central domain (NAC, 61-95) and the C-terminal acidic tail (96-140).

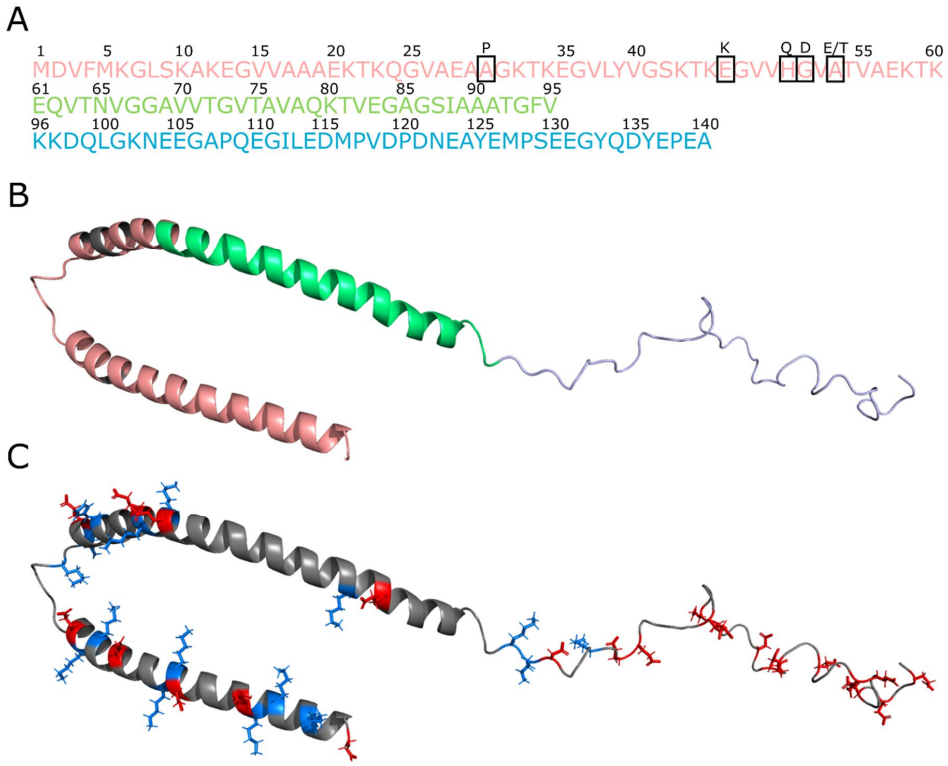

Figure 3: Primary structure and fold of α-synuclein. (A) The sequence of α-synuclein divided into three distinct sections: N-terminal (red), NAC (green) and C-terminal (blue) with known pathological mutations of α-synuclein. (B) Structure of micelle-bound α-synuclein (PDB entry 1XQ8 [149]). The sections are distinguished by color in the same manner as in panel A. (C) Structure of micelle-bound α-synuclein with charged amino acid side chains. The blue and red color represents positive and negative charge respectively. Figures in Panel B and C have been generated in Pymol software [150].

The positively charged N-terminal domain of α-synuclein contains non-perfect 11-amino acid long repeats. These repeats are highly conserved and unique only to vertebrates [136]. Each repeat contains a hexameric motif, KTKEGV, also found in apolipoproteins where it represents a small α-helical domain [137]. All pathologic mutations associated with PD – A53T, A30P, E46K, G51D, H50Q, and newly identified A53E – are clustered within this region [7,85,138–142]. The central NAC region is a highly hydrophobic segment that is prone to form inter-molecular cross β-structures [143], and it is directly involved in aggregation and fibril formation [144]. The C-terminal domain of α-synuclein is an acidic tail. This domain structurally represents

a random coil, has low hydrophobicity and high net negative charge. The reduction of pH neutralizes the negative charge and induce aggregation *in vitro* [145,146]. *In vivo,* this domain can be phosphorylated at multiple sites [147,148] which suggest a mechanism for regulation. The function of these phosphorylations is still not clear, but it has been showed that the C-terminal has a role in both regulating the interaction of α-synuclein with lipids [147] and inhibiting oligomerization [148].

1.2.4 Post-translational modification of α-synuclein

The α-synuclein can undergo several post-translational modifications in a cell, including phosphorylation, nitration, glycosylation, acetylation and truncation with various effects on oligomerization and cytotoxic properties of α-synuclein (reviewed in [151,152]). However, many of the studies have used an overexpression system without a relevant physiological localization of α-synuclein, and most of these modifications are likely rare events in normal cell environment [151].

However, there is one highly relevant post-translational modification of α-synuclein, observed in the brains of PD patients, and that is phosphorylation of Ser-129. In the brain of the healthy individual only circa 4% of α-synuclein is phosphorylated at this position [153]. However, this modification is very prevalent in Lewy bodies in which about 90% of α-synuclein is phosphorylated [153,154]. *In vivo,* it has been observed that Ser-129 phosphorylation increased the cytotoxicity of α-synuclein and accelerated the formation of α-synuclein inclusions [155,156]. Moreover, the accumulation of phosphorylated Ser-129 α-synuclein has been observed in mice models overexpressing the α--synuclein [127,157,158]. Furthermore, it has also been shown that phosphorylation of Ser-129 can inhibit fibrillation *in vitro,* potentially producing a higher population of toxic oligomers [159,160].

1.3 α-Synuclein pathology

α-Synuclein is involved in several neurodegenerative diseases: Parkinson disease (PD), Parkinson disease with dementia, Dementia with Lewy bodies, Multiple system atrophy and others [4,161]. A common denominator for all of them is the presence of fibril deposits containing α-synuclein in the brain. For PD and PD related dementia, the deposits are the in the form of Lewy bodies or Lewy neurites. These are round,

eosinophilic, cytoplasmic inclusions, which are particularly numerous in substantia nigra [162]. The progress of the PD (and PD related dementia) is associated with substantial loss of dopaminergic nerve cells in this region [163]. In Multiple-system atrophy the deposits of α-synuclein are found in glial cytoplasmic inclusions which resides predominantly in oligodendrocytes [32,164]. The glial deposits are generally more spread over the broader region of the brain affecting not only substantia nigra but also basal ganglia, cerebellum, spinal cord and other [161,164]. The different localization of deposits correlates with the different progress of the disease and different clinical symptoms.

However, the insoluble fibrils deposits of α-synuclein seem to be just a symptom of the disease, not its cause. There is accumulating evidence that soluble oligomeric forms may be toxic species involved in the disease. Firstly, there is an increase in the abundance of oligomeric α-synuclein in the brain of PD patient [165] and this increase correlates with the progress of disease [166]. Secondly, *in vitro* formed oligomers of α-synuclein are mostly neurotoxic [86,167,168]. Lastly, more soluble mutants of α-synuclein, which are more prone to oligomerization but not to fibrillation, are causing dopaminergic death *in vivo* [86,169]. Meanwhile, the α-synuclein fibrils are mostly inert and nontoxic [86]. This evidence points to a molecular basis of neuronal loss which we will discuss further.

1.3.1 Mitochondrial dysfunction

Mitochondrial dysfunction seems to be central to the pathogenesis of oligomeric α-synuclein and has also been described in other neurodegenerative diseases. The observations from experimental models and human biopsies provide strong evidence that α-synuclein oligomers can induce a mitochondrial depolarization and impair respiration through interaction with complex I [116,170], inducing the mitochondrial uptake of exogenous calcium [171]. α-Synuclein may also play an indirect role in modulating complex I activity by interaction with cardiolipin [172,173]. Cardiolipin, an anionic phospholipid, is almost exclusively found in the inner mitochondrial membrane [174] and it seems to be involved in the formation of mitochondrial supercomplex.

Therefore physical interaction between cardiolipin and α-synuclein could disrupt electron transfer [175–177].

There are also other theories about α-synuclein-induced mitochondrial death, usually backed up by several *in vitro* experiments. For example, the α-synuclein oligomers have been demonstrated to interact with the outer mitochondrial membrane receptor complex TOM20 and impair a mitochondrial protein import and an excessive ROS production [178]. The oligomers of α-synuclein also seem to be able to induce the selective oxidation of the ATP synthase beta unit and mitochondrial lipid peroxidation. These oxidation events could lead to a permeability transition pore opening, short-lived unspecific pores, which cause mitochondrial swelling and ultimately to cell death [179]. Moreover, overexpression of α-synuclein in *Caenorhabditis elegans* can lead to disruption of mitochondrial fusion and mitochondrial fragmentation [120]. These fusion deficits can be rescued by overexpressing several PD-related proteins (like PINK1, Parkin, and DJ-1) [120,121,180]. Besides, mutant α-synuclein A53T has been shown to modulate mitochondria morphology in the central nervous system (CNS) *in vivo* [181]. The reported pathological effect of α-synuclein on the mitochondria is heterogeneous, and for now, it is hard to identify which of these pathological pathways (or combination of those) are the key one in the progress of synucleinopathy.

1.3.2 Membrane permeabilization and calcium dysregulation

The monomers of α-synuclein can bind different synthetic and biological lipids (see more in section 1.5. α-Synuclein interaction with lipids). This binding seems to be able to initiate the self-aggregation of protein either by raising the local concentration of α-synuclein in the presence of membrane, by exposing hydrophobic residues (the NAC region) of α-synuclein or by the physiochemical properties of the surrounding lipids [182,183]. Once the oligomers are formed, they are able to disrupt the membrane and to integrate themselves into the lipid bilayer [184]. This membrane disruption can lead to ion flux across the membrane and dysregulation of the most common ion in a cell, calcium [168,185,186]. It is not yet known whenever this mechanism is based on a pore formation or a membrane disruption (membrane thinning) [187,188]. Recently, there has been report of a new possible calcium dysregulation mechanism involving the

interaction of α-synuclein oligomers and cellular PrP and formation of new complex hetero-oligomer. This complex can alter calcium homeostasis through interaction with metabotropic glutamate receptor and NMDA receptor [189].

1.3.3 Lysosomal and degradation dysfunction

Dysfunctional lysosomal clearance mechanism and the failure of the degradation pathway to remove the aggregated protein is another phenomenon that accompanies oligomer-mediated toxicity. It has been observed that α-synuclein oligomers are cleared through the lysosomal pathway and that inhibition of lysosomal activity accelerated the oligomer aggregation and toxicity [190]. Conversely, elevated lysosomal activity reduces the accumulation of oligomeric α-synuclein in neuronal cell lines [191]. It has also been observed that overexpression of transcription factor EB, a master regulator of lysosomal biogenesis, was able to reverse the lysosomal defects and accumulation of α-synuclein aggregates as more lysosomes were assembled [192]. Another factor is that heterozygous mutation in an important lysosomal gene GBA1, coding glucocerebrosidase (GCAse), is causing early onset and faster progress of PD in 7% of cases [193]. It is not yet clear how 30-50% reduction of GCAse concentration in a cell can cause an increase in oligomerization of α-synuclein. The theory is that this is caused by the accumulation of GCAse substrate, glucosylceramide (GluCer), which can directly interact with α-synuclein and promote the conformational conversion of α-synuclein monomers, into toxic oligomeric species [194].

1.3.4 Oxidative stress

Oxidative stress is another important pathological hallmark of α-synuclein oligomers presence [195]. It is caused by an imbalance between ROS species like O_2^-, H_2O_2 and $O^{\cdot}$, and antioxidants such as glutathione or enzymes such as manganese superoxidase dismutase [196,197]. The increased oxidative stress comes partially from disturbing the mitochondria homeostasis. The mitochondria are the major intracellular source of ROS, generated in Complex I and II of the respiratory chain. Any disturbance in mitochondria integrity can lead to the release of ROS to intracellular space of the cell [198]. However, oligomeric α-synuclein seems also to produce ROS independently of known

mitochondrial enzymatic pathways [199,200], and it is also able to induce increased lipid peroxidation activity [200].

1.3.5 Microglial activation and inflammation

Microglial activation is the critical component in the progress of amyloid neurodegenerative pathogenesis. The release of protein aggregates and oligomers from neurons activates microglia which consequently initiates an inflammation response [201]. The activation of microglia then results in elevation of cytokines, chemokines, ROS and interleukin levels which are crucially involved in neuronal death [202]. There are two mechanisms of α-synuclein associated microglia activation. The first one happens when α-synuclein oligomers are taken up by an astroglial cell where they trigger an inflammatory response [190]. The second mechanism is the interaction of α-synuclein oligomers and Toll-like receptors on both microglia and astrocytes [203–205].

The microglial activation can be viewed as a double-edged sword in neurodegenerative diseases. On the one hand, microglial activation is necessary to clear debris from apoptotic neurons, but on the other, it contributes to cell stress by an increasing the amount of ROS, cytokines, and chemokines [206]. The inflammation processes in a brain can also be viewed as a positive feedback loop: α-synuclein oligomers and aggregates can induce inflammation processes which then promotes even more oligomerization and aggregation. It has also been observed that other processes which lead to microglial activation can lead to faster progress of some neurodegenerative diseases. For example, traumatic brain injury can lead to an increase of the concentration of pro-inflammatory and amyloidogenic protein S100A9 and consequently into Aβ aggregation and AD [207]. It is possible that similar inflammatory positive feedback loop is present also for α-synuclein.

1.4 Folding, oligomerization and fibrillation of α-synuclein

α-Synuclein is structurally exciting protein. In its native state the protein is intrinsically disordered, but under specific conditions, it can gain α-helix structure, β-sheet structure or cross β-sheet fibrillary structure. This quite unusual behavior has led to the α-synuclein informal title: folding chameleon [208].

1.4.1 Native monomeric α-synuclein

In the cell, α-synuclein exists in equilibrium between a soluble and a membrane-bound state [151]. The soluble α-synuclein is primarily monomeric and intrinsically disordered [209,210]. The intrinsically disordered proteins have little or no ordered structure under physiological conditions and fall mostly into the category of random coils [208]. However, it was observed that α-synuclein monomers are slightly more compact than expected [211,212]. Further FTIR and NMR analysis revealed that ~ 70% of molecules is disordered, but a region between residue K6 and V37 has a preference towards helical conformation [211,213]. The possibility of a helical conformational presence in monomeric α-synuclein has also been confirmed by Raman spectroscopy [214]. The partial folding is visible at higher temperatures or low pH [211,212]. Lower pH can neutralize the excess negative charge of α-synuclein (pI = 4.7), increase the overall hydrophobicity of the protein and induce the helical formation on N-terminal. This pH-induced transition from unfolded to partially folded conformation was shown to be a completely reversible [211,212].

Upon binding to a membrane α-synuclein monomer will adopt α-helical structure on the N-terminal part of the protein [215–217]. Overall, the N-terminal ~100 amino acids will gain an α-helical conformation while the remaining ~40 amino acid in the C-terminal region stay unordered [218,219]. The truncation of the N-terminal domain has been showed to reduce lipid binding drastically and suggest a cooperative effect of the 11-residue repeats present in this region [151]. However, there are different reported structures where α-synuclein forms either a single extended helix or a helix broken around a central bend. It was later elucidated that these structural variations depend on the membrane curvature. Specifically, membranes with a larger diameter (>30 nm), which have lower curvature, induce an elongated α-helix in α-synuclein [218–221]. Meanwhile, when α-synuclein interacts with small highly curved vesicles, it adopts a broken α-helix conformation (Figure 4) [222–224].

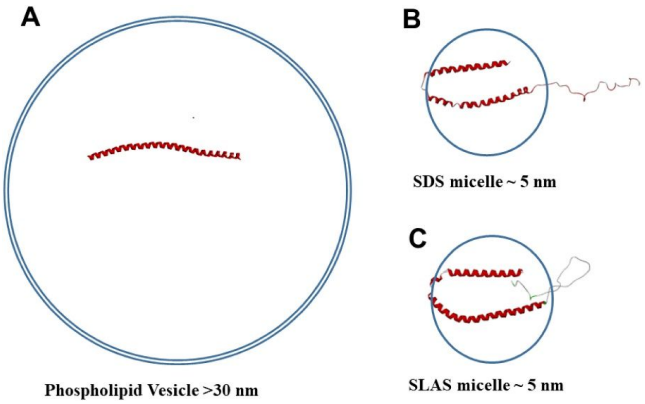

Figure 4: Membrane-bound α-synuclein. (A) When bound to a vesicle, α-synuclein has been reported to obtain an extended helical conformation [218]. (B, C) When bound to lipid models of smaller diameter, α-synuclein adopts the structure of a broken helix (PDB entry 1XQ8 and 2KKW, for panel B and C respectively) [149,225]. SDS - sodium dodecyl sulphate, SLAS - sodium lauroyl sarcosinate. The figure was replicated with permission from [226].

1.4.2 Dimers, Trimers, and Tetramers

There are two different structural variants of α-synuclein dimers referred to as the type 1 and type 2, both of them quite unstable and transient [227]. The type 1 dimer is more unstable with a lifetime around ~100 ms in neutral pH [228], and both molecules of α-synuclein in the dimer have similar globular shape [229]. The type 1 dimers form preferentially in certain circumstances, for example, by the mutant A30P, which is predisposed to form oligomers over fibrils *in vitro*. Both molecules in type 1 dimer seem to have only a single point of intermolecular contact [230,231], which explain type 1 dimer short lifetime. The type 2 dimer is less abundant (~ 20 % of dimers for wild-type α-synuclein) in neutral pH, but it is more stable with longer lifetime ~500ms [228]. The type 2 dimer population becomes more abundant in lower pH, probably due to stabilization of negative charge on C-terminal of protein. It was also shown that dimers from α-synuclein mutants E46K and A53T, which are more prone to fibrillation, have multiple intermolecular contacts and are more stable [230,231]. Structurally, the type 2 dimer consists of one globular molecule and one molecule with extended flexible tail [229]. The extended part of α-synuclein seems to be the N-terminal, forming a metastable α-helix [229]. This observation has led to the theory that lipid bilayer could lead to stabilization of type 2 dimer and through this mechanism to the promotion of fibrillation and neurotoxicity.

Trimers of α-synuclein are rarely studied as they seem to exist only in a mixed population with oligomers. There is one study which points out trimers in the mixture of small oligomers as a possible cause of *in vitro* liposome clustering (the model of mitochondrial fragmentation) [121]. α-synuclein trimers have also been identified in the presence of phosphoglycerol (PG) and oleic acid. In the presence of lipid molecules, α-synuclein has been observed to form trimeric nanoparticles, similar to the ones formed by apolipoprotein, i.e., ellipsoidal discs with a diameter of ~10 nm. In this trimeric form, α-synuclein seem to assume a broken helical conformation [232].

Native α-synuclein tetramers have been reported in 2012 [233]. The α-helical tetramer is hypothesized to be a non-toxic species that inhibits α-synuclein fibrillation pathway [234] and that up to 70% of native cytosolic α-synuclein is in this form [235]. Several studies have confirmed the observation of tetramers in the native neuronal cell [235,236], however other groups were unable to confirm this [209,237]. So, for now, the existence of tetramers *in vivo* remains a polarizing issue in the field [209].

1.4.3 On and Off-pathway α-synuclein oligomers

There is still little consensus on the exact mechanism of α-synuclein toxicity. However, soluble oligomers are widely regarded as the main culprit of PD and other synucleopathies. When analyzed by atomic force microscopy (AFM), the different morphologies of early oligomers were observed [208]. The early oligomers appeared to be predominantly spherical with a radius between 2.5 and 4.2 nm [238,239]. They are later converted into annular (doughnut) shape under appropriate conditions. The wild-type of α-synuclein seems to produce two types of annular structures: small, with a diameter range of 32-96 nm, and large, with a diameter range of 100 – 180 nm [239]. The PD-associated pathological mutations A53T was observed to form a smaller and more homogenous population of annular oligomers with diameter ~10 nm. It was suggested that the observed annular oligomers are not on the direct monomer-to-fibril pathway and that these annular structures must be reopened to be converted to fibrils [239]. The round shape oligomers can interact with phospholipid bilayers and are able to induce membrane permeabilization [240]. Another observed morphology of α-synuclein oligomers is rod shape. The rod-shape oligomers are formed when

α-synuclein binds dopamine which seems to be incorporated into the structure of the oligomer. These rod oligomers do not bind phospholipids or affect membrane permeability [241]. Stellate oligomers (star-shaped) have been observed *in vitro* in the presence of copper, these oligomers have also reduced the ability to associate with membranes [242,243]. It is not yet certain which of these species exist *in vivo*.

The early oligomers are transient, and they seem to be able disassemble into monomeric form. Still, there are several studies which have been able to use the modification of α-synuclein to isolate a stable homogenous population of oligomeric species. These modifications are: the oxidation of the methionine residues to methionine sulfoxide [244,245], the nitration of tyrosine residues [246,247], the interaction with polyphenols such as baicalein, rifampicin, epigallocatechin gallate (EGCG) [248–250], the covalent modification by 4-hydroxynonenal [251] or the tandem repeats of α-synuclein connected by peptide linker [252]. Many of these oligomers are incredibly stable with a prolonged rate of both dissociation and fibrillation. However, they are generally much less toxic than *in vivo* isolated oligomers suggesting they are biologically less relevant, inert, off-pathway oligomers.

Recently more insight into the structural difference between toxic and non-toxic oligomers of α-synuclein has been published [184]. Two general types of oligomers have been established – type A* and type B*. Both types have similar sizes and morphologies. However, they exhibit different abilities to disrupt the lipid bilayer. Type A* is the non-toxic type which can be generated, for example, by incubation of α-synuclein monomers with EGCG [248]. These oligomers can interact with membranes but do not to disrupt them [184]. Type A* oligomers are predominantly unstructured and have limited interaction with charged lipid headgroups, but no deep penetration into the membrane. Type B* oligomers are neurotoxic oligomers, generated by prolonged incubation of α-synuclein in 37 °C with shaking. They are able to interact with the membrane, and they induce membrane leakage in vesicle models [184]. Structurally, type B* oligomers contain both α-helix and β-sheet structures. It is hypothesized that α-helix interacts with charged lipid headgroups and β-sheets penetrates the hydrophobic part of the lipid membrane, distorting the lipid bilayer.

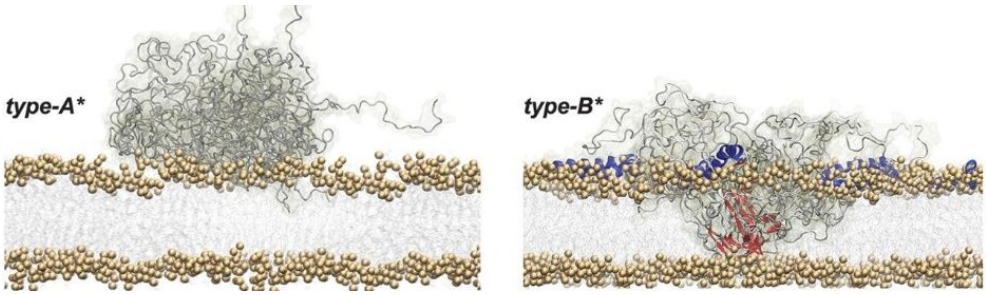

Figure 5: Two different types of α-synuclein oligomers. Type-A* oligomers, generated by incubation with EGCG, do not penetrate the lipid bilayer and are mostly unstructured. Type-B* oligomers, generated by incubation at 37 °C and shaking, penetrates lipid bilayer and contains both distinct α-helix and β-sheet domains. The figure was replicated with permission from [184].

1.4.4 Fibrils of α-synuclein

There are two final stages of α-synuclein aggregation pathway: amorphous aggregates and structured fibrils. The amorphous aggregate has only been observed *in vitro,* and it is similar to precipitation of non-amyloid proteins. It represents a non-reversible collapse into particles with highly hydrophobic cores [208,253]. The fibrillation is a more delicate process which contains a high amount of oligomer restructuralization.

During fibrillation, the α-synuclein oligomers assemble into a highly compact structure enriched in β-sheet content [254–256]. The core is formed mainly by NAC and by part of N-terminal domain, from residues 30-38 to residues 95-110, which are assembled into five to six β-strands separated by several loops [257,258]. The N- and C-terminal regions are unstructured and exposed to the solvent outside of the core. There are various fibril structures reported by AFM and by transmission electron microscopy and fulfill all general characteristics of amyloid fibril (1.1.1 Amyloid fibril structure). However, different subtypes of the α-synuclein fibrils has been characterized: twisted, curved, periodic, untwisted, straight and nonperiodic [259,260]. Such variability is caused by different aggregating conditions, or it can be the effect of the genetic mutation. Overall it is virtually impossible to define which of the observed structure subtypes, if any, represent the types of aggregates found in the brain of patients with synucleinopathy.

Fibrils do not appear to be toxic on its own. However, there are two fibril toxicity hypotheses, which are backed by several reports [227,253]. The first hypothesis is that fibrils can produce toxic oligomers by a dynamic equilibrium with fibril assembly/disassembly. It has been observed that when monomers are removed, the fibrils can slowly dissemble and generate a mixture of oligomers and monomers [167]. The products of fibril disassembly can serve as a seed to the growth of new fibrils from free monomers. This phenomenon also appears *in vivo* during apparent cell-to-cell transmission [50,53]. In addition, pre-formed fibrils applied to neuronal cell culture are able to seed the growth of endogenous α-synuclein aggregates, even in the absence of endogenous overexpression [261]. Moreover, there have been reports where cells seeded with α-synuclein aggregates shown the disruption of autophagic protein clearance and calcium homeostasis dysfunction [262].

The second fibril toxicity theory is that the process of fibril elongation is toxic through the phenomenon of "lipid extraction," which was initially observed in studies of amyloidogenic human islet amyloid polypeptide [263]. It has been observed that α-synuclein fibrils can absorb fluorescently labeled lipids. This effect accelerated when A53T and E57K α-synuclein mutants were used. However, the addition of dopamine prevents this binding, probably by stabilizing soluble oligomers [264]. So far, the lipid extraction has not been studied in cells, but it has been shown that fibrils can disrupt lysosomes and mitochondria isolated from cells [265]. The fibrils have also been shown to disrupt vesicles with smaller amounts of anionic lipids (from 20% of PG) than what was observed in the case of oligomers (from 50% of PG) [266,267]. This observation suggests the possibility that there is a different permeabilization mechanism for fibrils than the one described for oligomers.

1.5 α-Synuclein interaction with lipids

The lipid environment is an essential component in both the biological and pathological role of α-synuclein. The interaction between α-synuclein and the membrane has been found to affect not only properties of the protein but also those of the lipid membrane. It has been observed that α-synuclein presence in the membrane has an effect on its melting temperature [183,268,269] and that it causes membrane remodeling [270–272],

membrane thinning and membrane expansion [271,273]. Summary of α-synuclein and lipid interaction is in Figure 6.

The strength of α-synuclein binding to the lipid bilayer is affected by the membrane physical, chemical, and thermotropic properties. α-Synuclein binds preferably to: (i) membranes composed of negatively charged (anionic) phospholipids [112,274], (ii) membranes containing packing defects [273,275] and/or (iii) membranes in fluid phase [183,269]. From these three components, the effect of electrostatic interaction (negative charge on the membrane) is the strongest contributor to final binding affinity. This has been confirmed by the observation that change in ionic strength of buffer has a noticeable effect on α-synuclein lipid binding efficiency [60,215].

Although, structural information about α-synuclein bounded to lipid membrane has been characterized previously [111,276], the detail of binding and the mechanism by which lipid environment affects folding and aggregation of α-synuclein is not yet well understood. Part of the problem was that it was not until recently, that intro experiments elucidated that this effect is strongly dependent on lipid:protein ratio (L:P ratio) [182,277].

One molecule of α-synuclein can interact with *n* molecules of lipids. The *n* values differ between different lipid species and their mixtures [277]. For L:P molar ratios $< n$ there is an insufficient amount of binding places on lipid bilayer, and α-synuclein monomers compete for binding. This could lead to local upconcentration of α-synuclein which will affect both the oligomerization and toxic properties of oligomers, in particular those related to membrane damage. Bound α-synuclein on the lipid membrane can also serve as a nucleation site, and in combination with an excess of free monomers, this promotes faster oligomerization and aggregation. When L:P ratio is closer to the *n* value, the rate of oligomerization slows down as there are less available monomers in solution. Eventually, all α-synuclein interacts with lipids and aggregation is stopped completely.

1.5.1 Anionic phospholipids

It has been observed that α-synuclein favorably interacts with lipid system containing anionic phospholipids like PG or PS [182,183,278]. During this interaction, there is a change in the fold of α-synuclein monomers from the intrinsic disordered state into the α-helical fold (see section 1.4.1. Native monomeric α-synuclein). The newly formed α-helix binds the bilayer by interaction with lipid headgroups, and this binding affects the aggregation properties of α-synuclein. However, the results of how precisely the presence of anionic lipids affect oligomerization and aggregation properties were inconclusive. Some studies observed promotion of aggregation and an increase in toxicity [278,279], and others reported a decrease in aggregation [182,183]. It is believed that these conflicting reports arise from different L:P ratio used in different experiments (for more information see review [277]).

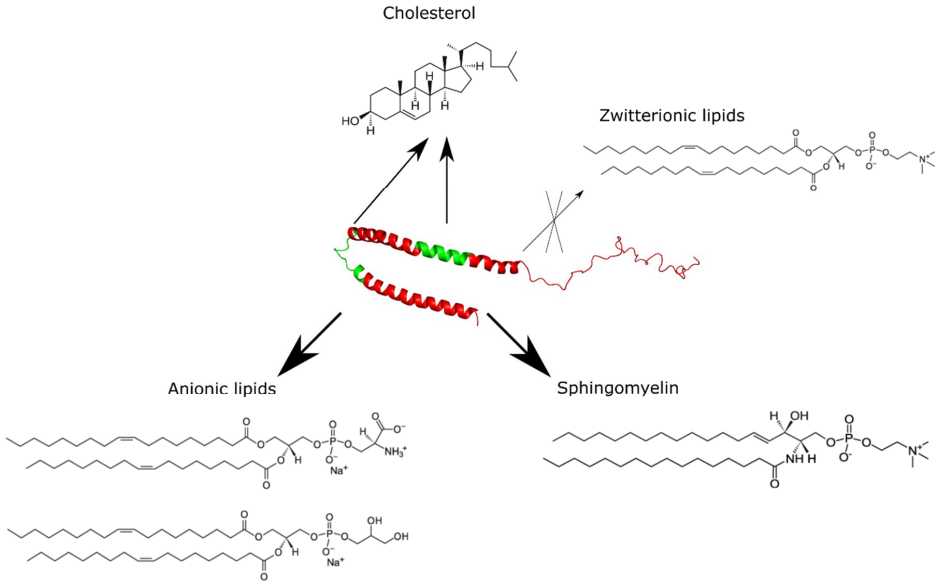

Figure 6: α-Synuclein interaction with lipids. α-Synuclein is able to interact with anionic lipids (in the picture: DOPS and DOPG) and sphingomyelin (in the picture: SM d18:1/16:0). Upon binding to the lipid bilayer, monomers of α-synuclein converts to a mainly α-helical conformation. α-Synuclein is also able to interact with cholesterol. The cholesterol binding sites are highlighted in green. Generally, α-synuclein does not interact with zwitterionic lipid bilayers (in the picture: DOPC), other factors (like high stored curvature stress in lipid vesicles) needs to be present for this interaction to occur.

It has also been observed that α-synuclein is co-localizing with synaptic vesicles in live cells which contains large amounts of anionic phospholipids [102] and the presence of anionic lipids and high curvature seems to be driving force behind α-synuclein localization into presynaptic vesicles of neuronal cells [273,277].

1.5.2 Sphingolipids

Sphingolipids have been the main suspect in more pronounced α-synuclein aggregation. The reason is that mutation of the GBA1 (gene coding GCase) is the most critical risk factor associated with PD. GCase converts GluCer to glucose and ceramide and the decrease in its activity leads to the accumulation of its substrates GluCer and glycosylsphingosine [194,280,281]. Mutation of GCase is associated with lysosomal degradation, which is one of the syndromes associated with synucleopathies (see 1.3.3 Lysosomal degradation and dysfunction for more information). However, elevated levels of several sphingolipids, including lactosylceramide, GM2, GD3 or GM3 has also been observed in Parkinson mice models [194] or the blood plasma of PD patients [282].

Two independent reports have found that Lewy bodies contain sphingolipids in its central core, especially sphingomyelin [283,284]. This was later confirmed using cellular models [285]. The sphingolipids, in general, seem to affect the ability of monomeric α-synuclein to bind to the membrane [286]. This interaction between α-synuclein and sphingolipids is in many ways similar to the interaction between α-synuclein and the anionic lipids. Both sphingolipids and anionic lipids seem to promote α-synuclein association with the membrane. Out of all sphingolipids species, α-synuclein has the highest affinity towards ganglioside GM1. The mixture of GM1 and DPPC (ratio 1:1) binds five times more molecules of α-synuclein than DPPC only [277].

In aggregation experiments, it was observed the vesicles containing sphingolipids are inhibiting oligomerization and aggregation of α-synuclein [278,286] Indeed, in this conditions a fraction of α-synuclein monomers is bound to the membrane which leads to the absence of available monomers which continue on the oligomerization pathway. However unlike for other tested anionic vesicles like DPPC or DMPS, in sphingolipid aggregating experiment, only lag phase seem to be affected and not fibrillation rate.

This suggest that, unlike anionic phospholipids, sphingolipids mainly affects the primary nucleation speed of α-synuclein, but once seeds are formed, the inhibition of oligomerization by sphingomyelins cease to have an effect [277,287].

1.5.3 Cholesterol

Cholesterol is one of the most abundant lipid species in the brain, and its dysregulation has been linked to faster progression of several neurodegenerative diseases including Alzheimer's disease [288,289], Huntington's disease [290] and Niemann-Pick disease type C [291,292]. However, the relationship between cholesterol and PD is less clear. Cholesterol is synthesized in brain *de novo* and cannot cross blood-brain barrier [293], and blood plasma levels of cholesterol do not reflect the abundance of cholesterol in the brain. This has led to contraindicating observations that elevated serum levels of cholesterol are related to an increased risk of PD [294], a decrease of risk of PD [295] or not correlated with PD at all [296,297]. However, the metabolites of cholesterol, like 27-hydroxycholesterol (27-OHC) are able to cross the blood-brain barrier freely and bear more accurate representation of total cholesterol abundance [293,298]. Indeed, it was observed that 27-OHC is more abundant in PD patients [299].

Nonetheless, a direct molecular link between the presence of cholesterol and α-synuclein fibrillation is still missing. This is because high cholesterol concentration in the cell could lead to α-synuclein fibrillation via other cellular processes other than direct α-synuclein/cholesterol interaction [277]. For example, a high concentration of cholesterol is known to affect lysosomal activity by inhibiting maturation of late endosomes into lysosomes [300–302]. This leads to a disruption of lysosomal activity, similar to that observed in the case of GCase deficiency. Insufficient clearing of α-synuclein monomers can favour oligomerization rate and can lead to toxic effects [280]. Moreover, the observed increased levels of 27-OHC could be the result of PD, not its cause. The increased oxidation of cholesterol sign of ROS presence generated by mitochondrial damage during the progress of PD [303]. However, *in vitro* experiment showed that α-synuclein molecule could interact with cholesterol directly.

The NAC region of α-synuclein has been reported to contain two cholesterol binding sites (residues 34-45 and 67-78), with the latter exhibiting a high affinity to cholesterol

[304,305]. The second binding site was used to design cholesterol-binding peptide, further proving high cholesterol binding ability. It was also reported that α-synuclein could serve as cholesterol acceptor and with combination with transmembrane protein ABCA1 it can promote cholesterol efflux from membrane [306]. Also, the formation of "amyloid pores" by α-synuclein oligomers has been reported to be possible only in the presence of cholesterol-rich membranes [304]. If such findings are verified, it would suggest that cholesterol could play an essential role in the toxic effect of α-synuclein oligomers. The other reports are inconclusive as cholesterol seems to promote [106], inhibit [307,308] or not affect [183] α-synuclein interaction with lipids. The role of cholesterol in α-synuclein physiological and pathological activity is yet to be entirely determined as the molecular mechanism behind this interaction is still poorly understood.

1.6 Neurolipidomics

The interaction between lipids and other amyloid proteins, including α-synuclein, is an active research field with many questions left unanswered. Among the most critical questions are: Which lipids come into direct contact with amyloid proteins? In what amounts do they occur in different tissues and subcellular compartments? How do they affect risks for developing misfolding diseases and how do lipid profiles change as the disease progresses? These questions are part of the driving forces behind amyloid neurolipidomics research [309].

It has been reported that the human brain is composed of around 900 neuroanatomically different subdivisions and each of these subdivisions have a different region-specific protein transcription profile [310]. This could lead to the assumption that also lipid composition is region specific or at least have some regional variation. However, this area of research is limited, and for now, we lack region and cell-specific lipidomics information. The focus of this section is to present current neurolipidomics knowledge with a focus on lipids which can be observed by ^{31}P NMR, i.e. the lipids containing phosphor atom. These are phospholipid species, cardiolipins, and sphingomyelins.

1.6.1 Lipid composition of brain

The adult human brain contains almost most of the human lipid mass, second only to the adipose tissue [311]. Lipids constitute around 5% of the wet weight of the whole brain and 7% of white matter. The brain lipids are also the most diverse, compared to other organs, and they consist of possible thousands of phospholipid and sphingolipid molecular species [312]. Brain tissue also contains an abundance of cholesterol. Indeed, one-quarter of total body cholesterol is localized in the brain, making it the organ with the highest concentration of cholesterol in the human body [313]. For a summary of brain lipid composition see Figure 7.

Quantitatively, the most abundant phospholipids isolated from brain matter are phosphatidylethanolamine (PE) [312,314–316]. They constitute about 35-36 % of all phospholipids in the human brain. The most of brain PE is in the form of ethanolamine plasmalogen or diacyl. The alkylacyl analogs of PE constitute less than 7% of total PE content in the brain. Regarding fatty acid (FA) composition, it has been reported that *sn-1* position is usually occupied by palmitic (16:0), stearic (18:0) or oleic acid (18:1). Position-2 contains more polyunsaturated FA chains. The second most abundant brain phospholipid is phosphatidylcholine (PC; ~30% of brain phospholipids) [314,315,317–319]. It is also the most predominant form of choline in the human brain. The major species is PC (16:0/18:1), and other forms of PC are reported to be in the minority. The choline plasmalogen and alkyl analogs account only for about 2% of total PC in the brain. The last major phospholipid group is formed by phosphatidylserines (PS) making up to ~17% of total phospholipids [314–316]. More than 90% of PS are in the form of diacyl, with the rest being mainly in plasmalogen form. FA profile of PS is composed mostly of steric (18:0), oleic (18:1) and docosahexaenoic acid (22:6). The long, unsaturated 22:6 chains of PS were observed particularly in the grey matter.

The phosphatidic acid (PA) is a minor phospholipid brain component (~3%) [312,314]. It is the simplest glycerophospholipid, and it is a central intermediary in the synthesis of both glycerophospholipids and neutral lipids. Another minor phospholipid component is phosphatidylinositol (PI) (~2%) [319,320]. The relative abundance of PI is low in comparison to other phospholipids present in the brain. However, it is still the

highest concentration of PI found among animal tissue. The main FA components of PI are steric (18:0) and arachidonic acid (20:4). Lastly, minor phospholipid components of the brain (less than 1%) are glycerol phosphatidylglycerol (PG) which include mainly its diacyl form and bis(monoacylglycerol) phosphate [321]. PG has been reported to have a wide range of FAs including 16:0, 16:1, 18:0, 18:1, 18:2, 18:3 and 20:4 and to be localized in the mitochondria, nuclear and synaptosomal fraction. Phosphatidylglycerol is also a metabolite precursor of cardiolipin, which is a specific type of diphosphatidylglycerol localized exclusively into inner leaflet of mitochondria [322].

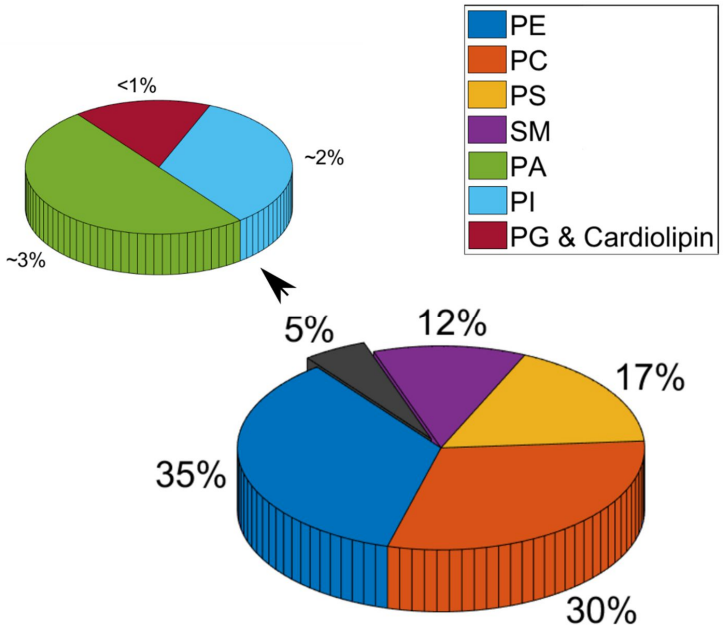

Figure 7: Phospholipid (including sphingomyelin) composition of the brain. Data taken from [312].

Sphingolipids are the second biggest group of complex brains observed in brain tissue. They are derived from *N*-acylsphingosine (ceramide) which is also the most abundant sphingolipid species [323,324]. A different modification of sphingolipid headgroup leads to the formation of sphingomyelin, cerebrosides, sulfatides, and gangliosides. Sphingomyelin (*N*-acylsphingosine-1-phosphocholine) is primary lipid of myelin membrane, and it is found in high concentration in peripheral nerves and white matter,

and it consists of ~12% of phospholipids in the brain [314,315,317,318]. Sphingomyelin FA chains comprise mainly of stearic (18:0), lignoceric (24:0) and nervonic acid (24:1).

1.6.2 Brain phospholipid changes during aging and Parkinson disease

The human brain ability to perform its wide range of functions decline with age, like any other part of the human body and this decline is even more pronounced during the progress of neurodegenerative diseases. It was observed that deterioration in structure and function is not uniform throughout the brain. It seems that brain aging and neurodegenerative processes are region- and cell-specific [312]. This phenomenon is called selective neuronal vulnerability (SNV), and it has been observed during the neurodegeneration, including both Alzheimer (AD) and Parkinson's disease (PD) [325–328]. The mechanism of SNV is still unknown, and this hinders further understanding of the neurodegeneration. One of the possible causes of SNV could be different regional lipid composition.

Regional SNV has been confirmed for both aging and neurodegenerative changes. During aging, the most affected brain regions are the association cortex, the neostriatum and the cerebellum [329–331]. For AD, the most affected region is the CA1 region of the hippocampus [332], and for PD it is substantia nigra [328]. The difference between these regions is studied by various techniques, including histological analysis, neuroimaging, and genomic and proteomic profiling. In these studies, however, the possible role of membrane lipids and lipid metabolism is mostly ignored. This is true even despite the knowledge that neuronal loss in these sensitive regions is relatively modest and most of the neurodegenerative processes are caused by changes in a number of synapses. The synapse can be affected by relatively subtle changes, like loss of dendrites, reduction in spine densities, altered spine morphologies or changes in the molecular profile of synapse [312,326,330]. All these changes can be associated with alteration of cell lipid profile.

Whole brain lipid analysis showed that the total amount of lipids increases until the age of 20 and then starts to decline [312,319,333]. This decrease speeds up after the age of 50. However, it is still very slow for several monitored phospholipids lipids: PI, PE, and PC as their level decrease only about 10% between age 40 and 100. There are two lipid

species where the observed decline was more pronounced; ethanolamine plasmalogen (PPE) and sphingomyelin [334]. The decrease is almost twice as fast as when compared to other lipid species and in case of PPE human brain lose 29% of PPE and 20% of sphingomyelin at age 100.

The study of regional brain lipid composition is limited, and so far such analyses have only been performed concerning FAs and cholesterol. McNamara *et al.* [335] observed that age inversely correlates with the amount of polyunsaturated fatty acids (PUFA), mainly docosahexaenoic (22:6) and lignoceric acid (20:4) in the grey matter of the orbitofrontal complex (decrease of 15% between groups of 30 and 80 years old). This age-related reduction in PUFA composition is inversely correlated with increased stearoyl-CoA desaturase activity, resulting in elevated levels of monounsaturated FAs. Regional cholesterol content seems to follow a similar trend as PUFA and its amount in brain decrease with age. So far, the decrease of cholesterol was observed in human frontal and temporal cortices, hippocampus, nucleus caudatus, medulla oblongata, and cerebellum. However, the rate of reduction in cholesterol content seems to be region-dependent, possibly mirroring differences in metabolic need if each specific region. [334,336].

There is a limited number of studies focusing on the lipidomics changes of the brain during the progress of PD. In the substantia nigra, it has been observed that there is the elevated activity of phospholipid biosynthetic enzymes relative [337] and there is an increase in cholesterol levels [338] relative to the rest of the brain. However, this increase has not been quantified. In the frontal cortex, there was a significant increase in diacylglycerol levels, similar to the increase observed in the frontal cortex of AD patients [339]. When the primary visual cortex of PD patients was investigated, changes in the lipid metabolism pathways of phosphoglycerol and cholesterol were observed [299]. Increase in levels of 24-OH cholesterol was observed. In response to that, the whole antioxidant response genes apparatus was upregulated. In the glycerophospholipid pathway, upregulation of the gene producing CDP-choline, the primary substrate for PC production, was found. However, the levels of PC remained

unchanged. Instead, there was an increase in the levels of PS, which suggest that excess of PC was metabolized into PS lipid species.

During aging, the overall levels of lipid in the brain dropping. However, during the progress of amyloid-forming neurodegenerative diseases, like PD, there is an apparent trend of upregulation of specific lipids in different areas of the brain. From current knowledge, most interesting is observed increased concentration of cholesterol and 24-OH cholesterol in the substantia nigra, most vulnerable part of the brain in PD.

1.7 Lipid nanodiscs - a tool for studying lipid-protein interactions

Research of how amyloid proteins interact with lipids is hindered by the complexity of natural lipid bilayers and by inadequate lipid models. The lipid vesicles are currently most commonly used lipid models. However, they suffer from several drawbacks like little stability or high-scattering. They also bring severe limitations to solution NMR experiments due to their size and high tumbling times. When searching for more suitable lipid model, it is possible to take into account α-synuclein behavior as a peripheral protein. This line of thought leads to novel lipid models used in membrane protein research, lipid nanodiscs (reviewed [340,341]).

Lipid nanodiscs are planar patches of the bilayer with diameters in the range of tens of nanometres. The lipids are encircled by amphipathic scaffold species which envelops lipids as a belt. Nanodiscs, along with micelles, bicelles, liposomes, and other colloid systems, belongs to the class of self-assembly lipid particles with defined structures [342]. These structures are in dynamic equilibrium with its environment, potentially exchanging their components. [340]. Compared to other self-assembled systems, the lipid nanodiscs are more stable and structurally better defined. The nanodiscs are not an entirely thermodynamically stable state of mixture of lipids and scaffold polymers as it has been observed that after prolonged incubation at increased temperature, they tend to separate irreversibly [343,344]. However, at physiological temperatures the stability is sufficient, and lipid nanodiscs can be stored for months at 4 °C with minimal aggregation and size variation. The scaffold species used in for lipid nanodiscs preparation can be either a membrane scaffold protein (MSP) or a non-peptide polymer – styrene maleic acid (SMA).

Originally, MSP was based on apolipoprotein A1 sequence [345]. This protein, however, produced a variety of lipoprotein particles of different sizes. Authors then modified the original protein several times to obtain more homogeneous and stable nanodiscs. The first modifications were extensions with additional α-helices, which yielded a larger protein envelope and resulted in larger and better-defined populations of lipid nanodiscs [346,347]. Later it was discovered that the N-terminal of the protein did not participate in the formation of the peripheral protein belt and after its deletion, the size of the formed nanodiscs were more homogeneous [346]. This version is denoted MSP1D1 and is currently the most commonly used in protein-lipid nanodisc preparation. One drawback of protein nanodiscs is the necessity to use detergent in their preparation. The lipid mixture needs to be dissolved in a detergent environment, and after addition of MSP protein, the detergent is removed by detergent absorbing particles. The lipid nanodiscs are then formed by self-assembly [343,344]. The preparation of lipid nanodiscs from the second scaffold species – styrene maleic acid (SMA) is entirely detergent free.

SMA lipid nanodiscs represent a new approach to lipid model preparation. This model is unique in its absence of detergent in all steps of nanodiscs preparation [341]. SMA is the hydrolyzed form of styrene-maleic anhydride copolymer synthesized by polymerization of styrene and maleic anhydride monomers (Figure 8). The method of SM anhydride preparation is a radical chain reaction which yields a wide distribution of molecular weights [348,349]. For lipid nanodisc preparation the range M_W of 7.5- 10 kDa is usually used [341]. This molecular weight variation also means that each new SMA batch needs to be optimized as it seems that lipid nanodiscs size varies with different SMA: lipid ratios. The process of SMA lipid nanodisc formation is still undergoing studies. For now, it has been observed that SMA insert itself into lipid bilayers which cause bilayer extension/swelling [350]. When SMA reach a critical concentration in the membrane, it will start to form lipid nanodiscs which will disassemble from lipid bilayer. This process seems to be in dynamic equilibrium as it has been observed that lipids from different nanodiscs population can come into close contact. It seems that lipid discs are disassembling and assembling continuously [350,351].

When SMA and MSP lipid nanodiscs are compared regarding suitability to use for α-synuclein: lipid interaction research, the SMA tends to surpass the MSP for two main reasons. The first reason is that MSP apolipoprotein, used for nanodiscs preparation, is structurally related to α-synuclein. The presence of another protein in the experiment could have a detrimental effect on results. The second reason is that the preparation of SMA lipid nanodiscs is also completely detergent-free.

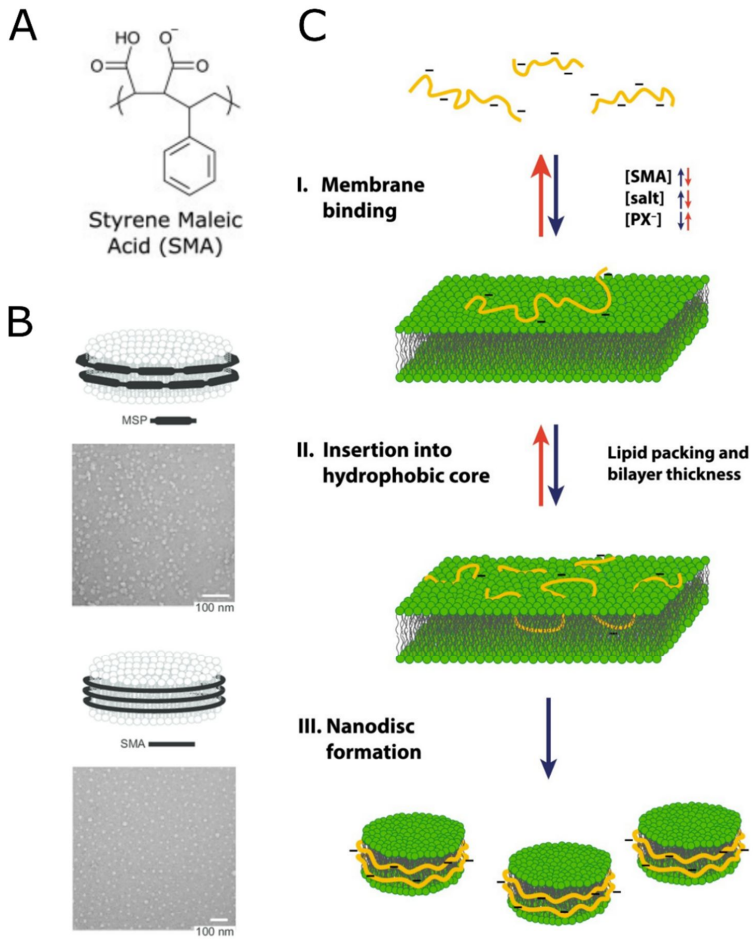

Figure 8: SMA Lipid nanodiscs. (A) The structure of the styrene-maleic acid polymer. (B) The MSP and SMA lipid nanodiscs structure. MSP lipid nanodiscs scaffold is formed by two molecules of MSP protein. Mutant forms of MSP of different lengths are used for exact size manipulation. Upper electron micrograph: MSP1E3 nanodiscs at a magnification of 180 000x [352]. SMA lipid nanodisc scaffold is formed by polymer species of styrene and maleic acid, usually in a ratio 3:1 or 2:1. Size is determined, besides other factors, by lipid concentration, the molecular weight of the SMA polymer and by what specific lipid species are present. Usually, another purification step (i.e., SEC chromatography) is needed to obtain homogenous nanodiscs size. Lower electron micrograph: SMA (3:1 ratio) lipid nanodiscs at a magnification of 120 000x [353]. Figure panel (B) was replicated with permission from [354]. (C) SMA lipid nanodiscs formation. (i) SMA binding to the membrane is determined by SMA concentration, salt concentration and by the charge of lipids in the bilayer [PX^-]. (ii) After binding to the lipid bilayer, the SMA hydrophobic core spontaneously insert into the lipid bilayer. In this step, it is possible to observe an increase in the size of the vesicles. (iii) After SMA reaches a critical concentration in the lipid bilayer, the solubilized lipid nanodiscs will start to form. Figure (C) was replicated with permission from [341].

2 Aims of the thesis

The transition of α-synuclein from inert monomers into toxic oligomers is a fascinating and complex process (see section 1.2 α-Synuclein). This transition is accompanied by a large restructuration of the protein, and it is affected by its lipid environment (see section 1.5 α-Synuclein and interaction with lipids). The lipids seem to be one of the important factor which strongly affects the transition of α-synuclein into oligomers and may play a role in disease etiology and toxic mechanisms. One of the lipid species which seems to affect α-synuclein fibrillation and toxicity behavior is cholesterol.

Our **overall aim** was to improve the state of knowledge in lipidomics and to investigate how lipids may influence protein misfolding events and lead to fibrillation. This aim led us to pursue three goals which are connected to our overall ambition of understanding the role of the lipid environment in α-synuclein misfolding behavior.

Our **first goal** was to investigate how the presence of cholesterol will affect oligomerization and fibrillation of α-synuclein. For this, we needed to establish cholesterol-containing lipid model systems that allowed us to track both interaction and fibrillation, and at the same time resolve effects that these events have on the protein conformation. We have prepared a novel lipid model: SMA lipid nanodiscs containing cholesterol. We have used biophysical techniques (HSQC NMR, SPR, and ThT fluorescence) to monitor the effect of cholesterol-containing nanodiscs on α-synuclein conformation, its affinity towards lipid bilayer and oligomerization behaviour.

In parallel, our **second goal** was to established lipidomics procedures involving efficient lipid isolation from limited cell sample for NMR studies. Initial work was done on *Listeria innocua* where we have improved standard methods for two-phase lipid isolation using dichloromethane and identified a new lyso-phospholipid species in ^{31}P NMR spectra. We have also investigated the effect that lipid changes in a cell population have on the physical properties of the lipid bilayers.

Our **third goal** was to improve the state of neurolipidomics knowledge so that potential lipid drivers of misfolding and oligomerization could be identified and quantified. We chose the SH-SY5Y neuroblastoma cell line, a much-used cellular model system for

studying PD, and we analyzed the whole cell and plasma membrane lipid composition by ^{31}P NMR and LC-MS/MS. We streamlined and automated the LC-MS/MS analysis of the FA chain and their distribution by writing and publishing Matlab script.

3 Summary of results

3.1 α-Synuclein interaction with lipid bilayer is affected by the presence of cholesterol

In Paper I we have investigated how cholesterol can affect α-synuclein affinity to lipid bilayer and its fibrillation. First, we used SPR to characterize the affinity of α-synuclein towards DOPC and DOPC:PE:PG (4:3:1) lipid vesicles with and without 30% cholesterol (w/w). Next, we prepared novel SMA lipid nanodiscs with the same lipid composition. We used these nanodiscs to measure changes in α-synuclein oligomerization rates in robust 384-well ThT fluorescence assay. We have then identified residue-specific apparent affinities of α-synuclein towards nanodiscs of the different lipid compositions using HSQC NMR.

We observed that α-synuclein has an overall lower affinity towards lipid vesicles containing cholesterol independently of lipid composition. When fibrillation speed was tested, using lipid nanodiscs, we have observed a significant increase in oligomerization rate, again, for both lipid models containing cholesterol. Fibrillation started almost immediately, suggesting that cholesterol lipid nanodiscs can act in a manner similar to seeds. However, individual amino acid apparent affinities differ significantly for both models. For DOPC lipid nanodiscs, the addition of cholesterol seems to promote the interaction of the NAC core part of α-synuclein towards lipid nanodiscs. Meanwhile, the affinity of the rest of the protein (N-terminal and C-terminal) did not change significantly. When DOPC:PE:PG lipid nanodiscs were used we observed the opposite trend. The NAC part of α-synuclein was not affected by the presence of cholesterol. However, both N-terminal and C-terminal apparent affinities decreased.

This observation suggests that different, lipid-dependent molecular mechanisms exist for α-synuclein binding to the lipid membrane. These mechanisms can be annotated as "N-terminal pathway," and "NAC-pathway." Cholesterol seems to promote "NAC-pathway" which leads to more volatile fibril formation. This different molecular mechanism could be crucial *in vivo* during pathological condition which can cause a local change in lipid composition.

3.2. Lipid composition and physical properties of prokaryote changes during the cell cycle

In Paper II we established tools for efficient lipid isolation and identification of lipid species. We selected *Listeria innocua* as a suitable prokaryotic model. Cultures of *L.* innocua were synchronized by rifampicin after elongation but before cell division, in the C/D boundary, at the end of the exponential growth phase. We then used a revised two-phase method for lipid isolation using dichloromethane and triethylammonium ions. This new method provided longer stability of isolated lipids and improved yield (> 99%) compared to traditional methods [355]. We used ^{31}P NMR to identify and quantify lipid species present in the samples. Furthermore, we have assigned lyso phospholipids species, including lyso-PG, and we proceed with LC-MS/MS identification of FA chains present for each headgroup.

We observed the modulation of lipid composition which occurs between the B period and the C/D boundary in *L. innocua*. Solid state (broad line) NMR revealed that this modulation in lipid composition during elongation of *L. innocua* represent a reduction in stored curvature membrane stress but without reduction to membrane fluidity. Curvature stress of the membrane is lowered by reduction of the PE fraction and fluidity is represented by an increase of PG (but not CL). Indeed, there seems to be coupling between membrane physical state and cell cycle of *L. innocua*. This study served as a proof-of-concept for further lipidomics experiments involving eukaryotic cells. It also suggests that the physical state of the membrane may be subject to functional modulations throughout the life-cycle of a cell.

3.3. SH-SY5Y lipid compositions differ from average brain tissue

In Paper III we used the method developed in Paper II for lipid isolation and identification of commonly used neuronal cell model SH-SY5Y. We have also adopted a method for plasma membrane isolation suitable for this cell line, and we have compared the composition of total cell lipid abundance with plasma membrane abundance. The lipid composition was analyzed by ^{31}P NMR and by improved LC-MS/MS analysis which offers automated analysis of relative FA abundance.

As part of this study, we developed an automated Matlab script for LC-MS/MS analysis of phospholipid samples. First, the script builds lipid fragmentation libraries based on data collected from literature and based on user input. The lipid search is based on a comparison of the MS2 spectrum with generated lipid libraries and score for each lipid species (based on a number of identified peaks and their intensity) is generated. The MS1 spectrum is then searched for identified lipid species in the observed retention time window, and an abundance of FA in each headgroup is calculated.

The abundance of individual phospholipids differs from a general lipid model of the brain cell. Among other findings, there was a higher abundance of PC lipids reaching up to 60% of the total phospholipids. There was also a more pronounced presence of PG which was on the same level as PS (5%). The SM was observed mostly in the PM-enriched sample, where they sum up until 18% of the total phospholipid content. The LC-MS/MS showed that the FA composition of PC is uniform in both whole cell and plasma membrane sample. The most abundant FA chains for PC was 18:1 and 16:0. FA abundance of PE has the highest variability from all the observed phospholipids. For the whole cell, the most abundant PE FA components were 18:1, 18:0 and 16:0. However, in the plasma membrane sample, there is a shift into FAs with longer chains and less saturation (like 20:1, 22:6 or 20:4). The difference between PE FA in the whole cell and the plasma membrane suggests a pronounced physiological role of PE in the membrane as storage component of curvature stress.

These novel observations of the lipid composition of the SH-SY5Y neuronal cell line could lead us to new, more reliable and relevant lipid model for use in protein/lipid interaction research. Moreover, the study has increased the knowledge available concerning the lipid profile of an important cell system used in especially PD research.

4 General discussion

4.1 Cholesterol role in α-synuclein:lipid interaction

Cholesterol is one of the most abundant lipid species in eukaryotes. It can constitute up to 50% mass of plasma membrane in mammals and has a considerable effect on the physical properties of the membrane [356,357]. Cholesterol has also been linked to the progress of several neurodegenerative diseases including AD [288,358], Huntington's disease [290] or Niemann-Pick type C [291,292]. However, the role of cholesterol in the interaction between α-synuclein and lipid bilayers is unclear as a consistent pattern of behavior has not been observed (see section 1.5.3 Cholesterol). We aimed to explore this interaction by monitoring α-synuclein affinity towards lipid bilayers of different compositions, both with and without cholesterol, and by monitoring changes in α-synuclein rates of fibrillation in the presence of these different lipid factors. First, we needed to established methods suitable for studying this particular lipid:protein interaction. For this, we had to choose and then establish a suitable lipid model system, design reliable ThT fluorescence assay and find a way to interpret peak broadening behavior of α-synuclein in solution NMR.

4.1.1 SMA Lipid nanodiscs preparation is affected by lipid composition

We searched for a suitable lipid model system which: (i) could contain cholesterol (ii) have enough long-term stability to be used in oligomerization experiments and (iii) have low molecular weight to maintain reasonably fast tumbling so that in-solution NMR experiments could be performed. This has been partially solved by using SMA lipid nanodisc (SMALN). However, SMALNs are still novel, and there are no reports of procedure for preparation of SMALN containing cholesterol available in the published literature. Our first practical goal was therefore to optimize the steps in SMALN preparation so that a sizeable population of cholesterol-containing lipid nanodiscs with narrow size distribution could be obtained. During this optimization, we have identified that SMALN formation is affected mainly by lipid composition.

SMALN formation is affected by the presence of non-zwitterionic lipids. The anionic lipids (PG), conically shaped lipids (PE) and cholesterol all turned out to have an

adverse effect on lipid nanodiscs formation. DOPC lipid nanodiscs prepared by the standard protocol were formed quickly in a uniform manner only with 1% SMA present [341]. For DOPC with 30% cholesterol (w/w) we observed only an increase in the size of lipid vesicles, but nanodiscs did not seem to form (Paper I, Figure 1B). One solution to this problem was to increase the SMA concentration in the nanodiscs preparation protocol. However, a simple increase of SMA concentration also leads to a higher diversity of lipid nanodiscs sizes (Paper I, Figure 1C). To obtain a uniform population of lipid nanodiscs the procedure needed to be further modified. In final iteration of the protocol, the SMA polymer was added into the hydrated dispersion of lipids before the vesicles were formed. This meant that SMA was present during the cycles of freeze-thawing and extrusion, and this seemingly helped to overcome the thermodynamic barrier in lipid nanodisc formation. With this new protocol, SMALN (both with and without cholesterol) were formed reliably (Paper I, Table 1).

This behavior of nanodiscs formation is in agreement with the three-step model of SMA lipid nanodiscs formation (Figure 8) suggested by Scheidelaar, *et al.* [350]. It seems that after insertion into the bilayer, SMA can relieve packing stress in the vesicles by the formation of thermodynamically more stable nanodiscs. However, this is hindered by the presence of cholesterol and conical lipids, like PE, which are also able to lower stored curvature stress. We also observed that cholesterol-containing nanodiscs overall are larger (~30nm), than noncholesterol nanodiscs (~10 nm, Paper I, Figure 1D). It is not clear what causes this difference. It is possible that larger diameter is a consequence of different lipid packing in nanodiscs containing cholesterol. Nevertheless, SMALN proved to be extraordinary stable with uniform and constant size even two weeks after preparation.

4.1.2 High throughput ThT fluorescence assay

The ThT fluorescence assay is an established method which is regularly used to monitor the progress of amyloid protein fibrillation (see section 1.1.1 The oligomerization and seeding properties of amyloid-forming proteins). The ThT molecule is a molecular rotor which can interact with a cross β-sheet grove of growing amyloid fibrils. As long as two parts of this molecule are free to move independently, fluorescence quenching is

efficient, and the fluorescence signal is very low. However, when ThT molecules interact with amyloid fibrils, the internal motion in the molecule is halted, and quenching is no longer efficient. ThT will then produce a strong fluorescence signal as a function of available sites on the growing fibril [22]. This behavior is used as the basis of a ThT fluorescence assay, an established assay, used to monitor amyloid fibril formation.

However, even though this method is widely established, its use in α-synuclein research is limited for several reasons. The most important one is the time required for fibril formation. The fibrils of wild-type α-synuclein will, generally, start to form after 20 hours of mechanical agitation. To be able to observe the whole fibrillation curve, an additional 20 hours are needed (Paper I, Figure 4B). In comparison – Aβ, is able to achieve fibrillation during 4 hours from the beginning of agitation [359]. This need for long–term agitation of α-synuclein means that small unilamellar lipid vesicles will not retain their structural properties and it is possible that after first 24 hours most of them will merge into large multilamellar vesicles or form lipid layer in the well, possibly affecting the results of the experiment [360].

The fibrillation of α-synuclein can be speeded up by using external seeds. Seeds are various particles which can serve as a hydrophobic platform for initiation of oligomerization and subsequently fibril growth. In general, seeds are usually introduced as preformed α-synuclein oligomers or small particles of fibrils. However, using externally provided seeds introduce additional variability of the experiment, mainly because it is difficult to control the quality and consistency of the seed used [361]. α-Synuclein oligomerization is very sensitive to the presence of any contaminant which can serve as seeding agent [362]. This sensitivity also applies to small differences in agitation and other hard to control variables, which is known to cause high variability between samples.

To overcome this problem, we have applied an adjusted version of the methodology of Afitska *et al.* [363]. By using 384 microwell plates, it is possible to do multiple repeats of experiments with minimal protein consumption. With more than >20 repeats per sample condition, it is possible to do a cumulative evaluation that increases reliability

and reproducibility of these experiments. In this approach, each well is evaluated only as positive or negative (in reference to negative control), and the cumulative percentage of positive wells can be plotted against the time (Paper I, Figure 4A). It is possible to use this cumulative curve to reconstruct fibrillation curve. While it is also possible to analyze the fluorescence intensity from each sample well independently (Paper I, Figure 4C, 4D), the very high variability between samples necessitates a more significant number of repeats. From our experience usually more than 30 repeats for one experimental condition would be needed, with at least three biological replicates. Hence, the approach using cumulative, positive wells saves both time and material, while providing sufficient experimental repeatability (Paper I, Figure 4A).

We also tested a new fluorescence dye - tetraphenylethene tethered with triphenylphosphonium (TPE-TPP), which is a structural analog of ThT [364]. TPE-TPP fluorescence yield is higher and can signal early fibrillation processes (Paper I, Figure 2B). The motivation for using this compound was to be able to detect early oligomers forming in the presence and absence of lipid models systems. However, based on our results, TPE-TPP seems also to interact with lipid nanodiscs, which deemed this probe to be unsuitable for lipid:protein interaction experiments (Paper I, Supplementary Figure S2).

4.1.3 α-Synuclein single amino acid affinity evaluation

Solution-state NMR experiments monitoring α-synuclein in the presence of lipids present their own challenges. It has been previously reported that signals from most of the α-synuclein residues keep broadening beyond the limit of detection in the presence of lipids [276,365,366]. This happens due to efficient relaxation pathways related to molecular motions [276]. We expected that lipid nanodiscs would mitigate this issue and that most peaks in the fingerprint would be observable even in the presence of significant amounts of nanodiscs. However, this was not the case, and we observed line broadening beyond detection with an increasing amount of lipid nanodiscs (Paper I, Figure 5A).

Still, we were able to extract some valuable information from collected data. First, it was possible to identify which residues are highly perturbed by the presence of lipids.

Those are residue which signal disappear first, with the lowest amount of lipids. These residues probably interact very strongly with a lipid bilayer (Paper I, Figure 5B). Indeed, all of these "invisible states" correspond with, among other, with non-perfect hexameric repeats KTKEGV and positively charged lysines, i.e. segments with high affinity to lipid environment [220,269,367]. Residues which did not interact with the lipid bilayer could also be observed directly. They are represented by peaks which did not broaden or move with increasing concentration of lipid nanodiscs (Paper I, Figure 5B). Again, this is in line with other reports as most of these residues were localized to C-terminal, which does not seem to interact with the lipid bilayer [213,276].

The rest of these residues are intermediately responsive to the presence of the nanodiscs, and these could be evaluated using the methodology presented by Shortridge *et al.* [368]. Changes in peak area with increasing concentration lipids can be fitted to a binding model (Paper I, Figure 6C) and an affinity constant (K_D) can be calculated for each residue. However, this affinity constant may also contain information about other possible molecular relaxation modes, like the interaction between two molecules of α-synuclein or broadening effects from the dynamic exchange of α-synuclein between the nanodisc and the solvent. Therefore, we treat this as an apparent affinity constant (aK_D), which reflect all changes caused by the presence of the lipid environment. However, it does not have to be only due to the direct binding of residue to the lipids.

4.1.4 Cholesterol and α-synuclein interaction is driven by lipid environment

Cholesterol seems to have a very complex role in α-synuclein behavior in a lipid environment. First, we have observed that cholesterol inhibits binding of α-synuclein with lipid vesicles (Paper I, Figure 3). This effect was similar for both lipid models (DOPC and DOPC:PE:PG), and the presence of 30% cholesterol caused a doubling of K_D in both cases. However, the presence of PE and PG has a more significant effect on α-synuclein than the presence of cholesterol. The K_D of α-synuclein towards DOPC:PE:PG vesicles containing cholesterol was still four-fold lower than for DOPC vesicles without cholesterol. This suggests that tighter packing of lipids, caused by the presence of cholesterol, has a negative impact on the α-synuclein bilayer interaction. However, the presence of anionic lipids (PG) and lipids able to store curvature stress

(PE) is a stronger determinant of α-synuclein affinity, and electrostatic interaction is the dominating force in the binding process. These findings are consistent with the previous reports of the adverse effect of cholesterol on α-synuclein binding [307].

Our next question was: What is the role of cholesterol in α-synuclein fibrillation? We explored this by setting up fibrillation assays monitored by ThT fluorescence in the presence and absence of lipid nanodiscs, with and without cholesterol included (Paper I, Figure 4). We observed that lipid nanodiscs lacking cholesterol cause a delay in α-synuclein fibrillation. For both lipid models, there was an almost three-fold increase in the lag-time, but no changes in fibrillation rate (see section 1.1.1 The oligomerization and seeding properties of amyloid-forming proteins). This suggests that the protein interaction with lipid environment caused an efficient decrease of free monomeric α-synuclein population. This results in slower oligomer formation and slower fibril formation [269,369]. However, when the lipid nanodiscs containing 30% cholesterol were present in the experiments, we observed a rapid increase in fibrillation processes - both lag time and fibrillation rate had been affected. It seems that lipid nanodiscs containing cholesterol could serve as a seeding agent and they can initiate almost immediate fibrillation, reducing lag time from 20 hours to less than an hour. Increase in fibrillation rate ratio shows that lipid nanodiscs containing cholesterol, not only act as a seed, but they can actively promote further growth of amyloid fibrils. Theories about the possible mechanism of actions, including molecular crowding [370] or aligning of NAC sequences [371] are further discussed in Paper I.

Solution NMR revealed that the mechanism of α-synuclein interaction with lipid bilayer containing cholesterol is defined by lipid composition. For the DOPC model, we could see that binding towards lipid is promoted mostly by NAC terminal (Paper I, Figure 6A). For DOPC:PE:PG model the situation is different and the presence of cholesterol is affecting C-terminal and N-terminal of protein (Paper I, Figure 6B). However, in this case, it is repulsion towards lipid bilayer. Cholesterol rich-sites seems to provide NAC-supported binding mode which is fundamentally different from standard N-terminal binding mode supported by high-charge and high-fluidity. The existence of two binding

modes can explain some discrepancy in the literature regarding the role of cholesterol in α-synuclein:lipid interaction.

Taken together our experiment shows that cholesterol inhibits binding of α-synuclein towards lipid bilayer and that it serves as a seeding agent in lipid nanodiscs, promoting faster fibrillation processes. This effect is seemingly independent of the other lipids present. The result is intriguing, as it is suggestive binding modes that are not reflected in standard affinity measurements. However, when examined by residue-specific HSQC NMR, we could see the contrasting difference of α-synuclein behavior. This difference can be explained by the possible existence of two-binding modes, a NAC-supported and an N-terminal supported binding mode.

The N-terminal binding is dominating mode in the presence of anionic lipids, and it leads to typical α-synuclein binding towards lipid bilayer which ends with the formation of α-helix. Further oligomerization is, generally slower because monomeric α-synuclein is localized on lipid bilayer and it is not available for oligomerization. The NAC binding mode is dominating in the presence of lipid bilayers containing cholesterol. In this case, α-synuclein binds towards lipid bilayer preferably by NAC segment. This could lead to different oligomerization pathway, which results in rapid oligomerization and fibrillation processes. The NAC binding could become dominant in case of a local increase of cholesterol concentration in neuronal cells.

4.2 Prokaryote modulate its lipid composition during the cell cycle

In parallel, we set out to established and improve the lipidomics methods available in our laboratory. The methods established should be able to discern changes in lipid profiles and assess whether these changes translated into modulations in physical properties of the membrane. Bacteria are, in general, easier to culture and have simpler lipidomes. Therefore, we aligned this goal with the investigation of the lipid content changes of Gram-positive bacteria during its life cycle. For this work, we selected the bacterial strain *Listeria innocua* NCTC 11288, mainly because it is biologically similar to pathogenic *L. monocytogenes* [372,373] and because it does not sporulate under

stress, unlike another commonly used Gram-positive model, *B. subtilis.* It has also been shown previously that Gram-negative *E. Coli* modulates its lipid composition [370]. This led us to a search for a similar trend in Gram-positive bacteria.

We used the bacteriostatic rifampicin to synchronize bacterial culture at the C/D boundary, just before bacterial division, which was confirmed by measuring the size of the cell (Paper II, Figure 1). Then, we implemented a new modification of the two-phase method of lipid isolation which addresses some shortcomings of other traditional methods [374]. In order to maximize lipid extraction efficiency, we implemented three changes relative to traditional methods: (i) We used triethylammonium ions (TEAC) as a counter-ion for lipid extraction, which is soluble in organic solvents and helps to mitigate migration of phospholipid species into the organic phase. (ii) Methanol, used in traditional lipid isolation methods, was replaced with dichloromethane to minimize lipid degradation. (iii) Before the two-phase isolation procedure, we washed the freeze-dried cell samples with a mixture of organic solvents (dichloromethane, methanol and TEAC). The combination of these measures yielded an isolation efficiency of >99% of total phospholipids (Paper II, Figure S3).

We observed significant modulation of lipid composition in *L. innocua* between C/D period boundary and unsynchronized culture. Most notably was the change in PE, CL and PG content (Paper II, Figure 2). We then investigated the phase behavior of the lipid system with the same composition as unsynchronized *L. innocua* and culture in C/D boundary using solid state (broad line) ^{31}P NMR (Paper II, Figure S7-S10). We observed that these differences were significant enough to represent changes in the physical properties of the lipid membranes as the bacterial moved into the C/D boundary. The reduction of PE content led to a reduction in stored curvature stress of the membrane. This reduction of curvature stress was compensated for by an increase in the PG content which provides an increased fluidity. There was no increase in CL content so the increase in PG can be interpreted as a regulation mechanism to maintain sufficient fluidity of the membrane. The observed changes in physical membrane properties were remarkably similar to lipid changes of the Gram-negative *E. Coli* [375].

The lipid changes during prokaryotic cell cycle present a question whenever also mitochondria do modulate its lipid content throughout its cell cycle and if so how this can affect potential interaction between mitochondria and α-synuclein. This result, as well as other works [376,377], suggests that the lipidome and the resulting properties of the cell membrane may vary significantly depending on the state of the cell.

4.3 Lipid composition of SH-SY5Y

Lastly, we have applied methods developed in Paper II to pursue our third goal: the lipidomics analysis of a neuroblastoma cell line – SH-SY5Y. This cell line is a frequently chosen model when studying neurodegenerative disease, including PD [378,379]. Lipids are implicated pathological factor in PD pathogenesis; however, so far, there is only one a phospholipidomics analysis of this cell model, using only ^{31}P NMR [380]. We have investigated the phospholipid content of a whole cell and plasma membrane fraction of SH-SY5Y using ^{31}P NMR and LC-MS/MS automated analysis.

An important part of this study was focused on developing LC-MS/MS automated fatty analysis. With the help of ^{31}P NMR, we have identified the phospholipid headgroups present in the sample and determined the relative amounts of each associated lipid species present. We have then used LC-MS/MS for detailed FA analysis. However, to be able to analyze a large amount of data obtained we needed to develop a suitable tool. For this, Matlab 2017b was used to build a script which can: (i) build lipid libraries of predicted fragmentations, based on information collected from literature, (ii) assign the signals in collected MS2 spectra to their corresponding precursor lipid and (iii) analyze the FA chain content in the MS1 chromatogram for each phospholipid headgroup (Paper III, Figure 2). This script, named the LipMat script, is available online on GitHub: https://github.com/MarJakubec/LipMat.

We observed several differences between a whole brain lipid content (See the section: 1.6 Neurolipidomics) and SH-SY5Y. The most striking one was the much higher PC (55%), and lower PE abundance (18%, Paper III, Figure 1) found. Also, SM content was much lower making it less abundant species than is generally observed in brain lipid analysis. SM in whole cell sample comprises 3% of the total lipids. However, when the PM was analyzed, it was the third most abundant lipid species with 18% of

abundance. These values reflect that most of the mass of SM in SH-SY5Y is present in the PM (Paper III, Figure 3). FA analysis showed that PC had the most uniform FA distribution (~75% of all PC lipids was composed of only one of the four types of FA chains detected). PE FAs were seemingly also non-variable in the same manner in a whole cell sample, and almost 90% of observed PE lipid species had one of the three detected FA. However, in the PM fraction, we observed for PE a much broader variety of FA chains that also contained long unsaturated chains (22:6 and 20:4). This FA distribution suggests that PE in the PM can act as one of the primary stores of curvature stress. Meanwhile, in the whole-cell sample, this role is performed by other conical lipid species with longer FA chains, like PG.

It is clear that the lipid composition of SH-SY5Y cell is different from generic models of cell lipid compositions, nor is it similar to a mean of brain lipid composition. This has to be taken into account in any further research which are focused on the role of lipids in neurodegenerative amyloid diseases and which are using SH-SY5Y as a model cell culture.

5 Concluding remarks and future perspectives

In this thesis, we have presented our current work in the amyloid protein:lipid interaction field. In Paper I we worked on establishing and improving several methods used to study amyloid protein and lipid interaction, which included SMA lipid nanodiscs, fibrillization assays and determination of residue specific apparent affinities by NMR. We applied these methods in the investigation of the role of cholesterol in α-synuclein affinity towards lipid bilayer and its fibrillation, and managed to link local affinities within the α-synuclein to the prescence of cholesterol and promotion of fibrillation. In Paper II we established a suite of lipidomics tools in the lab where the project took place, where no such tools existed beforehand. In some cases, it has also been possible to improve on current methodologies in the field, including reaching high lipid extraction efficiencies and better control of enzymatic lipid degradation. These tools have been tested on prokaryotic *L. innocua*. In Paper III we have used these tools for lipidomics analysis of SH-SY5Y neuroblastoma cell line, and we have developed an automated Matlab script for mass spectrometry analysis of FA chain abundance.

Taken together we are left with more questions than answers. Further research will aim to elucidate some of these questions, including: Is two-mode binding of α-synuclein towards the lipid membrane biologically relevant? If prokaryotic cells modulate its lipid content during cell growth does the same modulation happens in mitochondria and could these mitochondrial lipid changes affect the progress of PD? Does the lipid composition of SH-SY5Y cell correspond to a standard or abnormal neuronal cell? Which specific lipid species do α-synuclein come into contact with in neurons? What is the subcellular SH-SY5Y lipid distribution?

Our next experimental work will aim to answer some of these questions. We are currently working on a further improved PM isolation protocol which will allow us to obtain higher lipid mass and, hopefully, to observe also minor phospholipid species by ^{31}P NMR. We are also currently working on a suitable protocol which allows us simultaneously to perform phospholipidomics analysis and quantitative analysis of cholesterol in different compartments of SH-SY5Y cells. This new lipidomics information can then be used to build suitable lipid models which can be used for

relevant *in-vitro* testing of αsynuclein behavior in different lipid environment. It may also be possible to prepare nanodisc directly from live cell membranes instead of artificial vesciles, use these in oligomerization assays and in this way link further research on membrane component triggers more directly to *in vivo* situations.

6 References

[1] V.N. Uversky, A decade and a half of protein intrinsic disorder: Biology still waits for physics, Protein Sci. 22 (2013) 693–724. doi:10.1002/pro.2261.

[2] V. Receveur-Bréhot, J.M. Bourhis, V.N. Uversky, B. Canard, S. Longhi, Assessing protein disorder and induced folding, Proteins Struct. Funct. Genet. 62 (2006) 24–45. doi:10.1002/prot.20750.

[3] T.R. Jahn, S.E. Radford, The Yin and Yang of protein folding, FEBS J. 272 (2005) 5962–5970. doi:10.1111/j.1742-4658.2005.05021.x.

[4] F. Chiti, C.M. Dobson, Protein Misfolding, Amyloid Formation, and Human Disease: A Summary of Progress Over the Last Decade, Annu. Rev. Biochem. 86 (2017) 27–68. doi:10.1146/annurev-biochem-061516-045115.

[5] A. Goate, M.C. Chartier-Harlin, M. Mullan, J. Brown, F. Crawford, L. Fidani, L. Giuffra, A. Haynes, N. Irving, L. James, R. Mant, P. Newton, K. Rooke, P. Roques, C. Talbot, M. Pericak-Vance, A. Roses, R. Williamson, M. Rossor, M. Owen, J. Hardy, Segregation of a missense mutation in the amyloid precursor protein gene with familial Alzheimer's disease, Nature. 349 (1991) 704–706. doi:10.1038/349704a0.

[6] S.G. van Duinen, E.M. Castano, F. Prelli, G.T. Bots, W. Luyendijk, B. Frangione, Hereditary cerebral hemorrhage with amyloidosis in patients of Dutch origin is related to Alzheimer disease., Proc. Natl. Acad. Sci. 84 (1987) 5991–5994. doi:10.1073/pnas.84.16.5991.

[7] J.J. Zarranz, J. Alegre, J.C. Gómez-Esteban, E. Lezcano, R. Ros, I. Ampuero, L. Vidal, J. Hoenicka, O. Rodriguez, B. Atarés, V. Llorens, E. Gomez Tortosa, T. Del Ser, D.G. Muñoz, J.G. De Yebenes, The New Mutation, E46K, of α-Synuclein Causes Parkinson and Lewy Body Dementia, Ann. Neurol. 55 (2004) 164–173. doi:10.1002/ana.10795.

[8] L. V Kalia, A.E. Lang, Parkinson's disease, Lancet. 386 (2015) 896–912. doi:10.1016/S0140-6736(14)61393-3.

[9] M.G. Spillantini, M.L. Schmidt, V.M.-Y. Lee, J.Q. Trojanowski, R. Jakes, M. Goedert, α-synuclein in Lewy bodies, Nature. 388 (1997) 839–840. doi:10.1038/42166.

[10] G.A. Wells, A.C. Scott, C.T. Johnson, R.F. Gunning, R.D. Hancock, M. Jeffrey, M. Dawson, R. Bradley, A novel progressive spongiform encephalopathy in cattle., Vet. Rec. 121 (1987) 419–420. doi:10.1136/vr.121.18.419.

[11] R.G. Will, J.W. Ironside, M. Zeidler, S.N. Cousens, K. Estibeiro, A. Alperovitch, S. Poser, M. Pocchiari, A. Hofmar, P.G. Smith, A new variant of Creutzfeldt-Jakob disease in the UK, Lancet. 347 (1996) 921–925. doi:10.1016/S0140-6736(96)91412-9.

[12] S.B. Prusiner, Nobel Lecture: Prions, Proc. Natl. Acad. Sci. 95 (1998) 13363–13383. doi:10.1073/pnas.95.23.13363.

[13] V.M.-Y. Lee, M. Goedert, J.Q. Trojanowski, Neurodegenerative Tauopathies, Annu. Rev. Neurosci. 24 (2001) 1121–1159. doi:10.1146/annurev.neuro.24.1.1121.

[14] M. Hutton, C.L. Lendon, P. Rizzu, M. Baker, S. Froelich, H.H. Houlden, S. Pickering-Brown, S. Chakraverty, A. Isaacs, A. Grover, J. Hackett, J. Adamson, S. Lincoln, D. Dickson, P. Davies, R.C. Petersen, M. Stevena, E. De Graaff, E. Wauters, J. Van Baren, M. Hillebrand, M. Joosse, J.M. Kwon, P. Nowotny, L.K. Che, J. Norton, J.C. Morris, L.A. Reed, J. Trojanowski, H. Basun, L. Lannfelt, M. Neystat, S. Fahn, F. Dark, T. Tannenberg, P.R. Dodd, N. Hayward, J.B.J. Kwok, P.R. Schofield, A. Andreadis, J. Snowden, D. Craufurd, D. Neary, F. Owen, B.A. Costra, J. Hardy, A. Goate, J. Van Swieten, D. Mann, T. Lynch, P. Heutink, Association of missense and 5'-splice-site mutations in tau with the inherited dementia FTDP-17, Nature. 393 (1998) 702–704. doi:10.1038/31508.

[15] D. Neary, J.S. Snowden, L. Gustafson, U. Passant, D. Stuss, S. Black, M. Freedman, A. Kertesz, P.H. Robert, M. Albert, K. Boone, B.L. Miller, J. Cummings, D.F. Benson, Frontotemporal lobar degeneration: A consensus on clinical diagnostic criteria, Neurology. 51 (1998) 1546–1554. doi:10.1212/WNL.51.6.1546.

[16] M. DiFiglia, E. Sapp, K.O. Chase, S.W. Davies, G.P. Bates, J.P. Vonsattel, N. Aronin, Aggregation of huntingtin in neuronal intranuclear inclusions and dystrophic neurites in brain, Science (80-.). 277 (1997) 1990–1993. doi:10.1126/science.277.5334.1990.

[17] M.H. Baumann, T. Wisniewski, E. Levy, G.T. Plant, J. Ghiso, C-terminal fragments of α-and β-tubulin form amyloid fibrils in vitro and associate with amyloid deposits of familial cerebral amyloid angiopathy, British type, Biochem. Biophys. Res. Commun. 219 (1996) 238–242. doi:10.1006/bbrc.1996.0211.

[18] R. Vidal, T. Revesz, A. Rostagno, E. Kim, J.L. Holton, T. Bek, M. Bojsen-Moller, H. Braendgaard, G. Plant, J. Ghiso, B. Frangione, A decamer duplication in the 3' region of the BRI gene originates an amyloid peptide that is associated with dementia in a Danish kindred, Proc. Natl. Acad. Sci. 97 (2000) 4920–4925. doi:10.1073/pnas.080076097.

[19] T.P.J. Knowles, M. Vendruscolo, C.M. Dobson, The amyloid state and its association with protein misfolding diseases, Nat. Rev. Mol. Cell Biol. 15 (2014) 384–396. doi:10.1038/nrm3810.

[20] J.D. Harper, P.T. Lansbury, MODELS OF AMYLOID SEEDING IN ALZHEIMER'S DISEASE AND SCRAPIE:Mechanistic Truths and Physiological Consequences of the Time-Dependent Solubility of Amyloid Proteins, Annu. Rev. Biochem. 66 (1997) 385–407. doi:10.1146/annurev.biochem.66.1.385.

[21] A.M. Morris, M.A. Watzky, J.N. Agar, R.G. Finke, Fitting neurological protein aggregation kinetic data via a 2-step, minimal/"Ockham's razor" model: The Finke-Watzky mechanism of nucleation followed by autocatalytic surface growth, Biochemistry. 47 (2008) 2413–2427. doi:10.1021/bi701899y.

[22] M. Biancalana, S. Koide, Molecular mechanism of Thioflavin-T binding to amyloid fibrils, Biochim. Biophys. Acta - Proteins Proteomics. 1804 (2010) 1405–1412. doi:10.1016/j.bbapap.2010.04.001.

[23] T.R. Serio, A.G. Cashikar, A.S. Kowal, G.J. Sawicki, J.J. Moslehi, L. Serpell, M.F. Arnsdorf, S.L. Lindquist, Nucleated conformational conversion and the replication of conformational information by a prion determinant, Science (80-.). 289 (2000) 1317–1321. doi:10.1126/science.289.5483.1317.

[24] E.K. Kumar, N. Haque, N.P. Prabhu, Kinetics of protein fibril formation: Methods and mechanisms, Int. J. Biol. Macromol. 100 (2017) 3–10. doi:10.1016/j.ijbiomac.2016.06.052.

[25] I.A. Iashchishyn, D. Sulskis, M. Nguyen Ngoc, V. Smirnovas, L.A. Morozova-Roche, Finke-Watzky Two-Step Nucleation-Autocatalysis Model of S100A9 Amyloid Formation: Protein Misfolding as "nucleation" Event, ACS Chem. Neurosci. 8 (2017) 2152–2158. doi:10.1021/acschemneuro.7b00251.

[26] A.K. Paravastu, R.D. Leapman, W.-M. Yau, R. Tycko, Molecular structural basis for polymorphism in Alzheimer's -amyloid fibrils, Proc. Natl. Acad. Sci. 105 (2008) 18349–18354. doi:10.1073/pnas.0806270105.

[27] C. Wasmer, A. Lange, H. Van Melckebeke, A.B. Siemer, R. Riek, B.H. Meier, Amyloid fibrils of the HET-s(218-289) prion form a β solenoid with a triangular hydrophobic core, Science (80-.). 319 (2008) 1523–1526. doi:10.1126/science.1151839.

[28] M. SUNDE, C. BLAKE, The Structure of Amyloid Fibrils by Electron Microscopy and X-Ray Diffraction, in: Adv. Protein Chem. Vol. 50, 1997: pp. 123–159. doi:10.1016/S0065-3233(08)60320-4.

[29] G. Zandomeneghi, M.R.H. Krebs, M.G. McCammon, M. Fändrich, FTIR reveals structural differences between native β-sheet proteins and amyloid fibrils, Protein Sci. 13 (2009) 3314–3321. doi:10.1110/ps.041024904.

[30] R. Kayed, E. Head, J.L. Thompson, T.M. McIntire, S.C. Milton, C.W. Cotman, C.G. Glabel, Common structure of soluble amyloid oligomers implies common mechanism of pathogenesis, Science (80-.). 300 (2003) 486–489. doi:10.1126/science.1079469.

[31] E. Kuusisto, L. Parkkinen, I. Alafuzoff, Morphogenesis of Lewy bodies: Dissimilar incorporation of alpha-synuclein, ubiquitin, and p62, J. Neuropathol. Exp. Neurol. 62 (2003) 1241–1253. %3CGo.

[32] M.I. Papp, J.E. Kahn, P.L. Lantos, Glial cytoplasmic inclusions in the CNS of patients with multiple system atrophy (striatonigral degeneration, olivopontocerebellar atrophy and Shy-Drager syndrome), J. Neurol. Sci. 94 (1989) 79–100. doi:10.1016/0022-510X(89)90219-0.

[33] W.A. Rutala, D.J. Weber, Creutzfeldt-Jakob disease: recommendations for disinfection and sterilization., Clin. Infect. Dis. 32 (2001) 1348–1356. doi:10.1086/319997.

[34] T.P. Knowles, A.W. Fitzpatrick, S. Meehan, H.R. Mott, M. Vendruscolo, C.M. Dobson, M.E. Welland, Role of intermolecular forces in defining material properties of protein nanofibrils, Science (80-.). 318 (2007) 1900–1903. doi:10.1126/science.1150057.

[35] Y. Zhou, L.P. Blanco, D.R. Smith, M.R. Chapman, Bacterial amyloids, Methods Mol. Biol. 849 (2012) 303–320. doi:10.1007/978-1-61779-551-0_21.

[36] T. Scheibel, R. Parthasarathy, G. Sawicki, X.-M. Lin, H. Jaeger, S.L. Lindquist, Conducting nanowires built by controlled self-assembly of amyloid fibers and selective metal deposition, Proc. Natl. Acad. Sci. 100 (2003) 4527–4532. doi:10.1073/pnas.0431081100.

[37] S. Bolisetty, R. Mezzenga, Amyloid-carbon hybrid membranes for universal water purification, Nat. Nanotechnol. 11 (2016) 365–371. doi:10.1038/nnano.2015.310.

[38] J. Zhao, Y. Qu, H. Chen, R. Xu, Q. Yu, P. Yang, Self-assembled proteinaceous wound dressings attenuate secondary trauma and improve wound healing in vivo, J. Mater. Chem. B. 6 (2018) 4645–4655. doi:10.1039/c8tb01100a.

[39] A. Aguzzi, A.M. Calella, Prions: Protein Aggregation and Infectious Diseases, Physiol. Rev. 89 (2009) 1105–1152. doi:10.1152/physrev.00006.2009.

[40] C. Lacroux, E. Comoy, M. Moudjou, A. Perret-Liaudet, S. Lugan, C. Litaise, H. Simmons, C. Jas-Duval, I. Lantier, V. Beringue, M. Groschup, G. Fichet, P. Costes, N. Streichenberger, F. Lantier, J.P. Deslys, D. Vilette, O. Andreoletti, Preclinical Detection of Variant CJD and BSE Prions in Blood, Plos Pathog. 10 (2014). doi:10.1371/journal.ppat.1004202.

[41] M. Meyer-Luehmann, J. Coomaraswamy, T. Bolmont, S. Kaeser, C. Schaefer, E. Kilger, A. Neuenschwander, D. Abramowski, P. Frey, A.L. Jaton, J.M. Vigouret, P. Paganetti, D.M. Walsh, P.M. Mathews, J. Ghiso, M. Staufenbiel, L.C. Walker, M. Jucker, Exogenous induction of cerebral β-amyloidogenesis is governed by agent and host, Science (80-.). 313 (2006) 1781–1784. doi:10.1126/science.1131864.

[42] M.D. Kane, W.J. Lipinski, M.J. Callahan, F. Bian, R.A. Durham, R.D. Schwarz, A.E. Roher, L.C. Walker, Evidence for seeding of beta -amyloid by intracerebral infusion of Alzheimer brain extracts in beta -amyloid precursor protein-transgenic mice., J. Neurosci. 20 (2000) 3606–11. doi:20/10/3606 [pii].

[43] M. Jucker, L.C. Walker, Pathogenic protein seeding in Alzheimer disease and other neurodegenerative disorders, Ann. Neurol. 70 (2011) 532–540. doi:10.1002/ana.22615.

[44] T. Hamaguchi, Y.S. Eisele, N.H. Varvel, B.T. Lamb, L.C. Walker, M. Jucker, The presence of Aβ seeds, and not age per se, is critical to the initiation of Aβ deposition in the brain, Acta Neuropathol. 123 (2012) 31–37. doi:10.1007/s00401-011-0912-1.

[45] F. Clavaguera, T. Bolmont, R.A. Crowther, D. Abramowski, S. Frank, A. Probst, G. Fraser, A.K. Stalder, M. Beibel, M. Staufenbiel, M. Jucker, M. Goedert, M. Tolnay, Transmission and spreading of tauopathy in transgenic mouse brain, Nat. Cell Biol. 11 (2009) 909–913. doi:10.1038/ncb1901.

[46] C.A. Lasagna-Reeves, D.L. Castillo-Carranza, U. Sengupta, M.J. Guerrero-Munoz, T. Kiritoshi, V. Neugebauer, G.R. Jackson, R. Kayed, Alzheimer brain-derived tau oligomers propagate pathology from endogenous tau, Sci. Rep. 2 (2012) 700. doi:10.1038/srep00700.

[47] F. Clavaguera, H. Akatsu, G. Fraser, R.A. Crowther, S. Frank, J. Hench, A. Probst, D.T. Winkler, J. Reichwald, M. Staufenbiel, B. Ghetti, M. Goedert, M. Tolnay, Brain homogenates from human tauopathies induce tau inclusions in mouse brain, Proc. Natl. Acad. Sci. 110 (2013) 9535–9540. doi:10.1073/pnas.1301175110.

[48] J.H. Kordower, Y. Chu, R.A. Hauser, T.B. Freeman, C.W. Olanow, Lewy body-like pathology in long-term embryonic nigral transplants in Parkinson's disease, Nat. Med. 14 (2008) 504–506. doi:10.1038/nm1747.

[49] J.Y. Li, E. Englund, J.L. Holton, D. Soulet, P. Hagell, A.J. Lees, T. Lashley, N.P. Quinn, S. Rehncrona, A. Björklund, H. Widner, T. Revesz, O. Lindvall, P. Brundin, Lewy bodies in grafted neurons in subjects with Parkinson's disease suggest host-to-graft disease propagation, Nat. Med. 14 (2008) 501–503. doi:10.1038/nm1746.

[50] C. Hansen, E. Angot, A.L. Bergström, J.A. Steiner, L. Pieri, G. Paul, T.F. Outeiro, R. Melki, P. Kallunki, K. Fog, J.Y. Li, P. Brundin, α-Synuclein propagates from mouse brain to grafted dopaminergic neurons and seeds aggregation in cultured human cells, J. Clin. Invest. 121 (2011) 715–725. doi:10.1172/JCI43366.

[51] J.H. Kordower, H.B. Dodiya, A.M. Kordower, B. Terpstra, K. Paumier, L. Madhavan, C. Sortwell, K. Steece-Collier, T.J. Collier, Transfer of host-derived alpha synuclein to grafted dopaminergic neurons in rat, Neurobiol. Dis. 43 (2011) 552–557. doi:10.1016/j.nbd.2011.05.001.

[52] L.A. Volpicelli-Daley, K.C. Luk, T.P. Patel, S.A. Tanik, D.M. Riddle, A. Stieber, D.F. Meaney, J.Q. Trojanowski, V.M.-Y. Lee, Exogenous α-Synuclein Fibrils Induce Lewy Body Pathology Leading to Synaptic Dysfunction and Neuron Death, Neuron. 72 (2011) 57–71. doi:10.1016/j.neuron.2011.08.033.

[53] P. Desplats, H.-J. Lee, E.-J. Bae, C. Patrick, E. Rockenstein, L. Crews, B. Spencer, E. Masliah, S.-J. Lee, Inclusion formation and neuronal cell death through neuron-to-neuron transmission of α-synuclein, Proc. Natl. Acad. Sci. 106 (2009) 13010–13015. doi:10.1073/pnas.0903691106.

[54] A.L. Mougenot, S. Nicot, A. Bencsik, E. Morignat, J. Verchère, L. Lakhdar, S. Legastelois, T. Baron, Prion-like acceleration of a synucleinopathy in a transgenic mouse model, Neurobiol. Aging. 33 (2012) 2225–2228. doi:10.1016/j.neurobiolaging.2011.06.022.

[55] K.C. Luk, V.M. Kehm, B. Zhang, P. O'Brien, J.Q. Trojanowski, V.M.Y. Lee, Intracerebral inoculation of pathological α-synuclein initiates a rapidly progressive neurodegenerative α-synucleinopathy in mice, J. Exp. Med. 209 (2012) 975–986. doi:10.1084/jem.20112457.

[56] K.C. Luk, V. Kehm, J. Carroll, B. Zhang, P. O'Brien, J.Q. Trojanowski, V.M.Y. Lee, Pathological α-synuclein transmission initiates Parkinson-like neurodegeneration in nontransgenic mice, Science (80-.). 338 (2012) 949–953. doi:10.1126/science.1227157.

[57] M. Masuda-Suzukake, T. Nonaka, M. Hosokawa, T. Oikawa, T. Arai, H. Akiyama, D.M.A. Mann, M. Hasegawa, Prion-like spreading of pathological α-synuclein in brain, Brain. 136 (2013) 1128–1138. doi:10.1093/brain/awt037.

[58] B.R. Groveman, C.D. Orrù, A.G. Hughson, L.D. Raymond, G. Zanusso, B. Ghetti, K.J. Campbell, J. Safar, D. Galasko, B. Caughey, Rapid and ultra-sensitive quantitation of disease-associated α-synuclein seeds in brain and cerebrospinal fluid by αSyn RT-QuIC, Acta Neuropathol. Commun. 6 (2018) 7. doi:10.1186/s40478-018-0508-2.

[59] S.M. Butterfield, H.A. Lashuel, Amyloidogenic protein-membrane interactions: Mechanistic insight from model systems, Angew. Chemie - Int. Ed. 49 (2010) 5628–5654. doi:10.1002/anie.200906670.

[60] E.J. Jo, J. McLaurin, C.M. Yip, P. St George-Hyslop, P.E. Fraser, alpha-synuclein membrane interactions and lipid specificity, J. Biol. Chem. 275 (2000) 34328–34334. doi:10.1074/jbc.M004345200.

[61] A. Kakio, S. Nishimoto, K. Yanagisawa, Y. Kozutsumi, K. Matsuzaki, Cholesterol-dependent formation of GM1 ganglioside-bound amyloid beta-protein, an endogenous seed for Alzheimer amyloid, J. Biol. Chem. 276 (2001) 24985–24990. doi:10.1074/jbc.M100252200.

[62] K. Yanagisawa, A. Odaka, N. Suzuki, Y. Ihara, GM1 ganglioside–bound amyloid β–protein (Aβ): A possible form of preamyloid in Alzheimer's disease, Nat. Med. 1 (1995) 1062–1066. doi:10.1038/nm1095-1062.

[63] K. Matsuzaki, K. Kato, K. Yanagisawa, Aβ polymerization through interaction with membrane gangliosides, Biochim. Biophys. Acta - Mol. Cell Biol. Lipids. 1801 (2010) 868–877. doi:10.1016/j.bbalip.2010.01.008.

[64] A. Kakio, S. ichi Nishimoto, K. Yanagisawa, Y. Kozutsumi, K. Matsuzaki, Interactions of amyloid β-protein with various gangliosides in raft-like membranes: Importance of GM1 ganglioside-bound form as an endogenous seed for Alzheimer amyloid, Biochemistry. 41 (2002) 7385–7390. doi:10.1021/bi0255874.

[65] K. Ikeda, T. Yamaguchi, S. Fukunaga, M. Hoshino, K. Matsuzaki, Mechanism of amyloid β-protein aggregation mediated by GM1 ganglioside clusters, Biochemistry. 50 (2011) 6433–6440. doi:10.1021/bi200771m.

[66] P. Marie-claude, H. Linda, M. Catherine, Cholesterol and ApoE in Alzheimer's disease, OCL. 25 (2018) D407. doi:10.1051/ocl/2018038.

[67] H. Jang, L. Connelly, F.T. Arce, S. Ramachandran, R. Lal, B.L. Kagan, R. Nussinov, Alzheimer's disease: Which type of amyloid-preventing drug agents to employ?, Phys. Chem. Chem. Phys. 15 (2013) 8868–8877. doi:10.1039/c3cp00017f.

[68] S.A. Kotler, P. Walsh, J.R. Brender, A. Ramamoorthy, Differences between amyloid-β aggregation in solution and on the membrane: Insights into elucidation of the mechanistic details of Alzheimer's disease, Chem. Soc. Rev. 43 (2014) 6692–6700. doi:10.1039/c3cs60431d.

[69] N. Stahl, D.R. Borchelt, K. Hsiao, S.B. Prusiner, Scrapie prion protein contains a phosphatidylinositol glycolipid, Cell. 51 (1987) 229–240. doi:10.1016/0092-8674(87)90150-4.

[70] B.M. Coleman, C.F. Harrison, B. Guo, C.L. Masters, K.J. Barnham, V.A. Lawson, A.F. Hill, B.W. Caughey, Pathogenic Mutations within the Hydrophobic Domain of the Prion Protein Lead to the Formation of Protease-Sensitive Prion Species with Increased Lethality, J. Virol. 88 (2014) 2690–2703. doi:10.1128/JVI.02720-13.

[71] H.E. Radford, G.R. Mallucci, The role of GPI-anchored PrPC in mediating the neurotoxic effect of scrapie prions in neurons, Curr. Issues Mol. Biol. 12 (2010) 119–128. doi:v12/119 [pii].

[72] J. Singh, A.T. Sabareesan, M.K. Mathew, J.B. Udgaonkar, Development of the structural core and of conformational heterogeneity during the conversion of oligomers of the mouse prion protein to worm-like amyloid fibrils, J. Mol. Biol. 423 (2012) 217–231. doi:10.1016/j.jmb.2012.06.040.

[73] A.T. Sabareesan, J. Singh, S. Roy, J.B. Udgaonkar, M.K. Mathew, The pathogenic A116V mutation enhances ion-selective channel formation by prion protein in membranes, Biophys. J. 110 (2016) 1766–1776. doi:10.1016/j.bpj.2016.03.017.

[74] B. Caughey, G.S. Baron, B. Chesebro, M. Jeffrey, Getting a Grip on Prions: Oligomers, Amyloids, and Pathological Membrane Interactions, Annu. Rev. Biochem. 78 (2009) 177–204. doi:10.1146/annurev.biochem.78.082907.145410.

[75] X. Wang, F. Wang, L. Arterburn, R. Wollmann, J. Ma, The interaction between cytoplasmic prion protein and the hydrophobic lipid core of membrane correlates with neurotoxicity, J. Biol. Chem. 281 (2006) 13559–13565. doi:10.1074/jbc.M512306200.

[76] J. Singh, H. Kumar, A.T. Sabareesan, J.B. Udgaonkar, Rational stabilization of helix 2 of the prion protein prevents its misfolding and oligomerization, J. Am. Chem. Soc. 136 (2014) 16704–16707. doi:10.1021/ja510964t.

[77] D. Sarnataro, S. Paladino, V. Campana, J. Grassi, L. Nitsch, C. Zurzolo, PrPC is sorted to the basolateral membrane of epithelial cells independently of its association with rafts, Traffic. 3 (2002) 810–821. doi:10.1034/j.1600-0854.2002.31106.x.

[78] N. Naslavsky, R. Stein, A. Yanai, G. Friedlander, A. Taraboulos, Characterization of detergent-insoluble complexes containing the cellular prion protein and its scrapie isoform, J. Biol. Chem. 272 (1997) 6324–6331. doi:10.1074/jbc.272.10.6324.

[79] A. Taraboulos, A.J. Raeber, D.R. Borchelt, D. Serban, S.B. Prusiner, Synthesis and trafficking of prion proteins in cultured cells., Mol. Biol. Cell. 3 (1992) 851–63. doi:066/21.

[80] D. Sarnataro, A. Caputo, P. Casanova, C. Puri, S. Paladino, S.S. Tivodar, V. Campana, C. Tacchetti, C. Zurzolo, Lipid rafts and clathrin cooperate in the internalization of PrPC in epithelial FRT cells, PLoS One. 4 (2009) e5829. doi:10.1371/journal.pone.0005829.

[81] D. Sarnataro, V. Campana, S. Paladino, M. Stornaiuolo, L. Nitsch, C. Zurzolo, PrP(C) association with lipid rafts in the early secretory pathway stabilizes its cellular conformation., Mol. Biol. Cell. 15 (2004) 4031–42. doi:10.1091/mbc.e03-05-0271.

[82] E.M. Jones, M. Dubey, P.J. Camp, B.C. Vernon, J. Biernat, E. Mandelkow, J. Majewski, E.Y. Chi, Interaction of Tau protein with model lipid membranes induces tau structural compaction and membrane disruption, Biochemistry. 51 (2012) 2539–2550. doi:10.1021/bi201857v.

[83] S.S. Dicke, L. Tatge, P.E. Engen, M. Culp, L.R. Masterson, Isothermal titration calorimetry and vesicle leakage assays highlight the differential behaviors of tau repeat segments upon interaction with anionic lipid membranes, Biochem. Biophys. Res. Commun. 493 (2017) 1504–1509. doi:10.1016/j.bbrc.2017.10.007.

[84] J. Parkinson, An Essay on the Shaking Palsy - 1817, J. Neuropsychiatry Clin. Neurosci. 14 (2002) 223–236. doi:10.1176/jnp.14.2.223.

[85] M.H. Polymeropoulos, C. Lavedan, E. Leroy, S.E. Ide, A. Dehejia, A. Dutra, B. Pike, H. Root, J. Rubenstein, R. Boyer, E.S. Stenroos, S. Chandrasekharappa, A. Athanassiadou, T. Papapetropoulos, W.G. Johnson, A.M. Lazzarini, R.C. Duvoisin, G. Di Iorio, L.I. Golbe, R.L. Nussbaum, Mutation in the α-synuclein gene identified in families with Parkinson's disease, Science (80-.). 276 (1997) 2045–2047. doi:10.1126/science.276.5321.2045.

[86] B. Winner, R. Jappelli, S.K. Maji, P.A. Desplats, L. Boyer, S. Aigner, C. Hetzer, T. Loher, M. Vilar, S. Campioni, C. Tzitzilonis, A. Soragni, S. Jessberger, H. Mira, A. Consiglio, E. Pham, E.

Masliah, F.H. Gage, R. Riek, In vivo demonstration that alpha-synuclein oligomers are toxic, Proc. Natl. Acad. Sci. U. S. A. 108 (2011) 4194–4199. doi:10.1073/pnas.1100976108.

[87] L.M. de Lau, M.M. Breteler, Epidemiology of Parkinson's disease, Lancet Neurol. 5 (2006) 525–535. doi:10.1016/S1474-4422(06)70471-9.

[88] C. Sahin, L. Kjær, M.S. Christensen, J. Pedersen, G. Christiansen, A.M.W. Pérez, I.M. Møller, J.J. Enghild, J.S. Pedersen, K. Larsen, D.E. Otzen, α-Synucleins from Animal Species Show Low Fibrillation Propensities and Weak Oligomer Membrane Disruption, Biochemistry. 57 (2018) 5145–5158. doi:10.1021/acs.biochem.8b00627.

[89] R. Jakes, M.G. Spillantini, M. Goedert, Identification of two distinct synucleins from human brain, FEBS Lett. 345 (1994) 27–32. doi:10.1016/0014-5793(94)00395-5.

[90] K. Ueda, H. Fukushima, E. Masliah, Y. Xia, A. Iwai, M. Yoshimoto, D.A. Otero, J. Kondo, Y. Ihara, T. Saitoh, Molecular cloning of cDNA encoding an unrecognized component of amyloid in Alzheimer disease., Proc. Natl. Acad. Sci. 90 (1993) 11282–11286. doi:10.1073/pnas.90.23.11282.

[91] M. Hashimoto, M. Yoshimoto, A. Sisk, L.J. Hsu, M. Sundsmo, A. Kittel, T. Saitoh, A. Miller, E. Masliah, NACP, a synaptic protein involved in Alzheimer's disease, is differentially regulated during megakaryocyte differentiation, Biochem. Biophys. Res. Commun. 237 (1997) 611–616. doi:10.1006/bbrc.1997.6978.

[92] V. Askanas, W.K. Engel, R.B. Alvarez, J. McFerrin, A. Broccolini, Novel immunolocalization of α-synuclein in human muscle of inclusion- body myositis, regenerating and necrotic muscle fibers, and at neuromuscular junctions, J. Neuropathol. Exp. Neurol. 59 (2000) 592–598. doi:10.1093/jnen/59.7.592.

[93] E.C. Shin, S.E. Cho, D.-K. Lee, M.-W. Hur, S.R. Paik, J.H. Park, J. Kim, Expression Patterns of α-Synuclein in Human Hematopoietic Cells and in Drosophila at Different Developmental Stages, Mol. Cells. 10 (2000) 65–70. doi:10.1007/s10059-000-0065-x.

[94] Q.-X. Li, B.C.V. Campbell, C.A. McLean, D. Thyagarajan, W.-P. Gai, R.M. Kapsa, K. Beyreuther, C.L. Masters, J.G. Culvenor, Platelet α- and γ-synucleins in Parkinson's disease and normal control subjects, J. Alzheimer's Dis. 4 (2002) 309–315. doi:10.3233/JAD-2002-4406.

[95] W. Tamo, T. Imaizumi, K. Tanji, H. Yoshida, F. Mori, M. Yoshimoto, H. Takahashi, I. Fukuda, K. Wakabayashi, K. Satoh, Expression of α-synuclein, the precursor of non-amyloid β component of Alzheimer's disease amyloid, in human cerebral blood vessels, Neurosci. Lett. 326 (2002) 5–8. doi:10.1016/S0304-3940(02)00297-5.

[96] S. Kim, B.S. Jeon, C. Heo, P.S. Im, T.B. Ahn, J.H. Seo, H.S. Kim, C.H. Park, S.H. Choi, S.H. Cho, W.J. Lee, Y.H. Suh, Alpha-synuclein induces apoptosis by altered expression in human peripheral lymphocyte in Parkinson's disease, Faseb J. 18 (2004) 1615–1617. doi:10.1096/fj.04-1917fje.

[97] S. Baltic, M. Perovic, A. Mladenovic, N. Raicevic, S. Ruzdijic, L. Rakic, S. Kanazir, α-synuclein is expressed in different tissues during human fetal development, J. Mol. Neurosci. 22 (2004) 199–203. doi:10.1385/JMN:22:3:199.

[98] M. Nakai, M. Fujita, M. Waragai, S. Sugama, J. Wei, H. Akatsu, C. Ohtaka-Maruyama, H. Okado, M. Hashimoto, Expression of α-synuclein, a presynaptic protein implicated in Parkinson's disease, in erythropoietic lineage, Biochem. Biophys. Res. Commun. 358 (2007) 104–110. doi:10.1016/j.bbrc.2007.04.108.

[99] T.A. Bayer, P. Jäkälä, T. Hartmann, R. Egensperger, R. Buslei, P. Falkai, K. Beyreuther, Neural expression profile of α-synuclein in developing human cortex, Neuroreport. 10 (1999) 2799–2803. doi:10.1097/00001756-199909090-00019.

[100] J.E. Galvin, T.M. Schuck, V.M.-Y. Lee, J.Q. Trojanowski, Differential expression and distribution of α-, β-, and γ-synuclein in the developing human substantia nigra, Exp. Neurol. 168 (2001) 347–355. doi:10.1006/exnr.2000.7615.

[101] G.S. Withers, J.M. George, G.A. Banker, D.F. Clayton, Delayed localization of synelfin (synuclein, NACP) to presynaptic terminals in cultured rat hippocampal neurons, Dev. Brain Res. 99 (1997) 87–94. doi:10.1016/S0165-3806(96)00210-6.

[102] L. Maroteaux, J.T. Campanelli, R.H. Scheller, Synuclein: a neuron-specific protein localized to the nucleus and presynaptic nerve terminal., J. Neurosci. 8 (1988) 2804–2815. doi:10.1523/JNEUROSCI.08-08-02804.1988.

[103] J. Burré, The synaptic function of α-synuclein, J. Parkinsons. Dis. 5 (2015) 699–713. doi:10.3233/JPD-150642.

[104] J. Burré, M. Sharma, T. Tsetsenis, V. Buchman, M.R. Etherton, T.C. Südhof, α-Synuclein promotes SNARE-complex assembly in vivo and in vitro, Science (80-.). 329 (2010) 1663–1667. doi:10.1126/science.1195227.

[105] J. Burré, M. Sharma, T.C. Südhof, α-Synuclein assembles into higher-order multimers upon membrane binding to promote SNARE complex formation, Proc. Natl. Acad. Sci. 111 (2014) E4274–E4283. doi:10.1073/pnas.1416598111.

[106] D.L. Fortin, M.D. Troyer, K. Nakamura, S. Kubo, M.D. Anthony, R.H. Edwards, Lipid rafts mediate the synaptic localization of alpha-synuclein., J. Neurosci. 24 (2004) 6715–23. doi:10.1523/JNEUROSCI.1594-04.2004.

[107] P.J. Kahle, M. Neumann, L. Ozmen, V. Muller, H. Jacobsen, A. Schindzielorz, M. Okochi, U. Leimer, H. van Der Putten, A. Probst, E. Kremmer, H.A. Kretzschmar, C. Haass, Subcellular localization of wild-type and Parkinson's disease-associated mutant alpha -synuclein in human and transgenic mouse brain., J. Neurosci. 20 (2000) 6365–73. http://www.ncbi.nlm.nih.gov/pubmed/10964942 (accessed September 17, 2018).

[108] O.A. Ross, A.T. Braithwaite, L.M. Skipper, J. Kachergus, M.M. Hulihan, F.A. Middleton, K. Nishioka, J. Fuchs, T. Gasser, D.M. Maraganore, C.H. Adler, L. Larvor, M.C. Chartier-Harlin, C. Nilsson, J.W. Langston, K. Gwinn, N. Hattori, M.J. Farrer, Genomic investigation of α-synuclein multiplication and parkinsonism, Ann. Neurol. 63 (2008) 743–750. doi:10.1002/ana.21380.

[109] S. Wislet-Gendebien, C. D'Souza, T. Kawarai, P. St. George-Hyslop, D. Westaway, P. Fraser, A. Tandon, Cytosolic proteins regulate alpha-synuclein dissociation from presynaptic membranes, J. Biol. Chem. 281 (2006) 32148–32155. doi:10.1074/jbc.M605965200.

[110] T. Logan, J. Bendor, C. Toupin, K. Thorn, R.H. Edwards, alpha-Synuclein promotes dilation of the exocytotic fusion pore, Nat. Neurosci. 20 (2017) 681–+. doi:10.1038/nn.4529.

[111] C.R. Bodner, C.M. Dobson, A. Bax, Multiple Tight Phospholipid-Binding Modes of α-Synuclein Revealed by Solution NMR Spectroscopy, J. Mol. Biol. 390 (2009) 775–790. doi:10.1016/j.jmb.2009.05.066.

[112] J. Diao, J. Burré, S. Vivona, D.J. Cipriano, M. Sharma, M. Kyoung, T.C. Südhof, A.T. Brunger, Native α-synuclein induces clustering of synaptic-vesicle mimics via binding to phospholipids and synaptobrevin-2/VAMP2, Elife. 2013 (2013) e00592. doi:10.7554/eLife.00592.

[113] J.H. Soper, S. Roy, A. Stieber, E. Lee, R.B. Wilson, J.Q. Trojanowski, C.G. Burd, V.M.-Y. Lee, α-Synuclein–induced Aggregation of Cytoplasmic Vesicles in Saccharomyces cerevisiae, Mol. Biol. Cell. 19 (2008) 1093–1103. doi:10.1091/mbc.e07-08-0827.

[114] W.W. Li, R. Yang, J.C. Guo, H.M. Ren, X.L. Zha, J.S. Cheng, D.F. Cai, Localization of α-synuclein to mitochondria within midbrain of mice, Neuroreport. 18 (2007) 1543–1546. doi:10.1097/WNR.0b013e3282f03db4.

[115] N.B. Cole, D. DiEuliis, P. Leo, D.C. Mitchell, R.L. Nussbaum, Mitochondrial translocation of α-synuclein is promoted by intracellular acidification, Exp. Cell Res. 314 (2008) 2076–2089. doi:10.1016/j.yexcr.2008.03.012.

[116] L. Devi, V. Raghavendran, B.M. Prabhu, N.G. Avadhani, H.K. Anandatheerthavarada, Mitochondrial import and accumulation of α-synuclein impair complex I in human dopaminergic neuronal cultures and Parkinson disease brain, J. Biol. Chem. 283 (2008) 9089–9100. doi:10.1074/jbc.M710012200.

[117] K. Nakamura, V.M. Nemani, E.K. Wallender, K. Kaehlcke, M. Ott, R.H. Edwards, Optical Reporters for the Conformation of -Synuclein Reveal a Specific Interaction with Mitochondria, J. Neurosci. 28 (2008) 12305–12317. doi:10.1523/JNEUROSCI.3088-08.2008.

[118] G. Liu, C. Zhang, J. Yin, X. Li, F. Cheng, Y. Li, H. Yang, K. Uéda, P. Chan, S. Yu, α-Synuclein is differentially expressed in mitochondria from different rat brain regions and dose-dependently down-regulates complex I activity, Neurosci. Lett. 454 (2009) 187–192. doi:10.1016/j.neulet.2009.02.056.

[119] L.J. Hsu, Y. Sagara, A. Arroyo, E. Rockenstein, A. Sisk, M. Mallory, J. Wong, T. Takenouchi, M. Hashimoto, E. Masliah, α-synuclein promotes mitochondrial deficit and oxidative stress, Am. J. Pathol. 157 (2000) 401–410. doi:10.1016/S0002-9440(10)64553-1.

[120] F. Kamp, N. Exner, A.K. Lutz, N. Wender, J. Hegermann, B. Brunner, B. Nuscher, T. Bartels, A. Giese, K. Beyer, S. Eimer, K.F. Winklhofer, C. Haass, Inhibition of mitochondrial fusion by α-synuclein is rescued by PINK1, Parkin and DJ-1, EMBO J. 29 (2010) 3571–3589. doi:10.1038/emboj.2010.223.

[121] K. Nakamura, V.M. Nemani, F. Azarbal, G. Skibinski, J.M. Levy, K. Egami, L. Munishkina, J. Zhang, B. Gardner, J. Wakabayashi, H. Sesaki, Y. Cheng, S. Finkbeiner, R.L. Nussbaum, E. Masliah, R.H. Edwards, Direct membrane association drives mitochondrial fission by the Parkinson disease-associated protein α-synuclein, J. Biol. Chem. 286 (2011) 20710–20726. doi:10.1074/jbc.M110.213538.

[122] F. Mori, K. Tanji, M. Yoshimoto, H. Takahashi, K. Wakabayashi, Immunohistochemical comparison of α- and β-synuclein in adult rat central nervous system, Brain Res. 941 (2002) 118–126. doi:10.1016/S0006-8993(02)02643-4.

[123] S. Yu, X. Li, G. Liu, J. Han, C. Zhang, Y. Li, S. Xu, C. Liu, Y. Gao, H. Yang, K. Uéda, P. Chan, Extensive nuclear localization of α-synuclein in normal rat brain neurons revealed by a novel monoclonal antibody, Neuroscience. 145 (2007) 539–555. doi:10.1016/j.neuroscience.2006.12.028.

[124] S. Gonçalves, T.F. Outeiro, Assessing the subcellular dynamics of alpha-synuclein using photoactivation microscopy, Mol. Neurobiol. 47 (2013) 1081–1092. doi:10.1007/s12035-013-8406-x.

[125] E. Guerrero, P. Vasudevaraju, M.L. Hegde, G.B. Britton, K.S. Rao, Recent advances in α-synuclein functions, advanced glycation, and toxicity: implications for Parkinson's disease., Mol. Neurobiol. 47 (2013) 525–536. doi:10.1007/s12035-012-8328-z.

[126] M.K. Mbefo, K.E. Paleologou, A. Boucharaba, A. Oueslati, H. Schell, M. Fournier, D. Olschewski, G. Yin, M. Zweckstetter, E. Masliah, P.J. Kahle, H. Hirling, H.A. Lashuel, Phosphorylation of synucleins by members of the polo-like kinase family, J. Biol. Chem. 285 (2010) 2807–2822. doi:10.1074/jbc.M109.081950.

[127] H. Schell, T. Hasegawa, M. Neumann, P.J. Kahle, Nuclear and neuritic distribution of serine-129 phosphorylated α-synuclein in transgenic mice, Neuroscience. 160 (2009) 796–804. doi:10.1016/j.neuroscience.2009.03.002.

[128] E. Kontopoulos, J.D. Parvin, M.B. Feany, α-synuclein acts in the nucleus to inhibit histone acetylation and promote neurotoxicity, Hum. Mol. Genet. 15 (2006) 3012–3023. doi:10.1093/hmg/ddl243.

[129] T.F. Outeiro, E. Kontopoulos, S.M. Altmann, I. Kufareva, K.E. Strathearn, A.M. Amore, C.B. Volk, M.M. Maxwell, J.C. Rochet, P.J. McLean, A.B. Young, R. Abagyan, M.B. Feany, B.T. Hyman, A.G. Kazantsev, Sirtuin 2 inhibitors rescue α-synuclein-mediated toxicity in models of Parkinson's disease, Science (80-.). 317 (2007) 516–519. doi:10.1126/science.1143780.

[130] N. Gosavi, H.J. Lee, J.S. Lee, S. Patel, S.J. Lee, Golgi fragmentation occurs in the cells with prefibrillar alpha-synuclein aggregates and precedes the formation of fibrillar inclusion, J. Biol. Chem. 277 (2002) 48984–48992. doi:10.1074/jbc.M208194200.

[131] W.W. Smith, H. Jiang, Z. Pei, Y. Tanaka, H. Morita, A. Sawa, V.L. Dawson, T.M. Dawson, C.A. Ross, Endoplasmic reticulum stress and mitochondrial cell death pathways mediate A53T mutant alpha-synuclein-induced toxicity, Hum. Mol. Genet. 14 (2005) 3801–3811. doi:10.1093/hmg/ddi396.

[132] N. Thayanidhi, J.R. Helm, D.C. Nycz, M. Bentley, Y. Liang, J.C. Hay, α-Synuclein Delays Endoplasmic Reticulum (ER)-to-Golgi Transport in Mammalian Cells by Antagonizing ER/Golgi SNAREs, Mol. Biol. Cell. 21 (2010) 1850–1863. doi:10.1091/mbc.e09-09-0801.

[133] M.A. Alim, M.S. Hossain, K. Arima, K. Takeda, Y. Izumiyama, M. Nakamura, H. Kaji, T. Shinoda, S. Hisanaga, K. Uéda, Tubulin seeds α-synuclein fibril formation, J. Biol. Chem. 277 (2002) 2112–2117. doi:10.1074/jbc.M102981200.

[134] R.M. Zhou, Y.X. Huang, X.L. Li, C. Chen, Q. Shi, G.R. Wang, C. Tian, Z.Y. Wang, Y.Y. Jing, C. Gao, X.P. Dong, Molecular interaction of α-synuclein with tubulin influences on the polymerization of microtubule in vitro and structure of microtubule in cells, Mol. Biol. Rep. 37 (2010) 3183–3192. doi:10.1007/s11033-009-9899-2.

[135] W.S. Woods, J.M. Boettcher, D.H. Zhou, K.D. Kloepper, K.L. Hartman, D.T. Ladror, Z. Qi, C.M. Rienstra, J.M. George, Conformation-specific binding of alpha-synuclein to novel protein partners detected by phage display and NMR spectroscopy., J. Biol. Chem. 282 (2007) 34555–67. doi:10.1074/jbc.M705283200.

[136] D.J. Busch, J.R. Morgan, Synuclein accumulation is associated with cell-specific neuronal death after spinal cord injury, J. Comp. Neurol. 520 (2012) 1751–1771. doi:10.1002/cne.23011.

[137] J.M. George, H. Jin, W.S. Woods, D.F. Clayton, Characterization of a novel protein regulated during the critical period for song learning in the zebra finch, Neuron. 15 (1995) 361–372. doi:10.1016/0896-6273(95)90040-3.

[138] S. Appel-Cresswell, C. Vilarino-Guell, M. Encarnacion, H. Sherman, I. Yu, B. Shah, D. Weir, C. Thompson, C. Szu-Tu, J. Trinh, J.O. Aasly, A. Rajput, A.H. Rajput, A. Jon Stoessl, M.J. Farrer, Alpha-synuclein p.H50Q, a novel pathogenic mutation for Parkinson's disease, Mov. Disord. 28 (2013) 811–813. doi:10.1002/mds.25421.

[139] R. Krüger, W. Kuhn, T. Müller, D. Woitalla, M. Graeber, S. Kösel, H. Przuntek, J.T. Epplen, L. Schöls, O. Riess, Ala30Pro mutation in the gene encoding α-synuclein in Parkinson's disease, Nat. Genet. 18 (1998) 106–108. doi:10.1038/ng0298-106.

[140] S. Lesage, M. Anheim, F. Letournel, L. Bousset, A. Honoré, N. Rozas, L. Pieri, K. Madiona, A. Dürr, R. Melki, C. Verny, A. Brice, G51D α-synuclein mutation causes a novel Parkinsonian-pyramidal syndrome, Ann. Neurol. 73 (2013) 459–471. doi:10.1002/ana.23894.

[141] C. Proukakis, C.G. Dudzik, T. Brier, D.S. MacKay, J.M. Cooper, G.L. Millhauser, H. Houlden, A.H. Schapira, A novel α-synuclein missense mutation in Parkinson disease, Neurology. 80 (2013) 1062–1064. doi:10.1212/WNL.0b013e31828727ba.

[142] G.M. Mohite, A. Navalkar, R. Kumar, S. Mehra, S. Das, L.G. Gadhe, D. Ghosh, B. Alias, V. Chandrawanshi, A. Ramakrishnan, S. Mehra, S.K. Maji, The Familial α-Synuclein A53E Mutation Enhances Cell Death in Response to Environmental Toxins Due to a Larger Population of Oligomers, Biochemistry. 57 (2018) acs.biochem.8b00321. doi:10.1021/acs.biochem.8b00321.

[143] J.A. Rodriguez, M.I. Ivanova, M.R. Sawaya, D. Cascio, F.E. Reyes, D. Shi, S. Sangwan, E.L. Guenther, L.M. Johnson, M. Zhang, L. Jiang, M.A. Arbing, B.L. Nannenga, J. Hattne, J. Whitelegge, A.S. Brewster, M. Messerschmidt, S. Boutet, N.K. Sauter, T. Gonen, D.S. Eisenberg, Structure of the toxic core of α-synuclein from invisible crystals, Nature. 525 (2015) 486–490. doi:10.1038/nature15368.

[144] S. Rajagopalan, J.K. Andersen, Alpha synuclein aggregation: Is it the toxic gain of function responsible for neurodegeneration in Parkinson's disease?, Mech. Ageing Dev. 122 (2001) 1499–1510. doi:10.1016/S0047-6374(01)00283-4.

[145] M. Ahn, S.B. Kim, M. Kang, Y. Ryu, T. Doohun Kim, Chaperone-like activities of α-synuclein: α-Synuclein assists enzyme activities of esterases, Biochem. Biophys. Res. Commun. 346 (2006) 1142–1149. doi:10.1016/j.bbrc.2006.05.213.

[146] W. Hoyer, T. Antony, D. Cherny, G. Heim, T.M. Jovin, V. Subramaniam, Dependence of α-synuclein aggregate morphology on solution conditions, J. Mol. Biol. 322 (2002) 383–393. doi:10.1016/S0022-2836(02)00775-1.

[147] A. Oueslati, M. Fournier, H.A. Lashuel, Role of post-translational modifications in modulating the structure, function and toxicity of α-synuclein. Implications for Parkinson's disease pathogenesis and therapies, Prog. Brain Res. 183 (2010) 115–145. doi:10.1016/S0079-6123(10)83007-9.

[148] H. Sato, T. Kato, S. Arawaka, The role of Ser129 phosphorylation of α-synuclein in neurodegeneration of Parkinson ' s disease: A review of in vivo models, Rev. Neurosci. 24 (2013) 115–123. doi:10.1515/revneuro-2012-0071.

[149] T.S. Ulmer, A. Bax, N.B. Cole, R.L. Nussbaum, Structure and dynamics of micelle-bound human α-synuclein, J. Biol. Chem. 280 (2005) 9595–9603. doi:10.1074/jbc.M411805200.

[150] L. Schrödinger, The {PyMOL} Molecular Graphics System, Version~2.2, 2015.

[151] J. Burré, M. Sharma, T.C. Südhof, Cell biology and pathophysiology of α-synuclein, Cold Spring Harb. Perspect. Med. 8 (2018) a024091. doi:10.1101/cshperspect.a024091.

[152] P.J. Barrett, J. Timothy Greenamyre, Post-translational modification of α-synuclein in Parkinson's disease, Brain Res. 1628 (2015) 247–253. doi:10.1016/j.brainres.2015.06.002.

[153] H. Fujiwara, M. Hasegawa, N. Dohmae, A. Kawashima, E. Masliah, M.S. Goldberg, J. Shen, K. Takio, T. Iwatsubo, α-synuclein is phosphorylated in synucleinopathy lesions, Nat. Cell Biol. 4 (2002) 160–164. doi:10.1038/ncb748.

[154] M. Neumann, P.J. Kahle, B.I. Giasson, L. Ozmen, E. Borroni, W. Spooren, V. Müller, S. Odoy, H. Fujiwara, M. Hasegawa, T. Iwatsubo, J.Q. Trojanowski, H.A. Kretzschmar, C. Haass, Misfolded proteinase K-resistant hyperphosphorylated alpha-synuclein in aged transgenic mice with locomotor deterioration and in human alpha-synucleinopathies., J. Clin. Invest. 110 (2002) 1429–39. doi:10.1172/JCI15777.

[155] W.W. Smith, R.L. Margolis, X. Li, J.C. Troncoso, M.K. Lee, V.L. Dawson, T.M. Dawson, T. Iwatsubo, C.A. Ross, Alpha-synuclein phosphorylation enhances eosinophilic cytoplasmic inclusion formation in SH-SY5Y cells., J. Neurosci. 25 (2005) 5544–52. doi:10.1523/JNEUROSCI.0482-05.2005.

[156] N. Sugeno, A. Takeda, T. Hasegawa, M. Kobayashi, A. Kikuchi, F. Mori, K. Wakabayashi, Y. Itoyama, Serine 129 phosphorylation of α-synuclein induces unfolded protein response-mediated cell death, J. Biol. Chem. 283 (2008) 23179–23188. doi:10.1074/jbc.M802223200.

[157] C. Rieker, K.K. Dev, K. Lehnhoff, S. Barbieri, I. Ksiazek, S. Kauffmann, S. Danner, H. Schell, C. Boden, M.A. Ruegg, P.J. Kahle, H. van der Putten, D.R. Shimshek, Neuropathology in mice expressing mouse alpha-synuclein, PLoS One. 6 (2011) e24834. doi:10.1371/journal.pone.0024834.

[158] M. Wakamatsu, A. Ishii, Y. Ukai, J. Sakagami, S. Iwata, M. Ono, K. Matsumoto, A. Nakamura, N. Tada, K. Kobayashi, T. Iwatsubo, M. Yoshimoto, Accumulation of phosphorylated alpha-synuclein in dopaminergic neurons of transgenic mice that express human alpha-synuclein, J. Neurosci. Res. 85 (2007) 1819–1825. doi:10.1002/jnr.21310.

[159] E.A. Waxman, B.I. Giasson, Specificity and regulation of casein kinase-mediated phosphorylation of alpha-synuclein, J. Neuropathol. Exp. Neurol. 67 (2008) 402–416. doi:10.1097/NEN.0b013e3186fc995.

[160] K.E. Paleologou, A. Oueslati, G. Shakked, C.C. Rospigliosi, H.-Y. Kim, G.R. Lamberto, C.O. Fernandez, A. Schmid, F. Chegini, W.P. Gai, D. Chiappe, M. Moniatte, B.L. Schneider, P. Aebischer, D. Eliezer, M. Zweckstetter, E. Masliah, H.A. Lashuel, Phosphorylation at S87 Is Enhanced in Synucleinopathies, Inhibits -Synuclein Oligomerization, and Influences Synuclein-Membrane Interactions, J. Neurosci. 30 (2010) 3184–3198. doi:10.1523/JNEUROSCI.5922-09.2010.

[161] M. Goedert, Alpha-synuclein and neurodegenerative diseases, Nat. Rev. Neurosci. 2 (2001) 492–501. doi:10.1038/35081564.

[162] E. Engelhardt, M. Da, M. Gomes, Lewy and his inclusion bodies Discovery and rejection, 2017. http://www.demneuropsy.com.br/imageBank/pdf/v11n2a12.pdf (accessed September 18, 2018).

[163] L.S. Forno, Neuropathology of Parkinson's disease., J. Neuropathol. Exp. Neurol. 55 (1996) 259–72. http://www.ncbi.nlm.nih.gov/pubmed/8786384 (accessed September 18, 2018).

[164] P.L. Lantos, The definition of multiple system atrophy: a review of recent developments, J. Neuropathol. Exp. Neurol. 57 (1998) 1099–1111. http://www.ncbi.nlm.nih.gov/pubmed/9862632 (accessed September 18, 2018).

[165] R.F. Roberts, R. Wade-Martins, J. Alegre-Abarrategui, Direct visualization of alpha-synuclein oligomers reveals previously undetected pathology in Parkinson's disease brain, Brain. 138 (2015) 1642–1657. doi:10.1093/brain/awv040.

[166] Y. Compta, T. Valente, J. Saura, B. Segura, Á. Iranzo, M. Serradell, C. Junqué, E. Tolosa, F. Valldeoriola, E. Muñoz, J. Santamaria, A. Cámara, M. Fernández, J. Fortea, M. Buongiorno, J.L. Molinuevo, N. Bargalló, M.J. Martí, Correlates of cerebrospinal fluid levels of oligomeric- and total-α-synuclein in premotor, motor and dementia stages of Parkinson's disease, J. Neurol. 262 (2014) 294–306. doi:10.1007/s00415-014-7560-z.

[167] N. Cremades, S.I.A. Cohen, E. Deas, A.Y. Abramov, A.Y. Chen, A. Orte, M. Sandal, R.W. Clarke, P. Dunne, F.A. Aprile, C.W. Bertoncini, N.W. Wood, T.P.J. Knowles, C.M. Dobson, D. Klenerman, Direct observation of the interconversion of normal and toxic forms of α-synuclein, Cell. 149 (2012) 1048–1059. doi:10.1016/j.cell.2012.03.037.

[168] P.R. Angelova, M.H.R. Ludtmann, M.H. Horrocks, A. Negoda, N. Cremades, D. Klenerman, C.M. Dobson, N.W. Wood, E. V. Pavlov, S. Gandhi, A.Y. Abramov, Ca 2+ is a key factor in α-synuclein-induced neurotoxicity, J. Cell Sci. 129 (2016) 1792–1801. doi:10.1242/jcs.180737.

[169] C.Y. Chung, J.B. Koprich, H. Siddiqi, O. Isacson, Dynamic Changes in Presynaptic and Axonal Transport Proteins Combined with Striatal Neuroinflammation Precede Dopaminergic Neuronal Loss in a Rat Model of AAV -Synucleinopathy, J. Neurosci. 29 (2009) 3365–3373. doi:10.1523/JNEUROSCI.5427-08.2009.

[170] A.K. Reeve, M.H. Ludtmann, P.R. Angelova, E.M. Simcox, M.H. Horrocks, D. Klenerman, S. Gandhi, D.M. Turnbull, A.Y. Abramov, Aggregated α-synuclein and complex I deficiency: exploration of their relationship in differentiated neurons, Cell Death Dis. 6 (2015) e1820–e1820. doi:10.1038/cddis.2015.166.

[171] E.S. Luth, I.G. Stavrovskaya, T. Bartels, B.S. Kristal, D.J. Selkoe, Soluble, prefibrillar α-synuclein oligomers promote complex I-dependent, Ca2+-induced mitochondrial dysfunction, J. Biol. Chem. 289 (2014) 21490–21507. doi:10.1074/jbc.M113.545749.

[172] M. Fry, D.E. Green, Cardiolipin requirement for electron transfer in complex I and III of the mitochondrial respiratory chain., J. Biol. Chem. 256 (1981) 1874–1880. http://www.ncbi.nlm.nih.gov/pubmed/6257690 (accessed September 19, 2018).

[173] M. Zhang, E. Mileykovskaya, W. Dowhan, Gluing the respiratory chain together: Cardiolipin is required for supercomplex formation in the inner mitochondrial membrane, J. Biol. Chem. 277 (2002) 43553–43556. doi:10.1074/jbc.C200551200.

[174] S.I. Kubo, V.M. Nemani, R.J. Chalkley, M.D. Anthony, N. Hattori, Y. Mizuno, R.H. Edwards, D.L. Fortin, A combinatorial code for the interaction of α-synuclein with membranes, J. Biol. Chem. 280 (2005) 31664–31672. doi:10.1074/jbc.M504894200.

[175] E. Mileykovskaya, W. Dowhan, Cardiolipin-dependent formation of mitochondrial respiratory supercomplexes, Chem. Phys. Lipids. 179 (2014) 42–48. doi:10.1016/j.chemphyslip.2013.10.012.

[176] A. Camilleri, C. Zarb, M. Caruana, U. Ostermeier, S. Ghio, T. Högen, F. Schmidt, A. Giese, N. Vassallo, Mitochondrial membrane permeabilisation by amyloid aggregates and protection by polyphenols, Biochim. Biophys. Acta - Biomembr. 1828 (2013) 2532–2543. doi:10.1016/j.bbamem.2013.06.026.

[177] I.G. Zigoneanu, Y.J. Yang, A.S. Krois, M.E. Haque, G.J. Pielak, Interaction of α-synuclein with vesicles that mimic mitochondrial membranes, Biochim. Biophys. Acta - Biomembr. 1818 (2012) 512–519. doi:10.1016/j.bbamem.2011.11.024.

[178] R. Di Maio, P.J. Barrett, E.K. Hoffman, C.W. Barrett, A. Zharikov, A. Borah, X. Hu, J. McCoy, C.T. Chu, E.A. Burton, T.G. Hastings, J.T. Greenamyre, α-Synuclein binds to TOM20 and inhibits mitochondrial protein import in Parkinson's disease, Sci. Transl. Med. 8 (2016) 342ra78-342ra78. doi:10.1126/scitranslmed.aaf3634.

[179] M.H.R. Ludtmann, P.R. Angelova, M.H. Horrocks, M.L. Choi, M. Rodrigues, A.Y. Baev, A. V. Berezhnov, Z. Yao, D. Little, B. Banushi, A.S. Al-Menhali, R.T. Ranasinghe, D.R. Whiten, R. Yapom, K.S. Dolt, M.J. Devine, P. Gissen, T. Kunath, M. Jaganjac, E. V. Pavlov, D. Klenerman, A.Y. Abramov, S. Gandhi, α-synuclein oligomers interact with ATP synthase and open the permeability transition pore in Parkinson's disease, Nat. Commun. 9 (2018) 2293. doi:10.1038/s41467-018-04422-2.

[180] C. Guardia-Laguarta, E. Area-Gomez, C. Rüb, Y. Liu, J. Magrané, D. Becker, W. Voos, E.A. Schon, S. Przedborski, α-Synuclein is localized to mitochondria-associated ER membranes., J. Neurosci. 34 (2014) 249–59. doi:10.1523/JNEUROSCI.2507-13.2014.

[181] W. Xie, K.K.K. Chung, Alpha-synuclein impairs normal dynamics of mitochondria in cell and animal models of Parkinson's disease, J. Neurochem. 122 (2012) 404–414. doi:10.1111/j.1471-4159.2012.07769.x.

[182] C. Galvagnion, A.K. Buell, G. Meisl, T.C.T. Michaels, M. Vendruscolo, T.P.J. Knowles, C.M. Dobson, Lipid vesicles trigger α-synuclein aggregation by stimulating primary nucleation, Nat. Chem. Biol. 11 (2015) 229–234. doi:10.1038/nchembio.1750.

[183] C. Galvagnion, J.W.P. Brown, M.M. Ouberai, P. Flagmeier, M. Vendruscolo, A.K. Buell, E. Sparr, C.M. Dobson, Chemical properties of lipids strongly affect the kinetics of the membrane-induced aggregation of α-synuclein, Proc. Natl. Acad. Sci. 113 (2016) 7065–7070. doi:10.1073/pnas.1601899113.

[184] G. Fusco, S.W. Chen, P.T.F. Williamson, R. Cascella, M. Perni, J.A. Jarvis, C. Cecchi, M. Vendruscolo, F. Chiti, N. Cremades, L. Ying, C.M. Dobson, A. De Simone, Structural basis of

membrane disruption and cellular toxicity by a-synuclein oligomers, Science (80-.). 358 (2017) 1440–1443. doi:10.1126/science.aan6160.

[185] E. V. Mosharov, K.E. Larsen, E. Kanter, K.A. Phillips, K. Wilson, Y. Schmitz, D.E. Krantz, K. Kobayashi, R.H. Edwards, D. Sulzer, Interplay between Cytosolic Dopamine, Calcium, and α-Synuclein Causes Selective Death of Substantia Nigra Neurons, Neuron. 62 (2009) 218–229. doi:10.1016/j.neuron.2009.01.033.

[186] M.H.R. Ludtmann, A.Y. Abramov, Mitochondrial calcium imbalance in Parkinson's disease, Neurosci. Lett. 663 (2018) 86–90. doi:10.1016/j.neulet.2017.08.044.

[187] K.M. Danzer, D. Haasen, A.R. Karow, S. Moussaud, M. Habeck, A. Giese, H. Kretzschmar, B. Hengerer, M. Kostka, Different Species of alpha-Synuclein Oligomers Induce Calcium Influx and Seeding, J. Neurosci. 27 (2007) 9220–9232. doi:10.1523/JNEUROSCI.2617-07.2007.

[188] R. Kumar, R. Kumari, S. Kumar, D.K. Jangir, T.K. Maiti, Extracellular α-Synuclein Disrupts Membrane Nanostructure and Promotes S-Nitrosylation-Induced Neuronal Cell Death, Biomacromolecules. 19 (2018) 1118–1129. doi:10.1021/acs.biomac.7b01727.

[189] D.G. Ferreira, M. Temido-Ferreira, H.V. Miranda, V.L. Batalha, J.E. Coelho, É.M. Szegö, I. Marques-Morgado, S.H. Vaz, J.S. Rhee, M. Schmitz, I. Zerr, L. V Lopes, T.F. Outeiro, α-synuclein interacts with PrPC to induce cognitive impairment through mGluR5 and NMDAR2B, Nat. Neurosci. 20 (2017) 1569–1579. doi:10.1038/nn.4648.

[190] H.-J. Lee, F. Khoshaghideh, S. Patel, S.-J. Lee, Clearance of Alpha-Synuclein Oligomeric Intermediates via the Lysosomal Degradation Pathway, J. Neurosci. 24 (2004) 1888–1896. doi:10.1523/JNEUROSCI.3809-03.2004.

[191] J.H. Lu, J.Q. Tan, S.S.K. Durairajan, L.F. Liu, Z.H. Zhang, L. Ma, H.M. Shen, E. Chan, M. Li, Isorhynchophylline, a natural alkaloid, promotes the degradation of α-synuclein in neuronal cells via inducing autophagy, Autophagy. 8 (2012) 98–108. doi:10.4161/auto.8.1.18313.

[192] M. Decressac, B. Mattsson, P. Weikop, M. Lundblad, J. Jakobsson, A. Bjorklund, TFEB-mediated autophagy rescues midbrain dopamine neurons from alpha-synuclein toxicity, Proc. Natl. Acad. Sci. 110 (2013) E1817–E1826. doi:10.1073/pnas.1305623110.

[193] W.C. Nichols, N. Pankratz, D.K. Marek, V.E. Elsaesser, C.A. Halter, A. Rudolph, J. Wojcieszek, R.F. Pfeiffer, T. Foroud, P.S.G.-P. Investigators, Mutations in GBA are assoicated with familial Parkinson disease susceptibility and age at onset, Neurology. 73_ _ (2009) 310–316. doi:10.1212/WNL.0b013e3181b28601.

[194] J.R. Mazzulli, Y.H. Xu, Y. Sun, A.L. Knight, P.J. McLean, G.A. Caldwell, E. Sidransky, G.A. Grabowski, D. Krainc, Gaucher disease glucocerebrosidase and α-synuclein form a bidirectional pathogenic loop in synucleinopathies, Cell. 146 (2011) 37–52. doi:10.1016/j.cell.2011.06.001.

[195] S. Gandhi, A.Y. Abramov, Mechanism of Oxidative Stress in Neurodegeneration, Oxid. Med. Cell. Longev. 2012 (2012) 1–11. doi:10.1155/2012/428010.

[196] A.K. Holley, V. Bakthavatchalu, J.M. Velez-Roman, D.K. St. Clair, Manganese Superoxide Dismutase: Guardian of the Powerhouse, Int. J. Mol. Sci. 12 (2011) 7114–7162. doi:10.3390/ijms12107114.

[197] J.M. Flynn, S. Melovn, SOD2 in mitochondrial dysfunction and neurodegeneration, Free Radic. Biol. Med. 62 (2013) 4–12. doi:10.1016/j.freeradbiomed.2013.05.027.

[198] M. Ott, V. Gogvadze, S. Orrenius, B. Zhivotovsky, Mitochondria, oxidative stress and cell death, Apoptosis. 12 (2007) 913–922. doi:10.1007/s10495-007-0756-2.

[199] E. Deas, N. Cremades, P.R. Angelova, M.H.R. Ludtmann, Z. Yao, S. Chen, M.H. Horrocks, B. Banushi, D. Little, M.J. Devine, P. Gissen, D. Klenerman, C.M. Dobson, N.W. Wood, S. Gandhi, A.Y.

Abramov, Alpha-Synuclein Oligomers Interact with Metal Ions to Induce Oxidative Stress and Neuronal Death in Parkinson's Disease, Antioxid. Redox Signal. 24 (2016) 376–391. doi:10.1089/ars.2015.6343.

[200] P.R. Angelova, M.H. Horrocks, D. Klenerman, S. Gandhi, A.Y. Abramov, M.S. Shchepinov, Lipid peroxidation is essential for α-synuclein-induced cell death, J. Neurochem. 133 (2015) 582–589. doi:10.1111/jnc.13024.

[201] W. Zhang, Aggregated alpha-synuclein activates microglia: a process leading to disease progression in Parkinson's disease, FASEB J. 19 (2005) 533–542. doi:10.1096/fj.04-2751com.

[202] W.W. Chen, X. Zhang, W.J. Huang, Role of neuroinflammation in neurodegenerative diseases (Review), Mol. Med. Rep. 13 (2016) 3391–3396. doi:10.3892/mmr.2016.4948.

[203] C. Kim, D.H. Ho, J.E. Suk, S. You, S. Michael, J. Kang, S.J. Lee, E. Masliah, D. Hwang, H.J. Lee, S.J. Lee, Neuron-released oligomeric α-synuclein is an endogenous agonist of TLR2 for paracrine activation of microglia, Nat. Commun. 4 (2013) 1562. doi:10.1038/ncomms2534.

[204] L. Fellner, R. Irschick, K. Schanda, M. Reindl, L. Klimaschewski, W. Poewe, G.K. Wenning, N. Stefanova, Toll-like receptor 4 is required for alpha-synuclein dependent activation of microglia and astroglia, Glia. 61 (2013) 349–360. doi:10.1002/glia.22437.

[205] E.H. Rannikko, S.S. Weber, P.J. Kahle, Exogenous α-synuclein induces toll-like receptor 4 dependent inflammatory responses in astrocytes, BMC Neurosci. 16 (2015) 57. doi:10.1186/s12868-015-0192-0.

[206] M.L. Choi, S. Gandhi, Crucial role of protein oligomerization in the pathogenesis of Alzheimer's and Parkinson's diseases, FEBS J. (2018). doi:10.1111/febs.14587.

[207] C. Wang, I.A. Iashchishyn, J. Pansieri, S. Nyström, O. Klementieva, J. Kara, I. Horvath, R. Moskalenko, R. Rofougaran, G. Gouras, G.G. Kovacs, S.K. Shankar, L.A. Morozova-Roche, S100A9-Driven Amyloid-Neuroinflammatory Cascade in Traumatic Brain Injury as a Precursor State for Alzheimer's Disease, Sci. Rep. 8 (2018) 12836. doi:10.1038/s41598-018-31141-x.

[208] V.N. Uversky, A protein-chameleon: Conformational plasticity of α-synuclein, a disordered protein involved in neurodegenerative disorders, J. Biomol. Struct. Dyn. 21 (2003) 211–234. doi:10.1080/07391102.2003.10506918.

[209] H.A. Lashuel, C.R. Overk, A. Oueslati, E. Masliah, The many faces of α-synuclein: From structure and toxicity to therapeutic target, Nat. Rev. Neurosci. 14 (2013) 38–48. doi:10.1038/nrn3406.

[210] R.L. Hamilton, Lewy Bodies in Alzheimer's Disease: A Neuropathological Review of 145 Cases Using α-Synuclein Immunohistochemistry, Brain Pathol. 10 (2006) 378–384. doi:10.1111/j.1750-3639.2000.tb00269.x.

[211] V.N. Uversky, J. Li, A.L. Fink, Evidence for a Partially Folded Intermediate in α-Synuclein Fibril Formation, J. Biol. Chem. 276 (2001) 10737–10744. doi:10.1074/jbc.M010907200.

[212] V.N. Uversky, J. Li, P. Souillac, I.S. Millett, S. Doniach, R. Jakes, M. Goedert, A.L. Fink, Biophysical properties of the synucleins and their propensities to fibrillate: Inhibition of α-synuclein assembly by β- and γ-synucleins, J. Biol. Chem. 277 (2002) 11970–11978. doi:10.1074/jbc.M109541200.

[213] D. Eliezer, E. Kutluay, R. Bussell, G. Browne, Conformational properties of alpha-synuclein in its free and lipid-associated states, J. Mol. Biol. 307 (2001) 1061–1073. doi:10.1006/jmbi.2001.4538.

[214] C.D. Syme, E.W. Blanch, C. Holt, R. Jakes, M. Goedert, L. Hecht, L.D. Barron, A Raman optical activity study of rheomorphism in caseins, synucleins and tau: New insight into the structure and behaviour of natively unfolded proteins, Eur. J. Biochem. 269 (2002) 148–156. doi:10.1046/j.0014-2956.2001.02633.x.

[215] W.S. Davidson, A. Jonas, D.F. Clayton, J.M. George, Stabilization of α-Synuclein secondary structure upon binding to synthetic membranes, J. Biol. Chem. 273 (1998) 9443–9449. doi:10.1074/jbc.273.16.9443.

[216] R. Bussell, T.F. Ramlall, D. Eliezer, Helix periodicity, topology, and dynamics of membrane-associated alpha-synuclein, Protein Sci. 14 (2005) 862–872. doi:10.1110/ps.041255905.

[217] B. Nuscher, F. Kamp, T. Mehnert, S. Odoy, C. Haass, P.J. Kahle, K. Beyer, α-synuclein has a high affinity for packing defects in a bilayer membrane: A thermodynamics study, J. Biol. Chem. 279 (2004) 21966–21975. doi:10.1074/jbc.M401076200.

[218] C.C. Jao, B.G. Hegde, J. Chen, I.S. Haworth, R. Langen, Structure of membrane-bound alpha-synuclein from site-directed spin labeling and computational refinement, Proc. Natl. Acad. Sci. 105 (2008) 19666–19671. doi:10.1073/pnas.0807826105.

[219] A.J. Trexler, E. Rhoades, α-Synuclein binds large unilamellar vesicles as an extended helix, Biochemistry. 48 (2009) 2304–2306. doi:10.1021/bi900114z.

[220] R. Bussell, D. Eliezer, A structural and functional role for 11-mer repeats in α-synuclein and other exchangeable lipid binding proteins, J. Mol. Biol. 329 (2003) 763–778. doi:10.1016/S0022-2836(03)00520-5.

[221] E.R. Georgieva, T.F. Ramlall, P.P. Borbat, J.H. Freed, D. Eliezer, Membrane-bound α-synuclein forms an extended helix: Long-distance pulsed ESR measurements using vesicles, bicelles, and rodlike micelles, J. Am. Chem. Soc. 130 (2008) 12856–12857. doi:10.1021/ja804517m.

[222] S. Chandra, X. Chen, J. Rizo, R. Jahn, T.C. Südhof, A broken α-helix in folded α-synuclein, J. Biol. Chem. 278 (2003) 15313–15318. doi:10.1074/jbc.M213128200.

[223] P. Borbat, T.F. Ramlall, J.H. Freed, D. Eliezer, Inter-helix distances in lysophospholipid micelle-bound α-synuclein from pulsed ESR measurements, J. Am. Chem. Soc. 128 (2006) 10004–10005. doi:10.1021/ja063122l.

[224] M. Drescher, G. Veldhuis, B.D. Van Rooijen, S. Milikisyants, V. Subramaniam, M. Huber, Antiparallel arrangement of the helices of vesicle-bound α-synuclein, J. Am. Chem. Soc. 130 (2008) 7796–7797. doi:10.1021/ja801594s.

[225] J.N. Rao, C.C. Jao, B.G. Hegde, R. Langen, T.S. Ulmer, A combinatorial NMR and EPR approach for evaluating the structural ensemble of partially folded proteins, J. Am. Chem. Soc. 132 (2010) 8657–8668. doi:10.1021/ja100646t.

[226] A. Rawat, R. Langen, J. Varkey, Membranes as modulators of amyloid protein misfolding and target of toxicity, Biochim. Biophys. Acta - Biomembr. (2018) 0–1. doi:10.1016/J.BBAMEM.2018.04.011.

[227] H.L. Roberts, D.R. Brown, Seeking a mechanism for the toxicity of oligomeric α-synuclein, Biomolecules. 5 (2015) 282–305. doi:10.3390/biom5020282.

[228] Z. Lv, A. V. Krasnoslobodtsev, Y. Zhang, D. Ysselstein, J.C. Rochet, S.C. Blanchard, Y.L. Lyubchenko, Effect of acidic pH on the stability of α-synuclein dimers, Biopolymers. 105 (2016) 715–724. doi:10.1002/bip.22874.

[229] Y. Zhang, M. Hashemi, Z. Lv, B. Williams, K.I. Popov, N. V. Dokholyan, Y.L. Lyubchenko, High-speed atomic force microscopy reveals structural dynamics of α-synuclein monomers and dimers, J. Chem. Phys. 148 (2018) 123322. doi:10.1063/1.5008874.

[230] J. Li, V.N. Uversky, A.L. Fink, Effect of familial Parkinson's disease point mutations A30P and A53T on the structural properties, aggregation, and fibrillation of human α-synuclein, Biochemistry. 40 (2001) 11604–11613. doi:10.1021/bi010616g.

[231] A. V. Krasnoslobodtsev, I.L. Volkov, J.M. Asiago, J. Hindupur, J.-C. Rochet, Y.L. Lyubchenko, α-Synuclein Misfolding Assessed with Single Molecule AFM Force Spectroscopy: Effect of Pathogenic Mutations, Biochemistry. 52 (2013) 7377–7386. doi:10.1021/bi401037z.

[232] J. Varkey, N. Mizuno, B.G. Hegde, N. Cheng, A.C. Steven, R. Langen, α-synuclein oligomers with broken helical conformation form lipoprotein nanoparticles, J. Biol. Chem. 288 (2013) 17620–17630. doi:10.1074/jbc.M113.476697.

[233] T. Bartels, J.G. Choi, D.J. Selkoe, α-Synuclein occurs physiologically as a helically folded tetramer that resists aggregation, Nature. 477 (2011) 107–111. doi:10.1038/nature10324.

[234] E. Kara, P.A. Lewis, H. Ling, C. Proukakis, H. Houlden, J. Hardy, α-Synuclein mutations cluster around a putative protein loop, Neurosci. Lett. 546 (2013) 67–70. doi:10.1016/j.neulet.2013.04.058.

[235] N. Gould, D.E. Mor, R. Lightfoot, K. Malkus, B. Giasson, H. Ischiropoulos, Evidence of native α-synuclein conformers in the human brain, J. Biol. Chem. 289 (2014) 7929–7934. doi:10.1074/jbc.C113.538249.

[236] U. Dettmer, A.J. Newman, E.S. Luth, T. Bartels, D. Selkoe, In vivo cross-linking reveals principally oligomeric forms of α-synuclein and β-synuclein in neurons and non-neural cells, J. Biol. Chem. 288 (2013) 6371–6385. doi:10.1074/jbc.M112.403311.

[237] B. Fauvet, M.K. Mbefo, M.B. Fares, C. Desobry, S. Michael, M.T. Ardah, E. Tsika, P. Coune, M. Prudent, N. Lion, D. Eliezer, D.J. Moore, B. Schneider, P. Aebischer, O.M. El-Agnaf, E. Masliah, H.A. Lashuel, α-Synuclein in central nervous system and from erythrocytes, mammalian cells, and Escherichia coli exists predominantly as disordered monomer, J. Biol. Chem. 287 (2012) 15345–15364. doi:10.1074/jbc.M111.318949.

[238] K.A. Conway, S.J. Lee, J.C. Rochet, T.T. Ding, R.E. Williamson, P.T. Lansbury, Acceleration of oligomerization, not fibrillization, is a shared property of both alpha-synuclein mutations linked to early-onset Parkinson's disease: implications for pathogenesis and therapy., Proc. Natl. Acad. Sci. U. S. A. 97 (2000) 571–6. http://www.ncbi.nlm.nih.gov/pubmed/10639120 (accessed September 23, 2018).

[239] T.T. Ding, S.J. Lee, J.C. Rochet, P.T. Lansbury, Annular α-synuclein protofibrils are produced when spherical protofibrils are incubated in solution or bound to brain-derived membranes, Biochemistry. 41 (2002) 10209–10217. doi:10.1021/bi020139h.

[240] N. Lorenzen, S.B. Nielsen, A.K. Buell, J.D. Kaspersen, P. Arosio, B.S. Vad, W. Paslawski, G. Christiansen, Z. Valnickova-Hansen, M. Andreasen, J.J. Enghild, J.S. Pedersen, C.M. Dobson, T.P.J. Knowles, D.E. Otzen, The role of stable α-synuclein oligomers in the molecular events underlying amyloid formation, J. Am. Chem. Soc. 136 (2014) 3859–3868. doi:10.1021/ja411577t.

[241] C.L.L. Pham, R. Cappai, The interplay between lipids and dopamine on α-synuclein oligomerization and membrane binding, Biosci. Rep. 33 (2013) 807–814. doi:10.1042/BSR20130092.

[242] J.A. Wright, X. Wang, D.R. Brown, Unique copper-induced oligomers mediate alpha-synuclein toxicity, FASEB J. 23 (2009) 2384–2393. doi:10.1096/fj.09-130039.

[243] X. Wang, D. Moualla, J.A. Wright, D.R. Brown, Copper binding regulates intracellular alpha-synuclein localisation, aggregation and toxicity, J. Neurochem. 113 (2010) 704–714. doi:10.1111/j.1471-4159.2010.06638.x.

[244] M.J. Hokenson, V.N. Uversky, J. Goers, G. Yamin, L.A. Munishkina, A.L. Fink, Role of Individual Methionines in the Fibrillation of Methionine-Oxidized Alpha-Synuclein, Biochemistry. 43 (2004) 4621–4633. doi:10.1021/bi049979h.

[245] C.B. Glaser, G. Yamin, V.N. Uversky, A.L. Fink, Methionine oxidation, α-synuclein and Parkinson's disease, Biochim. Biophys. Acta - Proteins Proteomics. 1703 (2005) 157–169. doi:10.1016/j.bbapap.2004.10.008.

[246] G. Yamin, V.N. Uversky, A.L. Fink, Nitration inhibits fibrillation of human α-synuclein in vitro by formation of soluble oligomers, FEBS Lett. 542 (2003) 147–152. doi:10.1016/S0014-5793(03)00367-3.

[247] V.N. Uversky, G. Yamin, L.A. Munishkina, M.A. Karymov, I.S. Millett, S. Doniach, Y.L. Lyubchenko, A.L. Fink, Effects of nitration on the structure and aggregation of α-synuclein, Mol. Brain Res. 134 (2005) 84–102. doi:10.1016/j.molbrainres.2004.11.014.

[248] D.E. Ehrnhoefer, J. Bieschke, A. Boeddrich, M. Herbst, L. Masino, R. Lurz, S. Engemann, A. Pastore, E.E. Wanker, EGCG redirects amyloidogenic polypeptides into unstructured, off-pathway oligomers, Nat. Struct. Mol. Biol. 15 (2008) 558–566. doi:10.1038/nsmb.1437.

[249] J. Li, M. Zhu, S. Rajamani, V.N. Uversky, A.L. Fink, Rifampicin inhibits α-synuclein fibrillation and disaggregates fibrils, Chem. Biol. 11 (2004) 1513–1521. doi:10.1016/j.chembiol.2004.08.025.

[250] M. Zhu, S. Rajamani, J. Kaylor, S. Han, F. Zhou, A.L. Fink, The Flavonoid Baicalein Inhibits Fibrillation of α-Synuclein and Disaggregates Existing Fibrils, J. Biol. Chem. 279 (2004) 26846–26857. doi:10.1074/jbc.M403129200.

[251] Z. Qin, D. Hu, S. Han, S.H. Reaney, D.A. Di Monte, A.L. Fink, Effect of 4-Hydroxy-2-nonenal Modification on α-Synuclein Aggregation, J. Biol. Chem. 282 (2007) 5862–5870. doi:10.1074/jbc.M608126200.

[252] C. Dong, M. Hoffmann, X. Li, M. Wang, C.R. Garen, N.O. Petersen, M.T. Woodside, Structural characteristics and membrane interactions of tandem α -synuclein oligomers, Sci. Rep. 8 (2018) 1–11. doi:10.1038/s41598-018-25133-0.

[253] A. Villar-Piqué, T. Lopes da Fonseca, T.F. Outeiro, Structure, function and toxicity of alpha-synuclein: the Bermuda triangle in synucleinopathies, J. Neurochem. 139 (2016) 240–255. doi:10.1111/jnc.13249.

[254] L.C. Serpell, J. Berriman, R. Jakes, M. Goedert, R.A. Crowther, Fiber diffraction of synthetic alpha -synuclein filaments shows amyloid-like cross-beta conformation, Proc. Natl. Acad. Sci. 97 (2000) 4897–4902. doi:10.1073/pnas.97.9.4897.

[255] Z. Qin, D. Hu, S. Han, D.P. Hong, A.L. Fink, Role of different regions of alpha-synuclein in the assembly of fibrils, Biochemistry. 46 (2007) 13322–13330. doi:10.1021/bi7014053.

[256] M.S. Celej, R. Sarroukh, E. Goormaghtigh, G.D. Fidelio, J.-M. Ruysschaert, V. Raussens, Toxic prefibrillar α-synuclein amyloid oligomers adopt a distinctive antiparallel β-sheet structure, Biochem. J. 443 (2012) 719–726. doi:10.1042/BJ20111924.

[257] M. Vilar, H.-T. Chou, T. Luhrs, S.K. Maji, D. Riek-Loher, R. Verel, G. Manning, H. Stahlberg, R. Riek, The fold of alpha-synuclein fibrils, Proc. Natl. Acad. Sci. 105 (2008) 8637–8642. doi:10.1073/pnas.0712179105.

[258] G. Lv, A. Kumar, K. Giller, M.L. Orcellet, D. Riedel, C.O. Fernández, S. Becker, A. Lange, Structural comparison of mouse and human α-synuclein amyloid fibrils by solid-state NMR, J. Mol. Biol. 420 (2012) 99–111. doi:10.1016/j.jmb.2012.04.009.

[259] M.E. Van Raaij, J. Van Gestel, I.M.J. Segers-Nolten, S.W. De Leeuw, V. Subramaniam, Concentration dependence of α-synuclein fibril length assessed by quantitative atomic force microscopy and statistical-mechanical theory, Biophys. J. 95 (2008) 4871–4878. doi:10.1529/biophysj.107.127464.

[260] L. Bousset, L. Pieri, G. Ruiz-Arlandis, J. Gath, P.H. Jensen, B. Habenstein, K. Madiona, V. Olieric, A. Böckmann, B.H. Meier, R. Melki, Structural and functional characterization of two alpha-synuclein strains, Nat. Commun. 4 (2013) 2575. doi:10.1038/ncomms3575.

[261] N. Plotegher, E. Greggio, M. Bisaglia, L. Bubacco, Biophysical groundwork as a hinge to unravel the biology of α-synuclein aggregation and toxicity, Q. Rev. Biophys. 47 (2014) 1–48. doi:10.1017/S0033583513000097.

[262] S.A. Tanik, C.E. Schultheiss, L.A. Volpicelli-Daley, K.R. Brunden, V.M.Y. Lee, Lewy Body-like α-Synuclein Aggregates Resist Degradation and Impair Macroautophagy, J. Biol. Chem. 288 (2013) 15194–15210. doi:10.1074/jbc.M113.457408.

[263] E. Sparr, M.F.M. Engel, D. V. Sakharov, M. Sprong, J. Jacobs, B. De Kruijff, J.W.M. Höppener, J. Antoinette Killian, Islet amyloid polypeptide-induced membrane leakage involves uptake of lipids by forming amyloid fibers, FEBS Lett. 577 (2004) 117–120. doi:10.1016/j.febslet.2004.09.075.

[264] N.P. Reynolds, A. Soragni, M. Rabe, D. Verdes, E. Liverani, S. Handschin, R. Riek, S. Seeger, Mechanism of membrane interaction and disruption by α-synuclein, J. Am. Chem. Soc. 133 (2011) 19366–19375. doi:10.1021/ja2029848.

[265] J.H. Lee, C.S. Hong, S. Lee, J.E. Yang, Y. Il Park, D. Lee, T. Hyeon, S. Jung, S.R. Paik, Radiating Amyloid Fibril Formation on the Surface of Lipid Membranes through Unit-Assembly of Oligomeric Species of α-Synuclein, PLoS One. 7 (2012) e47580. doi:10.1371/journal.pone.0047580.

[266] B.D. van Rooijen, M.M.A.E. Claessens, V. Subramaniam, Lipid bilayer disruption by oligomeric α-synuclein depends on bilayer charge and accessibility of the hydrophobic core, Biochim. Biophys. Acta - Biomembr. 1788 (2009) 1271–1278. doi:10.1016/j.bbamem.2009.03.010.

[267] H. Chaudhary, A.N.D. Stefanovic, V. Subramaniam, M.M.A.E. Claessens, Membrane interactions and fibrillization of α-synuclein play an essential role in membrane disruption, FEBS Lett. 588 (2014) 4457–4463. doi:10.1016/j.febslet.2014.10.016.

[268] M. Pantusa, B. Vad, O. Lillelund, L. Kjær, D. Otzen, R. Bartucci, Alpha-synuclein and familial variants affect the chain order and the thermotropic phase behavior of anionic lipid vesicles, Biochim. Biophys. Acta - Proteins Proteomics. 1864 (2016) 1206–1214. doi:10.1016/j.bbapap.2016.05.003.

[269] K. Pirc, N.P. Ulrih, α-Synuclein interactions with phospholipid model membranes: Key roles for electrostatic interactions and lipid-bilayer structure, Biochim. Biophys. Acta - Biomembr. 1848 (2015) 2002–2012. doi:10.1016/j.bbamem.2015.06.021.

[270] A.R. Braun, M.M. Lacy, V.C. Ducas, E. Rhoades, J.N. Sachs, α-synuclein-induced membrane remodeling is driven by binding affinity, partition depth, and interleaflet order asymmetry, J. Am. Chem. Soc. 136 (2014) 9962–9972. doi:10.1021/ja5016958.

[271] Z. Shi, J.N. Sachs, E. Rhoades, T. Baumgart, Biophysics of α-synuclein induced membrane remodelling, Phys. Chem. Chem. Phys. 17 (2015) 15561–15568. doi:10.1039/c4cp05883f.

[272] C.H. Westphal, S.S. Chandra, Monomeric synucleins generate membrane curvature, J. Biol. Chem. 288 (2013) 1829–1840. doi:10.1074/jbc.M112.418871.

[273] M.M. Ouberai, J. Wang, M.J. Swann, C. Galvagnion, T. Guilliams, C.M. Dobson, M.E. Welland, α-Synuclein senses lipid packing defects and induces lateral expansion of lipids leading to membrane remodeling, J. Biol. Chem. 288 (2013) 20883–20895. doi:10.1074/jbc.M113.478297.

[274] M. Stöckl, P. Fischer, E. Wanker, A. Herrmann, α-Synuclein Selectively Binds to Anionic Phospholipids Embedded in Liquid-Disordered Domains, J. Mol. Biol. 375 (2008) 1394–1404. doi:10.1016/j.jmb.2007.11.051.

[275] M. Garten, C. Prévost, C. Cadart, R. Gautier, L. Bousset, R. Melki, P. Bassereau, S. Vanni, Methyl-branched lipids promote the membrane adsorption of α-synuclein by enhancing shallow lipid-packing defects, Phys. Chem. Chem. Phys. 17 (2015) 15589–15597. doi:10.1039/c5cp00244c.

[276] G. Fusco, A. De Simone, T. Gopinath, V. Vostrikov, M. Vendruscolo, C.M. Dobson, G. Veglia, Direct observation of the three regions in α-synuclein that determine its membrane-bound behaviour, Nat. Commun. 5 (2014) 3827. doi:10.1038/ncomms4827.

[277] C. Galvagnion, The Role of Lipids Interacting with α-Synuclein in the Pathogenesis of Parkinson's Disease, J. Parkinsons. Dis. 7 (2017) 433–450. doi:10.3233/JPD-171103.

[278] G. Marie, C.J. Dunning, R. Gaspar, C. Grey, P. Brundin, E. Sparr, S. Linse, Acceleration of α-synuclein aggregation by exosomes, J. Biol. Chem. 290 (2015) 2969–2982. doi:10.1074/jbc.M114.585703.

[279] M. Zhu, J. Li, A.L. Fink, The association of α-synuclein with membranes affects bilayer structure, stability, and fibril formation, J. Biol. Chem. 278 (2003) 40186–40197. doi:10.1074/jbc.M305326200.

[280] J. Magalhaes, M.E. Gegg, A. Migdalska-Richards, M.K. Doherty, P.D. Whitfield, A.H.V. Schapira, Autophagic lysosome reformation dysfunction in glucocerebrosidase deficient cells: Relevance to Parkinson disease, Hum. Mol. Genet. 25 (2015) 3432–3445. doi:10.1093/hmg/ddw185.

[281] G.A. Grabowski, Phenotype, diagnosis, and treatment of Gaucher's disease, Lancet. 372 (2008) 1263–1271. doi:10.1016/S0140-6736(08)61522-6.

[282] R.B. Chan, A.J. Perotte, B. Zhou, C. Liong, E.J. Shorr, K.S. Marder, U.J. Kang, C.H. Waters, O.A. Levy, Y. Xu, H. Bin Shim, I. Pe'Er, G. Di Paolo, R.N. Alcalay, Elevated GM3 plasma concentration in idiopathic Parkinson's disease: A lipidomic analysis, PLoS One. 12 (2017) e0172348. doi:10.1371/journal.pone.0172348.

[283] W.A. Den Hartog Jager, Sphingomyelin in Lewy Inclusion Bodies in Parkinson's Disease, Arch. Neurol. 21 (1969) 615–619. doi:10.1001/archneur.1969.00480180071006.

[284] M.R. Issidorides, C. Mytilineou, M.T. Panayotacopoulou, M.D. Yahr, Lewy bodies in parkinsonism share components with intraneuronal protein bodies of normal brains, J. Neural Transm. - Park. Dis. Dement. Sect. 3 (1991) 49–61. doi:10.1007/BF02251136.

[285] H.-J. Lee, C. Choi, S.-J. Lee, Membrane-bound alpha-synuclein has a high aggregation propensity and the ability to seed the aggregation of the cytosolic form., J. Biol. Chem. 277 (2002) 671–8. doi:10.1074/jbc.M107045200.

[286] Z. Martinez, M. Zhu, S.B. Han, A.L. Fink, GM1 specifically interacts with alpha-synuclein and inhibits fibrillation, Biochemistry. 46 (2007) 1868–1877. doi:10.1021/bi061749a.

[287] P. Arosio, M. Vendruscolo, C.M. Dobson, T.P.J. Knowles, Chemical kinetics for drug discovery to combat protein aggregation diseases, Trends Pharmacol. Sci. 35 (2014) 127–135. doi:10.1016/j.tips.2013.12.005.

[288] E. Kojro, G. Gimpl, S. Lammich, W. Marz, F. Fahrenholz, Low cholesterol stimulates the nonamyloidogenic pathway by its effect on the alpha-secretase ADAM 10, Proc. Natl. Acad. Sci. 98 (2001) 5815–5820. doi:10.1073/pnas.081612998.

[289] M. Simons, P. Keller, B. De Strooper, K. Beyreuther, C.G. Dotti, K. Simons, Cholesterol depletion inhibits the generation of beta-amyloid in hippocampal neurons, Proc. Natl. Acad. Sci. U. S. A. 95 (1998) 6460–6464. doi:10.1073/pnas.95.11.6460.

[290] M. Valenza, D. Rigamonti, D. Goffredo, C. Zuccato, S. Fenu, L. Jamot, A. Strand, A. Tarditi, B. Woodman, M. Racchi, C. Mariotti, S. Di Donato, A. Corsini, G. Bates, R. Pruss, J.M. Olson, S.

Sipione, M. Tartari, E. Cattaneo, Dysfunction of the Cholesterol Biosynthetic Pathway in Huntington's Disease, J. Neurosci. 25 (2005) 9932–9939. doi:10.1523/JNEUROSCI.3355-05.2005.

[291] J.E. Vance, Transfer of cholesterol by the NPC team, Cell Metab. 12 (2010) 105–106. doi:10.1016/j.cmet.2010.07.004.

[292] M.L. Wang, M. Motamed, R.E. Infante, L. Abi-Mosleh, H.J. Kwon, M.S. Brown, J.L. Goldstein, Identification of surface residues on Niemann-Pick C2 essential for hydrophobic handoff of cholesterol to NPC1 in lysosomes, Cell Metab. 12 (2010) 166–173. doi:10.1016/j.cmet.2010.05.016.

[293] D. Lutjohann, O. Breuer, G. Ahlborg, I. Nennesmo, A. Siden, U. Diczfalusy, I. Bjorkhem, Cholesterol homeostasis in human brain: evidence for an age-dependent flux of 24S-hydroxycholesterol from the brain into the circulation., Proc. Natl. Acad. Sci. 93 (1996) 9799–9804. doi:10.1073/pnas.93.18.9799.

[294] G. Hu, R. Antikainen, P. Jousilahti, M. Kivipelto, J. Tuomilehto, Total cholesterol and the risk of Parkinson disease, Neurology. 70 (2008) 1972–1979. doi:10.1212/01.wnl.0000312511.62699.a8.

[295] K.M. Powers, T. Smith-Weller, G.M. Franklin, W.T. Longstreth, P.D. Swanson, H. Checkoway, H. Checkoway, Dietary fats, cholesterol and iron as risk factors for Parkinson's disease., Parkinsonism Relat. Disord. 15 (2009) 47–52. doi:10.1016/j.parkreldis.2008.03.002.

[296] L.M.L. de Lau, M. Bornebroek, J.C.M. Witteman, A. Hofman, P.J. Koudstaal, M.M.B. Breteler, Dietary fatty acids and the risk of Parkinson disease: The Rotterdam Study, Neurology. 64 (2005) 2040–2045. doi:10.1212/01.WNL.0000166038.67153.9F.

[297] X. Huang, P. Auinger, S. Eberly, D. Oakes, M. Schwarzschild, A. Ascherio, R. Mailman, H. Chen, Serum cholesterol and the progression of parkinson's disease: Results from DATATOP, PLoS One. 6 (2011) e22854. doi:10.1371/journal.pone.0022854.

[298] D.A. Bosco, D.M. Fowler, Q. Zhang, J. Nieva, E.T. Powers, P. Wentworth, R.A. Lerner, J.W. Kelly, Elevated levels of oxidized cholesterol metabolites in Lewy body disease brains accelerate α-synuclein fibrilization, Nat. Chem. Biol. 2 (2006) 249–253. doi:10.1038/nchembio782.

[299] D. Cheng, A.M. Jenner, G. Shui, W.F. Cheong, T.W. Mitchell, J.R. Nealon, W.S. Kim, H. McCann, M.R. Wenk, G.M. Halliday, B. Garner, Lipid pathway alterations in parkinson's disease primary visual cortex, PLoS One. 6 (2011) e17299. doi:10.1371/journal.pone.0017299.

[300] D.J. Sillence, V. Puri, D.L. Marks, T.D. Butters, R.A. Dwek, R.E. Pagano, F.M. Platt, Glucosylceramide modulates membrane traffic along the endocytic pathway, J. Lipid Res. 43 (2002) 1837–1845. doi:10.1194/jlr.M200232-JLR200.

[301] Y. Takahashi, S. Nada, S. Mori, T. Soma-Nagae, C. Oneyama, M. Okada, The late endosome/lysosome-anchored p18-mTORC1 pathway controls terminal maturation of lysosomes, Biochem. Biophys. Res. Commun. 417 (2012) 1151–1157. doi:10.1016/j.bbrc.2011.12.082.

[302] C. Bissig, J. Gruenberg, Lipid sorting and multivesicular endosome biogenesis, Cold Spring Harb. Perspect. Biol. 5 (2013) a016816–a016816. doi:10.1101/cshperspect.a016816.

[303] V. Dias, E. Junn, M.M. Mouradian, The role of oxidative stress in parkinson's disease, J. Parkinsons. Dis. 3 (2013) 461–491. doi:10.3233/JPD-130230.

[304] C. Di Scala, N. Yahi, S. Boutemeur, A. Flores, L. Rodriguez, H. Chahinian, J. Fantini, Common molecular mechanism of amyloid pore formation by Alzheimer's beta-amyloid peptide and alpha-synuclein, Sci. Rep. 6 (2016) 28781. doi:10.1038/srep28781.

[305] J. Fantini, D. Carlus, N. Yahi, The fusogenic tilted peptide (67–78) of α-synuclein is a cholesterol binding domain, Biochim. Biophys. Acta - Biomembr. 1808 (2011) 2343–2351. doi:10.1016/J.BBAMEM.2011.06.017.

[306] J.H.T. Hsiao, G.M. Halliday, W.S. Kim, α-Synuclein regulates neuronal cholesterol efflux, Molecules. 22 (2017) 1769. doi:10.3390/molecules22101769.

[307] E.I. O'Leary, Z. Jiang, M.-P. Strub, J.C. Lee, E.I. O'Leary, Z. Jiang, M.-P. Strub, J.C. Lee, Effects of phosphatidylcholine membrane fluidity on the conformation and aggregation of N-terminally acetylated α-synuclein, J. Biol. Chem. (2018) jbc.RA118.002780. doi:10.1074/jbc.RA118.002780.

[308] V. V. Shvadchak, L.J. Falomir-Lockhart, D.A. Yushchenko, T.M. Jovin, Specificity and Kinetics of α-Synuclein Binding to Model Membranes Determined with Fluorescent Excited State Intramolecular Proton Transfer (ESIPT) Probe, J. Biol. Chem. 286 (2011) 13023–13032. doi:10.1074/jbc.M110.204776.

[309] C. Power, K.D. Patel, Neurolipidomics: An inflammatory perspective on fat in the brain, Neurology. 63 (2004) 608–609. doi:10.1002/jcc.22981.

[310] M.J. Hawrylycz, E.S. Lein, A.L. Guillozet-Bongaarts, E.H. Shen, L. Ng, J.A. Miller, L.N. Van De Lagemaat, K.A. Smith, A. Ebbert, Z.L. Riley, C. Abajian, C.F. Beckmann, A. Bernard, D. Bertagnolli, A.F. Boe, P.M. Cartagena, M. Mallar Chakravarty, M. Chapin, J. Chong, R.A. Dalley, B.D. Daly, C. Dang, S. Datta, N. Dee, T.A. Dolbeare, V. Faber, D. Feng, D.R. Fowler, J. Goldy, B.W. Gregor, Z. Haradon, D.R. Haynor, J.G. Hohmann, S. Horvath, R.E. Howard, A. Jeromin, J.M. Jochim, M. Kinnunen, C. Lau, E.T. Lazarz, C. Lee, T.A. Lemon, L. Li, Y. Li, J.A. Morris, C.C. Overly, P.D. Parker, S.E. Parry, M. Reding, J.J. Royall, J. Schulkin, P.A. Sequeira, C.R. Slaughterbeck, S.C. Smith, A.J. Sodt, S.M. Sunkin, B.E. Swanson, M.P. Vawter, D. Williams, P. Wohnoutka, H. Ronald Zielke, D.H. Geschwind, P.R. Hof, S.M. Smith, C. Koch, S.G.N. Grant, A.R. Jones, An anatomically comprehensive atlas of the adult human brain transcriptome, Nature. 489 (2012) 391–399. doi:10.1038/nature11405.

[311] X. Han, Neurolipidomics: challenges and developments., Front. Biosci. 12 (2007) 2601–15. http://www.ncbi.nlm.nih.gov/pubmed/17127266 (accessed November 26, 2018).

[312] A. Naudí, R. Cabré, M. Jové, V. Ayala, H. Gonzalo, M. Portero-Otín, I. Ferrer, R. Pamplona, Lipidomics of Human Brain Aging and Alzheimer's Disease Pathology, in: Int. Rev. Neurobiol., 2015: pp. 133–189. doi:10.1016/bs.irn.2015.05.008.

[313] J.M. Dietschy, S.D. Turley, Cholesterol metabolism in the brain, Curr. Opin. Lipidol. 12 (2001) 105–112. doi:10.1097/00041433-200104000-00003.

[314] J.S. O'Brien, E.L. Sampson, Lipid composition of the normal human brain: gray matter, white matter, and myelin., J. Lipid Res. 6 (1965) 537–44. http://www.ncbi.nlm.nih.gov/pubmed/5865382 (accessed November 26, 2018).

[315] J.S. O'Brien, E.L. Sampson, Fatty acid and fatty aldehyde composition of the major brain lipids in normal human gray matter, white matter, and myelin., J. Lipid Res. 6 (1965) 545–51. http://www.ncbi.nlm.nih.gov/pubmed/5865383 (accessed November 26, 2018).

[316] R. V Panganamala, L.A. Horrocks, J.C. Geer, D.G. Cornwell, Positions of double bonds in the monounsaturated alk-1-enyl groups from the plasmalogens of human heart and brain, Chem. Phys. Lipids. 6 (1971) 97–102. doi:10.1016/0009-3084(71)90031-4.

[317] G. Rouser, C. Galli, G. Kritchevsky, Lipid class composition of normal human brain and variations in metachromatic leucodystrophy, Tay-Sachs, Niemann-Pick, chronic gaucher's and Alzheimer's diseases, J. Am. Oil Chem. Soc. 42 (1965) 404–410. doi:10.1007/BF02635576.

[318] G. Rouser, G. Feldman, C. Galli, Fatty acid compositions of human brain lecithin and sphingomyelin in normal individuals, senile cerebral cortical atrophy, Alzheimer's disease, metachromatic leucodystrophy, Tay-Sachs and Niemann-Pick diseases, J. Am. Oil Chem. Soc. 42 (1965) 411–412. doi:10.1007/BF02635577.

[319] G. Rouser, A. Yamamoto, Curvilinear regression course of human brain lipid composition changes with age, Lipids. 3 (1968) 284–287. doi:10.1007/BF02531202.

[320] W.T. Norton, S.E. Poduslo, K. Suzuki, Subacute sclerosing leukoencephalitis: II. Chemical studies including abnormal myelin and an abnormal ganglioside pattern, J. Neuropathol. Exp. Neurol. 25 (1966) 582–597. doi:10.1097/00005072-196610000-00006.

[321] K. Kahma, J. Brotherus, M. Haltia, O. Renkonen, Low and moderate concentrations of lysobisphosphatidic acid in brain and liver of patients affected by some storage diseases, Lipids. 11 (1976) 539–544. doi:10.1007/BF02532899.

[322] R.H. Houtkooper, F.M. Vaz, Cardiolipin, the heart of mitochondrial metabolism, Cell. Mol. Life Sci. 65 (2008) 2493–2506. doi:10.1007/s00018-008-8030-5.

[323] M. Maceyka, S. Spiegel, Sphingolipid metabolites in inflammatory disease, Nature. 510 (2014) 58–67. doi:10.1038/nature13475.

[324] P.S. Sastry, Lipids of nervous tissue: Composition and metabolism, Prog. Lipid Res. 24 (1985) 69–176. doi:10.1016/0163-7827(85)90011-6.

[325] M. Jové, M. Portero-Otín, A. Naudí, I. Ferrer, R. Pamplona, Metabolomics of human brain aging and age-related neurodegenerative diseases, J. Neuropathol. Exp. Neurol. 73 (2014) 640–657. doi:10.1097/NEN.0000000000000091.

[326] M.P. Mattson, T. Magnus, Ageing and neuronal vulnerability, Nat. Rev. Neurosci. 7 (2006) 278–294. doi:10.1038/nrn1886.

[327] X. Wang, M. L. Michaelis, E. K. Michaelis, Functional Genomics of Brain Aging and Alzheimers Disease: Focus on Selective Neuronal Vulnerability, Curr. Genomics. 11 (2010) 618–633. doi:10.2174/138920210793360943.

[328] H. Braak, K. Del Tredici, U. Rüb, R.A.I. De Vos, E.N.H. Jansen Steur, E. Braak, Staging of brain pathology related to sporadic Parkinson's disease, Neurobiol. Aging. 24 (2003) 197–211. doi:10.1016/S0197-4580(02)00065-9.

[329] J.H. Morrison, P.R. Hof, Life and death of neurons in the aging brain., Science. 278 (1997) 412–9. http://www.ncbi.nlm.nih.gov/pubmed/9334292 (accessed November 29, 2018).

[330] B.M. Morrison, P.R. Hof, J.H. Morrison, Determinants of neuronal vulnerability in neurodegenerative diseases, Ann. Neurol. 44 (1998) S32–S44. doi:10.1016/S1474-4422(07)70295-8.

[331] R.D. Terry, R. DeTeresa, L.A. Hansen, Neocortical cell counts in normal human adult aging, Ann. Neurol. 21 (1987) 530–539. doi:10.1002/ana.410210603.

[332] P. Giannakopoulos, G. Gold, J.P. Michel, C. Bouras, Cellular vulnerability in brain aging and Alzheimer's disease. Clinical correlates and molecular background., Ann. Med. Interne (Paris). 149 (1998) 187–91. http://www.ncbi.nlm.nih.gov/pubmed/11490545 (accessed November 29, 2018).

[333] M. BURGER, K. SEIDEL, [Chemical biomorphosis of the human brain and sciatic nerve; a survey]., Z. Alternsforsch. 12 (1958) 52–79. http://www.ncbi.nlm.nih.gov/pubmed/13593524 (accessed November 30, 2018).

[334] L. Svennerholm, K. Boström, B. Jungbjer, L. Olsson, Membrane lipids of adult human brain: lipid composition of frontal and temporal lobe in subjects of age 20 to 100 years., J. Neurochem. 63 (1994) 1802–11. http://www.ncbi.nlm.nih.gov/pubmed/7931336 (accessed November 30, 2018).

[335] R.K. McNamara, Y. Liu, R. Jandacek, T. Rider, P. Tso, The aging human orbitofrontal cortex: Decreasing polyunsaturated fatty acid composition and associated increases in lipogenic gene expression and stearoyl-CoA desaturase activity, Prostaglandins Leukot. Essent. Fat. Acids. 78 (2008) 293–304. doi:10.1016/j.plefa.2008.04.001.

[336] M. Söderberg, C. Edlund, K. Kristensson, G. Dallner, Lipid Compositions of Different Regions of the Human Brain During Aging, J. Neurochem. 54 (1990) 415–423. doi:10.1111/j.1471-4159.1990.tb01889.x.

[337] B.M. Ross, N. Mamalias, A. Moszczynska, A.H. Rajput, S.J. Kish, Elevated activity of phospholipid biosynthetic enzymes in substantia nigra of patients with Parkinson's disease, Neuroscience. 102 (2001) 899–904. doi:10.1016/S0306-4522(00)00501-7.

[338] G.M. Halliday, A. Ophof, M. Broe, P.H. Jensen, E. Kettle, H. Fedorow, M.I. Cartwright, F.M. Griffiths, C.E. Shepherd, K.L. Double, α-Synuclein redistributes to neuromelanin lipid in the substantia nigra early in Parkinson's disease, Brain. 128 (2005) 2654–2664. doi:10.1093/brain/awh584.

[339] P.L. Wood, S. Tippireddy, J. Feriante, R.L. Woltjer, Augmented frontal cortex diacylglycerol levels in Parkinson's disease and Lewy Body Disease, PLoS One. 13 (2018) e0191815. doi:10.1371/journal.pone.0191815.

[340] I.G. Denisov, S.G. Sligar, Nanodiscs in Membrane Biochemistry and Biophysics, Chem. Rev. 117 (2017) 4669–4713. doi:10.1021/acs.chemrev.6b00690.

[341] J.M. Dörr, S. Scheidelaar, M.C. Koorengevel, J.J. Dominguez, M. Schäfer, C.A. van Walree, J.A. Killian, The styrene–maleic acid copolymer: a versatile tool in membrane research, Eur. Biophys. J. 45 (2016) 3–21. doi:10.1007/s00249-015-1093-y.

[342] A. Wlodawer, J.P. Segrest, B.H. Chung, R. Chiovetti, J.N. Weinstein, High-density lipoprotein recombinants: evidence for a bicycle tire micelle structure obtained by neutron scattering and electron microscopy, FEBS Lett. 104 (1979) 231–235. doi:10.1016/0014-5793(79)80821-2.

[343] T.H. Bayburt, S.G. Sligar, Membrane protein assembly into Nanodiscs, FEBS Lett. 584 (2010) 1721–1727. doi:10.1016/j.febslet.2009.10.024.

[344] T.H. Bayburt, Y. V. Grinkova, S.G. Sligar, Self-Assembly of Discoidal Phospholipid Bilayer Nanoparticles with Membrane Scaffold Proteins, Nano Lett. 2 (2002) 853–856. doi:10.1021/nl025623k.

[345] C.G. Brouillette, G.M. Anantharamaiah, J.A. Engler, D.W. Borhani, Structural models of human apolipoprotein A-I: A critical analysis and review, Biochim. Biophys. Acta - Mol. Cell Biol. Lipids. 1531 (2001) 4–46. doi:10.1016/S1388-1981(01)00081-6.

[346] I.G. Denisov, Y. V. Grinkova, A.A. Lazarides, S.G. Sligar, Directed Self-Assembly of Monodisperse Phospholipid Bilayer Nanodiscs with Controlled Size, J. Am. Chem. Soc. 126 (2004) 3477–3487. doi:10.1021/ja0393574.

[347] T.K. Ritchie, Y. V Grinkova, T.H. Bayburt, I.G. Denisov, J.K. Zolnerciks, W.M. Atkins, S.G. Sligar, Chapter 11 - Reconstitution of membrane proteins in phospholipid bilayer nanodiscs., Methods Enzymol. 464 (2009) 211–31. doi:10.1016/S0076-6879(09)64011-8.

[348] Z. Yao, B.G. Li, W.J. Wang, Z.R. Pan, Continuous thermal bulk copolymerization of styrene and maleic anhydride, J. Appl. Polym. Sci. 73 (1999) 615–622. doi:10.1002/(SICI)1097-4628(19990801)73:5<615::AID-APP1>3.0.CO;2-1.

[349] B. Klumperman, Mechanistic considerations on styrene-maleic anhydride copolymerization reactions, Polym. Chem. 1 (2010) 558–562. doi:10.1039/b9py00341j.

[350] S. Scheidelaar, M.C. Koorengevel, J.D. Pardo, J.D. Meeldijk, E. Breukink, J.A. Killian, Molecular Model for the solubilization of membranes into nanodisks by styrene maleic acid copolymers, Biophys. J. 108 (2015) 279–290. doi:10.1016/j.bpj.2014.11.3464.

[351] A. Grethen, D. Glueck, S. Keller, Role of Coulombic Repulsion in Collisional Lipid Transfer Among SMA(2:1)-Bounded Nanodiscs, J. Membr. Biol. 251 (2018) 443–451. doi:10.1007/s00232-018-0024-0.

[352] C.T. Schwall, V.L. Greenwood, N.N. Alder, The stability and activity of respiratory Complex II is cardiolipin-dependent, Biochim. Biophys. Acta - Bioenerg. 1817 (2012) 1588–1596. doi:10.1016/j.bbabio.2012.04.015.

[353] A.R. Long, C.C. O'Brien, K. Malhotra, C.T. Schwall, A.D. Albert, A. Watts, N.N. Alder, A detergent-free strategy for the reconstitution of active enzyme complexes from native biological membranes into nanoscale discs, BMC Biotechnol. 13 (2013) 41. doi:10.1186/1472-6750-13-41.

[354] K. Malhotra, N.N. Alder, Advances in the use of nanoscale bilayers to study membrane protein structure and function, Biotechnol. Genet. Eng. Rev. 30 (2014) 79–93. doi:10.1080/02648725.2014.921502.

[355] E.G. Bligh, W.J. Dyer, A Rapid Method Of Total Lipid Extraction And Purification, Can. J. Biochem. Physiol. 37 (1959) 911–917. doi:10.1139/o59-099.

[356] G. van Meer, A.I.P.M. de Kroon, Lipid map of the mammalian cell, J. Cell Sci. 124 (2011) 5–8. doi:10.1242/jcs.071233.

[357] T. Róg, M. Pasenkiewicz-Gierula, I. Vattulainen, M. Karttunen, Ordering effects of cholesterol and its analogues, Biochim. Biophys. Acta - Biomembr. 1788 (2009) 97–121. doi:10.1016/j.bbamem.2008.08.022.

[358] M. Simons, P. Keller, B. De Strooper, K. Beyreuther, C.G. Dotti, K. Simons, Cholesterol depletion inhibits the generation of beta-amyloid in hippocampal neurons., Proc. Natl. Acad. Sci. U. S. A. 95 (1998) 6460–4. http://www.ncbi.nlm.nih.gov/pubmed/9600988 (accessed October 2, 2018).

[359] H. LeVine, Quantification of β-sheet amyloid fibril structures with thioflavin T, Methods Enzymol. 309 (1999) 274–284. doi:10.1016/S0076-6879(99)09020-5.

[360] J. Jass, T. Tjärnhage, G. Puu, From liposomes to supported, planar bilayer structures on hydrophilic and hydrophobic surfaces: An atomic force microscopy study, Biophys. J. 79 (2000) 3153–3163. doi:10.1016/S0006-3495(00)76549-0.

[361] E.S. Voropai, M.P. Samtsov, K.N. Kaplevskii, A.A. Maskevich, V.I. Stepuro, O.I. Povarova, I.M. Kuznetsova, K.K. Turoverov, A.L. Fink, V.N. Uverskii, Spectral properties of thioflavin T and its complexes with amyloid fibrils, J. Appl. Spectrosc. 70 (2003) 868–874. doi:10.1023/B:JAPS.0000016303.37573.7e.

[362] S.A. Hudson, H. Ecroyd, T.W. Kee, J.A. Carver, The thioflavin T fluorescence assay for amyloid fibril detection can be biased by the presence of exogenous compounds, FEBS J. 276 (2009) 5960–5972. doi:10.1111/j.1742-4658.2009.07307.x.

[363] K. Afitska, A. Fucikova, V. V. Shvadchak, D.A. Yushchenko, Modification of C Terminus Provides New Insights into the Mechanism of α -Synuclein Aggregation, Biophys. J. 113 (2017) 2182–2191. doi:10.1016/j.bpj.2017.08.027.

[364] C.W.T. Leung, F. Guo, Y. Hong, E. Zhao, R.T.K. Kwok, N.L.C. Leung, S. Chen, N.N. Vaikath, O.M. El-Agnaf, Y. Tang, W.P. Gai, B.Z. Tang, Detection of oligomers and fibrils of α-synuclein by AIEgen with strong fluorescence, Chem. Commun. 51 (2015) 1866–1869. doi:10.1039/c4cc07911f.

[365] B. Liang, L.K. Tamm, Solution NMR of SNAREs, complexin and α-synuclein in association with membrane-mimetics, Prog. Nucl. Magn. Reson. Spectrosc. 105 (2018) 41–53. doi:10.1016/j.pnmrs.2018.02.001.

[366] M.S. Terakawa, Y.-H. Lee, M. Kinoshita, Y. Lin, T. Sugiki, N. Fukui, T. Ikenoue, Y. Kawata, Y. Goto, Membrane-induced initial structure of α-synuclein control its amyloidogenesis on model membranes, Biochim. Biophys. Acta - Biomembr. 1860 (2018) 757–766. doi:10.1016/J.BBAMEM.2017.12.011.

[367] K. Beyer, Mechanistic aspects of Parkinson's disease: α-synuclein and the biomembrane, Cell Biochem. Biophys. 47 (2007) 285–299. doi:10.1007/s12013-007-0014-9.

[368] M.D. Shortridge, D.S. Hage, G.S. Harbison, R. Powers, Estimating Protein-Ligand Binding Affinity using High- Throughput Screening by NMR, J Comb Chem. 10 (2009) 948–958. doi:10.1021/cc800122m.Estimating.

[369] M. Grey, S. Linse, H. Nilsson, P. Brundin, E. Sparr, Membrane interaction of α-synuclein in different aggregation states, J. Parkinsons. Dis. 1 (2011) 359–371. doi:10.3233/JPD-2011-11067.

[370] V.N. Uversky, E. M. Cooper, K.S. Bower, J. Li, A.L. Fink, Accelerated α-synuclein fibrillation in crowded milieu, FEBS Lett. 515 (2002) 99–103. doi:10.1016/S0014-5793(02)02446-8.

[371] T. Viennet, M.M. Wördehoff, B. Uluca, C. Poojari, H. Shaykhalishahi, D. Willbold, B. Strodel, H. Heise, A.K. Buell, W. Hoyer, M. Etzkorn, Structural insights from lipid-bilayer nanodiscs link α-Synuclein membrane-binding modes to amyloid fibril formation, Commun. Biol. 1 (2018) 44. doi:10.1038/s42003-018-0049-z.

[372] T. Jemmi, R. Stephan, Listeria monocytogenes: food-borne pathogen and hygiene indicator., Rev. Sci. Tech. 25 (2006) 571–80. http://www.ncbi.nlm.nih.gov/pubmed/17094698 (accessed January 12, 2019).

[373] T. Chakraborty, T. Hain, E. Domann, Genome organization and the evolution of the virulence gene locus in Listeria species, Int. J. Med. Microbiol. 290 (2000) 167–174. doi:10.1016/S1438-4221(00)80086-7.

[374] S. Furse, M.R. Egmond, J.A. Killian, Isolation of lipids from biological samples, Mol. Membr. Biol. 32 (2015) 55–64. doi:10.3109/09687688.2015.1050468.

[375] S. Furse, H. Wienk, R. Boelens, A.I.P.M. de Kroon, J.A. Killian, E. coli MG1655 modulates its phospholipid composition through the cell cycle, Febs Lett. 589 (2015) 2726–2730. doi:10.1016/j.febslet.2015.07.043.

[376] I. Pradas, K. Huynh, R. Cabré, V. Ayala, P.J. Meikle, M. Jové, R. Pamplona, Lipidomics reveals a tissue-specific fingerprint, Front. Physiol. 9 (2018). doi:10.3389/fphys.2018.01165.

[377] C. Klose, M.A. Surma, M.J. Gerl, F. Meyenhofer, A. Shevchenko, K. Simons, Flexibility of a eukaryotic lipidome - insights from yeast lipidomics, PLoS One. 7 (2012) e35063. doi:10.1371/journal.pone.0035063.

[378] H. Xicoy, B. Wieringa, G.J.M. Martens, The SH-SY5Y cell line in Parkinson's disease research: a systematic review, Mol. Neurodegener. 12 (2017) 1–11. doi:10.1186/s13024-017-0149-0.

[379] J. Kovalevich, D. Langford, Considerations for the use of SH-SY5Y neuroblastoma cells in neurobiology, Methods Mol. Biol. 1078 (2013) 9–21. doi:10.1007/978-1-62703-640-5_2.

[380] B.T. Layden, A.M. Abukhdeir, C. Malarkey, L.A. Oriti, W. Salah, C. Stigler, C.F.G.C. Geraldes, D.M. De Freitas, Identification of Li+binding sites and the effect of Li+treatment on phospholipid composition in human neuroblastoma cells: A7Li and31P NMR study, Biochim. Biophys. Acta - Mol. Basis Dis. 1741 (2005) 339–349. doi:10.1016/j.bbadis.2005.07.004.

I

II

SCIENTIFIC REPORTS

OPEN

Evidence that *Listeria innocua* modulates its membrane's stored curvature elastic stress, but not fluidity, through the cell cycle

Received: 13 January 2017
Accepted: 20 June 2017
Published online: 14 August 2017

Samuel Furse[1], Martin Jakubec[1], Frode Rise[3], Huw E. Williams[2], Catherine E. D. Rees[4] & Øyvind Halskau[1]

This paper reports that the abundances of endogenous cardiolipin and phosphatidylethanolamine halve during elongation of the Gram-positive bacterium *Listeria innocua*. The lyotropic phase behaviour of model lipid systems that describe these modulations in lipid composition indicate that the average stored curvature elastic stress of the membrane is reduced on elongation of the cell, while the fluidity appears to be maintained. These findings suggest that phospholipid metabolism is linked to the cell cycle and that changes in membrane composition can facilitate passage to the succeding stage of the cell cycle. This therefore suggests a means by which bacteria can manage the physical properties of their membranes through the cell cycle.

The bacterial cell cycle is an example of binary fission that is typically both rapid and reliable. It is characterised by periods known as B, C and D[1–4]. The B period represents the phase between division and the initiation of replication, whereas the C period (sometimes called the replication phase) represents the phase in which the nucleolus is replicated and in which the bacterium reaches its mature size. The D period is that between the replication of the DNA and fission of the cell envelope. The B, C and D periods can therefore considered analogous to the eukaryotic G_1, S and G_2 phases, respectively. However, despite considerable research, little is understood about how progress from the B to D periods is controlled.

In Eukaryotes it is known that the cell cycle is controlled through the interaction of cyclin and cyclin-dependent kinases[5–7]. However, to date there is no evidence for the presence of homologues of cyclin in bacteria. Furthermore, studies of Gram-negative species have been unable to produce evidence for regulation of cell division either through changes in gene expression[8] or changes in the concentration of the proteins that comprise the divisome[9,10]. Existing models for the control of bacterial cell division allow for several possible mechanisms. One is based on regulation of increase in cell size (the size adder theory[11–13]). Another is that cell size is regulated in advance of division, possibly through dilution of a 'timekeeper' protein, though the mechanism underlying this model is not known[13,14] and it is not clear whether such proteins would control, or are rate-limiting, with respect to the cell cycle. There are also hints that cell structure is a determinant in controlling the binary fission in bacteria[15]. In principle, control of progress through the cell cycle through changes in cell structure could be based on both structural proteins and lipids, but knowledge of the role of lipids in this is lacking.

Recent work on lipids and their metabolism in the Gram-positive bacterium *Bacillus subtilis* has revealed a link between the synthesis of phospholipids and the divisome. This evidence suggests that *de novo* synthesised lipids are produced at the septum during fission[16]. Furthermore, there is evidence for an overall change in the lipid profile of the Gram-negative *Escherichia coli* through its cell cycle[15]. The latter work showed that the abundance of curvature-forming cardiolipin (CL) falls whilst that of the bilayer-forming phosphatidylglycerol (PG) increased on elongation of the cell at the C/D boundary. Evidence from biophysical studies conducted over the

[1]Department of Molecular Biology, University of Bergen, Thormøhlensgate 55, NO-5006, Bergen, Norway. [2]Centre for Biomolecular Sciences, University of Nottingham, University Park, NG7 2RD, Nottingham, United Kingdom. [3]Department of Chemistry, University of Oslo, P. O. Box 1033, Blindern, NO-0315, Oslo, Norway. [4]School of Biosciences, University of Nottingham, Sutton Bonington Campus, LE12 5RD, Nottinghamshire, United Kingdom. Correspondence and requests for materials should be addressed to Ø.H. (email: oyvind.halskau@uib.no)

last half-century shows that modulation of lipid composition can have a considerable impact on the lyotropic phase behaviour of lipid systems[17,18]. For example, an increase in the fraction size of phosphatidylethanolamine (PE) increases the propensity of a lipid system to assemble into curved phases rather than bilayer-like ones[19,20]. This is known as increasing stored curvature elastic stress, SCES[21].

Determining the relationship between lipid composition and phase behaviour complements the interpretation of lipid profiling studies. Data from studies of the phase behaviour of lipids suggest that the increase in abundance of a bilayer-forming lipid and the reduction in abundance of a non-bilayer forming lipid that occurs in *E. coli* on elongation, reduces SCES[22–25]. This is consistent with the changes in morphology of the cell during elongation because average curvature is lower in elongated cells and the evidence that the location of the Z-ring may be determined by cell membrane geometry[26–28]. This led us to the hypothesis that the production and shape of the cell envelope is involved in controlling the cell cycle of bacteria. If correct, this hypothesis implies that the topology of the plasma membrane and thus the physical properties of its lipids play a significant role in progress through the cell cycle in bacteria.

In order to investigate whether modulation of lipid composition through the cell cycle is a general feature of bacteria we measured global changes in the lipid profile of a bacterium that is evolutionarily distinct from *E. coli*. *Listeria innocua* NCTC 11288 was chosen because, unlike the commonly studied model Gram-positive *B. subtilis*, it does not sporulate under stress. *L. innocua* also has clinical relevance[29], due to its biological similarity to the pathogen *L. monocytogenes*[30,31].

Cultures of *L. innocua* in the exponential phase were stopped after elongation but before cell division (around the C/D period boundary) with the bacteriostatic antibiotic rifampicin (RIF) using an adapted[15] version of an established method[32–34]. The lipid fractions (LF) were isolated from freeze-dried, pelleted cultures whose cell walls had been thoroughly digested. The LFs were profiled using a combination of solution phase ^{31}P NMR and HR-MS/MS[35]. The relationship between changes in lipid composition and membrane morphology observed in *L. innocua* was investigated using broad line ^{31}P NMR to characterise the phase behaviour of model systems that corresponded to the lipid compositions observed.

Results

Culture growth and synchronisation. Cultures of *L. innocua* NCTC 11288 were grown in tryptic soya broth at 37 °C and the growth phase synchronised using RIF[15]. A growth curve was used to identify the appropriate point to administer the arrest drug (determined empirically to be 240 min (Fig. 1).

The experimental steps for preparation of samples and collection of profiling data are shown in Fig. S1. Based on their size distribution the synchrony of the untreated exponentially growing cultures was determined to be >80% (and the cell size analysis suggested that these were predominantly in the B period) (Fig. 1). The cell size was measured using cells stained with Nile Red observed using fluorescence microscopy. These data were used to establish the efficacy of RIF in arresting and holding cells at the C/D boundary and cells from such cultures were found to be significantly longer (mean = 1.92 µm, ± 0.44 µm) than those in the untreated samples (mean = 1.34 µm, ± 0.29), with only 6.7% being as short or shorter than those seen to predominate in the untreated samples (*t*-test, $p = <0.01$). Based on these results the untreated samples were taken to be representative of cells in the B period, and the RIF-treated samples representative of cells at the C/D boundary.

We took several steps in order to avoid chemical and enzymatic degradation of lipids. After centrifugation cells were resuspended in PBS to suppress PI-PLC activity[36], and a mixture of lipase inhibitors was added to suppress the activity of these enzymes *ex vivo*[15,35]. A mixture of mutanolysin[37], lysozyme and RNAase was added to digest the cell wall and thus maximise access to the lipid fraction[38].

Possible contamination of the cultures was checked for by inspecting the ^{1}H spectrum of the FA fraction but none was found (that of *Listeria ssp.*[39–42] is distinct from other commonplace bacteria, such as *E. coli*[43–46]. See *Preparation of fatty acid isolates* in *Experimental Methods*, and Fig. S2).

Isolation of the lipid fraction. The LFs were extracted using a two-step method that was designed to address the apparent short-comings of traditional methods[47] (see *Experimental* for details). Triethylammonium ions were used to provide a counter-ion that is soluble in organic solvents and thus favours migration of phospholipid species into the organic phase. Dichloromethane was used in place of chloroform in order to minimise chemical degradation of lipid species[47]. Lastly, in order to maximise the extraction efficacy, the freeze-dried free-flowing powdered cellular matter was washed in a mixture of organic solvents (dichloromethane/methanol/triethylammonium chloride, 3:1:0.0005, *v/v/w*) before being dispersed in water and methanol, and extracted with dichloromethane. In order to test the effectiveness of this procedure, the aqueous fraction and precipitate from the isolation of the LF were freeze-dried and treated with strong acid (5% H_2SO_4) in order to hydrolyse any FA ester bonds and thus release any remaining FAs. The amount of FA found is treated as proportional to the mass of the lipid not collected during the isolation. The data from these measurements (^{1}H NMR, see *Experimental* and Fig. S3) suggest that the procedure used in this study extracted >99% of the LF. This compares favourably with around 85% for the original Bligh & Dyer method[48].

Profiling of the lipid fraction. The LFs were profiled using a combination of solution phase ^{31}P NMR and HRMS/MS[35]. ^{31}P NMR was used for quantification because it allows non-destructive and unambiguous high-resolution spectroscopy of the organically-soluble phosphorus-containing molecular species present. Lysylated lipids have not been profiled using ^{31}P NMR before and so the shifts of lysyl-dioleoyl phosphatidylglycerol (lysyl-DOPG) were determined (Fig. S4). Representative spectra of the lipid profiling and the relative abundance of lipids in the B period and at the C/D boundary are shown in Fig. 2A. A combination of high resolution and tandem mass spectrometry were used to identify both the head groups present and the range of lipid

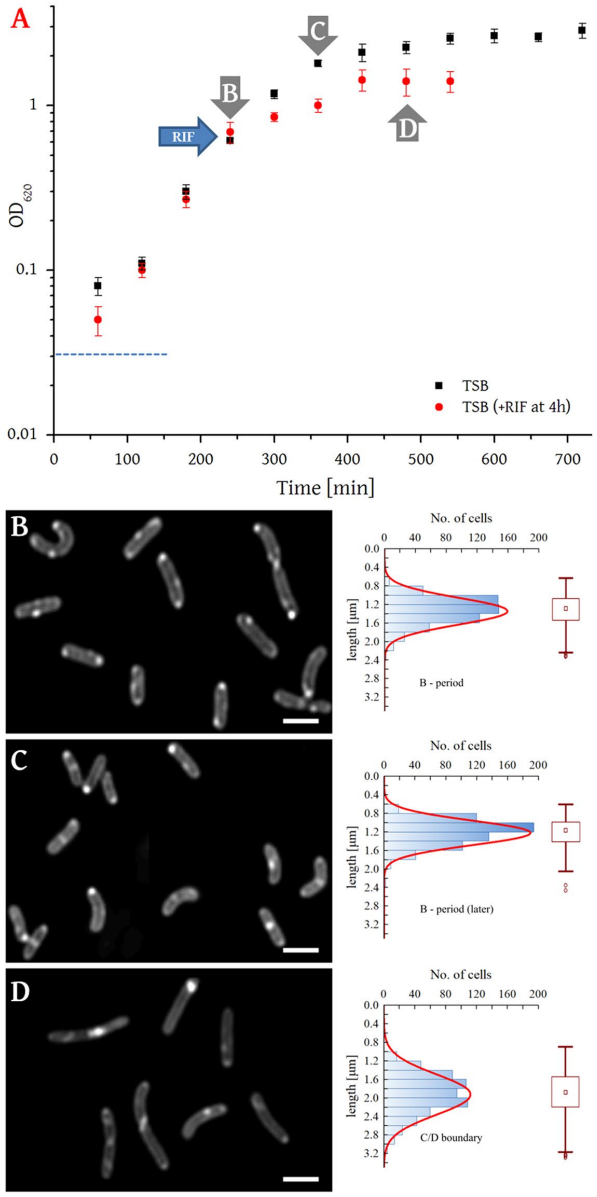

Figure 1. Identification of growth phases and image analysis of cultures. Panel A, Growth curve for L. innocua NCTC 11288 grown in TSB at 37 °C ($n = 3$ independent experimental measurements per point). The lag phase lasted for approximately 150 min (------); exponential phase (untreated cultures) began at about 150 min and by 400 min the cells were in the stationary phase. In cultures treated with RIF, stationary phase was induced immediately although some growth was still detected for ~120 min. Samples in panels B and C (untreated controls) were collected after 240 and 360 min and sample in panel C was collected 240 min after RIF administration (at 480 min). Panels B–D show light and fluorescence micrographs of *L. innocua*; for fluorescent imaging samples were stained with Nile red (1000 × magnification; scale bar = 1 µm). A graph of the distribution of cell lengths is shown for each sample with Gaussian distribution (red line). Data represents 180–200 cells from at least three images from four independent cultivations. The Box plots show medians, 50% of data in the range (box), non-outliers range (whiskers) and outliers (circles and stars). Sample B is representative of cells in exponential phase growth (240 min after inoculation) with the majority of cells appearing to be in the B period (>80% synchrony; mean = 1.34 µm, ± 0.29 µm). Sample C is

representative of cells at the end of the exponential phase (360 min after inoculation) and represents the B period of older cultures (>80% synchrony; mean = 1.22 μm, ±0.26 μm). Sample D is representative of cells arrested at the C/D boundary by RIF (80-90% synchrony; mean = 1.92 μm, ±0.44 μm). Only 6.7% of cells in the C/D boundary samples are as short or shorter than those seen to predominate in the untreated samples (t-test, p = < 0.01).

isoforms present (Table S1 shows the lipid abundance and isoform profiles. Representative lipid fragmentation is shown in Fig. S5).

These data show that the abundance of both cardiolipin (CL) and phosphatidylethanolamine (PE) fall significantly between the B period and at the C/D period boundary. The fraction size of CL falls by around 40% whereas that of PE falls by about 60%. The absolute value for the abundance of PG varies between cultures, but does not appear to be statistically significant. This is perhaps surprising in view of the significant decreases in both CL and PE, however it is not clear why this should be. It seems unlikely that this is due to lysylation as the abundance of lysyl-PG is also not statistically significant, despite notable shifts in the absolute values. The abundance of major structural lipids CL and PE does not change substantially between cultures at the beginning and end of the exponential phase, while PG changes to some extent (Table S1). Unlike *E. coli*, the age of cultures of *Listeria* does not appear to correlate with changes in its lipid profile.

Profiling of the fatty acid residues (FARs) of the total lipid fraction did not indicate a difference in the FA profile between periods, suggesting that FA production is not linked to the cell cycle in this organism (Fig. S6). These data therefore indicate that although the lipid profile changes through the cell cycle of *L. innocua* it does not change with the age of rapidly-dividing cells. Furthermore, cell-cycle dependent changes are restricted to the head groups of the major structural species. Taken together, these data suggest that synthesis of the principal head groups in particular is linked to the expansion of the membrane during the B and C periods.

These data (Fig. 2B, Table S1) are consistent with the published evidence that the bulk of the *Listeria* LF comprises PE[49] and lysyl-derivatives of PG and CL[50], but is at odds with reports in which PE appears not to have been found[39,50]. Conversely, phosphatidylinositol (PI) was not detected in any sample in this study despite the presence of several PLC inhibitors, contrasting with reports of the presence of PI in a closely-related strain of *Listeria*[42,51]. We note that the lipid profile of biological samples can be influenced by myriad factors, including the medium used, how cultures are incubated and handled, how the LF is isolated, handled and profiled, and even the activity of endogenous lipases *ex vivo*[47].

Lyotropic phase behaviour of model membrane systems. The evidence for modulations in the abundance of CL and PE during cell elongation raises the question of whether membrane properties change with these changes in composition. Studies of the phase behaviour of PG, PE and CL over the last half-century have shown that they have distinct properties. PE's spontaneous curvature is negative[19,52–54], as is CL's but only in the presence of a high concentration of divalent cations[23,55,56]. PG's phase behaviour is dominated by lamellar phases, suggesting that its spontaneous curvature is negligible[24,25,57–59]. Modulation of the abundance of PE and CL (with a low concentration of divalent cations) is therefore a change in the abundance of two major structural lipids with contrasting spontaneous curvature. That these changes in abundance occur through the cell cycle therefore suggests that the stored curvature elastic stress of the membrane also changes through the cell cycle. We investigated this by modelling the behaviour of two-lipid mixtures using broad line ^{31}P NMR.

Model systems comprised the di-oleoyl isoforms of PG and PE (DOPG and DOPE), and tetra-oleoyl isoform of CL (TOCL). Temperature scans of the individual lipids revealed the established behaviour, *i.e.* systems comprising either TOCL or DOPG showed fluid lamellar (L_α) phase over the temperature range studied (Fig. S7A,B), with DOPE undergoing a transition from L_α to inverse hexagonal (H_{II}) only above 273 K (Fig. S7C).

Mixtures of DOPG with TOCL show a strong preference for L_α, even at relatively low temperatures (273 K, Fig. 3A; Fig. S8A–C), suggesting that both lipids confer fluidity on systems in which they are present. The L_α phase also dominates across most of the concentration range in mixtures of DOPG and DOPE at 273 K (Fig. 3B), but higher temperatures favour curved phases (*e.g.* 310 K, Fig. 3C; Fig. S9). These data indicate that PE confers stored curvature elastic stress on PG systems. In particular, a reduction in PE from 36% to 18%, similar to that on elongation of *L. innocua*, reduces the ability of that system to form curved phases, suggesting a significant reduction in SCES. The L_α dominates in mixtures of DOPE with TOCL where the concentration of DOPE is below 50% (273 K, Fig. 3D). This also indicates the preference for lamellar phase(s) by TOCL at low concentrations of divalent cations (Fig. S10A), and curved phases by PE (Fig. S10C). Thus, although the fraction of CL shrinks on elongation of *L. innocua*, the increase in that of the DOPG ensures that the reduction in the abundance of PE reduces SCES.

However, it appears that doping DOPE with rather small quantities of DOPG (22-13:1, 4.3-7.1%) or TOCL (~36-12:1, 2.7-7.7%) allows the formation of curved phases at 273 K, particularly the H_{II} phase (Figs 3B and S9, and Figs 3D and S10). Importantly, the phase transition from fluid lamellar to the H_{II} phase occurs in DOPE around 10 K higher than this, at ~ 281K[60]. This suggests that the presence of small quantities of these lipids can relieve the packing stress of the H_{II} phase.

Data from a mixture of lysyl-DOPG with TOCL suggest that lysyl-DOPG has similar fluid properties to DOPG (Fig. S8C and D) but does not reduce the packing stress of DOPE systems as DOPG does (Fig. S9E and F). Notably, the behaviour of DOPE:lysyl-DOPG (22:1, Fig. S9F) is very similar to that of pure DOPE (Fig. S7C), and both are distinct from DOPE:DOPG (22:1, Fig. S9E). In the latter, the less abundant lipid appears to reduce the packing stress of the inverse hexagonal phase. This suggests that the role of lysyl-DOPG in the membrane differs from that of PG and may be related more to modulations in SCES and/or lipid packing than to fluidity.

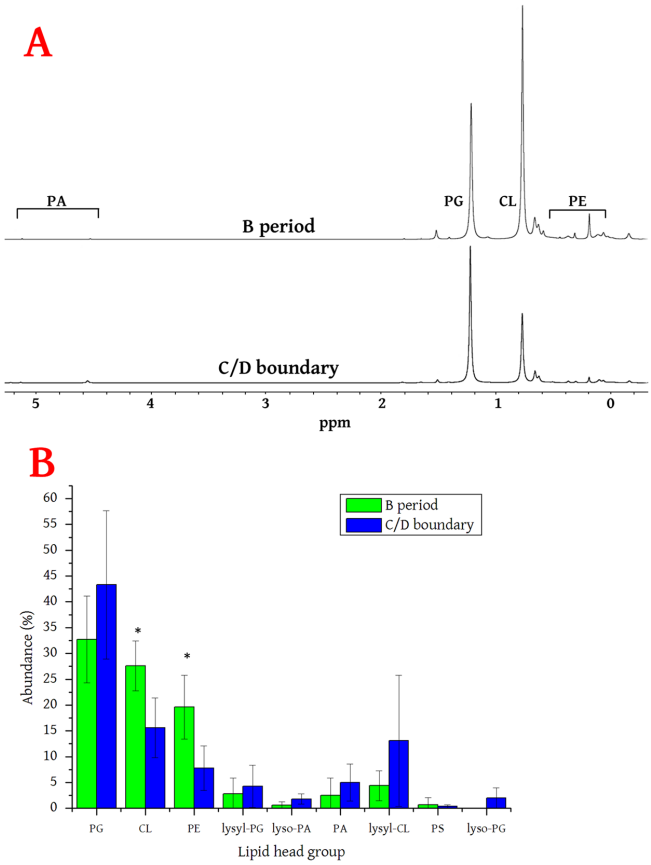

Figure 2. Profiling of the phospholipids in *L. innocua* NCTC 11288 at different stages of the cell cycle. Panel A shows representative ^{31}P NMR spectra of the lipid fraction collected from B period cultures and cultures at the boundary of the C and D periods. The relative area of the integrations of the appropriate resonance(s) were taken as a fraction of the total integrations for each spectrum and used to generate the fraction size given for each sample. The shift of phosphate *mono*-ester-containing lipids such as PA, is pH dependent. PE exhibits several resonances due to concentration and pH-dependent solvent interactions[15,78]. Panel B shows the abundance of lipids in the B period and at the C/D period boundary from cells collected in the exponential phase. Asterisks mark the head groups (CL, PE) for which the difference in abundance is considerable (when comparing standard deviations, $n = 5$ independent samples profiled using quantitative ^{31}P NMR). CL, cardiolipin; *lyso*-PA, lyso-phosphatidic acid; *lyso*-PG, *lyso*-phosphatidylglycerol; lysyl-CL, lysyl-cardiolipin; lysyl-PG, lysyl-phosphatidylglycerol; PA, phosphatidic acid, PE, phosphatidylethanolamine; PG, phosphatidylglycerol; PS, phosphatidylserine.

Discussion

The evidence from this study indicates that the modulations in lipid composition in *L. innocua* that occur between the B period and C/D boundary are statistically significant. The behaviour of model systems suggests that the modulations in lipid composition on elongation of *L. innocua* represent a reduction in the SCES of the membrane (observed as a reduction in size of PE fraction, Fig. 3B) but without a reduction in its fluidity (with an increase in PG and despite a decrease in CL; Fig. 3A and D). This suggests that the physical properties of the membrane are linked to the cell cycle.

The behaviour of model lipid systems observed in this study supports the conclusion that changes in lipid composition favour changes in morphology of the membrane on a cellular scale. Comparison of the lipid profile and distribution between different rod-shaped bacteria (such as *E. coli* and *B. subtilis*) and between rod-shaped and spherical bacteria (such as *Staphylococcus aureus*) are therefore of interest in understanding the cellular structure of prokaryotes. However, comprehensive cell-cycle-based lipid profiling of prokaryotes is lacking at present. What is known, is that *E. coli* and *B. subtilis* have very different distributions of lipids in their membranes, which

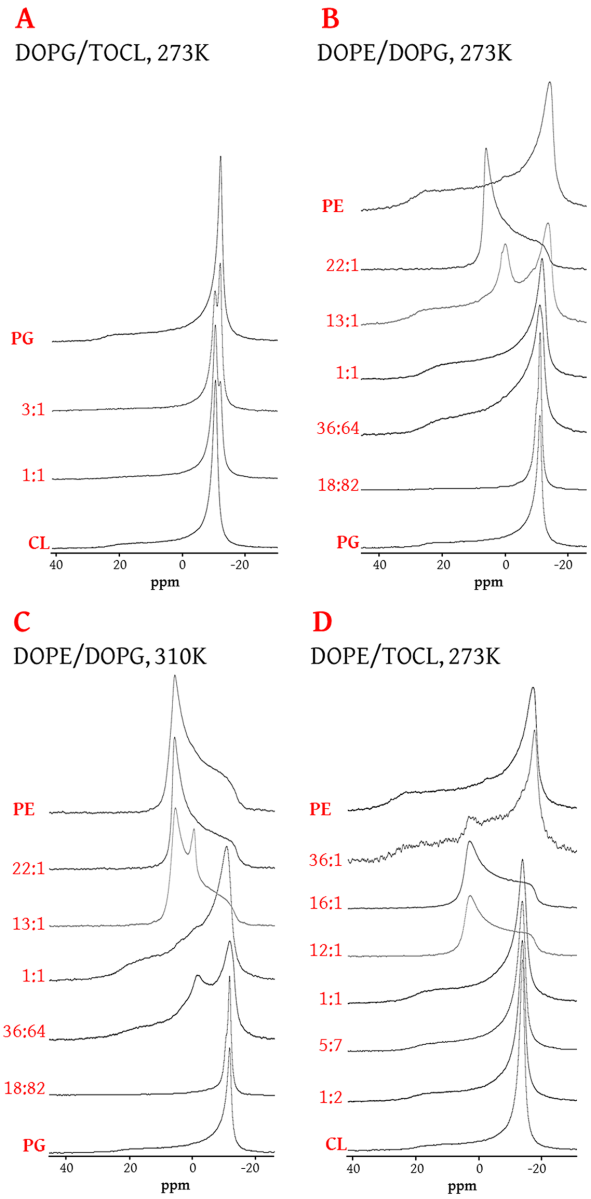

Figure 3. Stacked spectra showing the phase behaviour of two-lipid systems as a function of lipid head group composition. (**A**), DOPG/TOCL mixtures at 273 K; (**B**), DOPE/DOPG at 273 K; (**C**), DOPE/DOPG at 310 K; (**D**), DOPE/TOCL scan at 273 K. The 36:64 and 18:82 mixtures of DOPE:DOPG represent the ratio of these two lipids in the B period and at the C/D boundary, respectively. DOPG, dioleoylphosphatidylglycerol; TOCL, tetraoleoylcardiolipin; DOPE, phosphatidylethanolamine. Full temperature scans of each lipid mixture can be found in Figs S8–10.

are linked to differences in proteins associated with cell division, and therefore cell shape is not expected to be the only factor that determines this change[61].

We note that the modulations in lipid composition of the Gram-positive *L. innocua* are analogous to those reported for the Gram-negative bacterium, *E. coli*. In the latter organism, the abundance of the bilayer-forming

PG increases during its elongation (from ~1:22 to ~1:16 against PE), with a reduction in the abundance of CL (from ~1:16 to ~1:36 against PE)[15]. Physical data from the present study suggest that there is also a reduction in the tendency to form the hexagonal phase (lower SCES) in *E. coli*, without a reduction in fluidity on progression from the B period to the C/D boundary. This indicates that *E. coli* has adopted the same pattern with respect to modulation of lyotropic phase behaviour between the B period and C/D boundary as seen in *L. innocua*.

This remarkable similarity between two bacteria that are quite separate in evolutionary terms raises the question of whether such modulations are important for the structure of rod-like cells in general. However, it is not clear from these data whether this trend is limited to cells with a cell wall; further work is required to establish what effects modulations in lipid composition have in other cell types.

It is appealing to speculate what further effects the modulations in lipid composition may have on membrane properties. The folding and function of proteins of both bacterial and eukaryotic origin have been shown to be sensitive to lipid membrane composition[62–64], and to SCES and packing defects[65,66]. This coupling between the membrane's physical state and the proteins' folding can also manifest itself in problematic rather than functional ways. For instance, there is evidence that charged head groups such as those of PG and phosphatidylserine enhance the membrane binding and mis-folding behaviour of α-Synuclein[67], and that packing defects are involved in promoting mis-folding of a protein linked to Parkinson's disease[68,69]. Particular constellations of ganglioside and cholesterol have also been proposed to promote both membrane binding and mis-folding in α-Synuclein and β-amyloid peptide[70].

It is clear that further work is required to fully characterise the relationship between lipid composition and distribution in bacteria[71] and in eukaryotic[72] cells. Data such as that acquired in this study indicate the extents to which the lipid composition and phase behaviour vary with the cell cycle. These alterations may in turn have an impact on the structural and functional properties of the membrane they comprise.

Experimental Methods

Reagents and chemicals. Growth medium, solvents and fine chemicals were purchased from *SigmaAldrich* (Gillingham, Dorset, UK) and used without purification. PhosSTOP tablets were purchased from Roche (Welwyn, Hertfordshire, UK) and stored at 4 °C. Purified lipids were purchased from *Avanti Polar lipids Inc.* (Alabaster, Alamaba, US) and used without further purification.

Cultivation of *L. innocua*. The growth kinetics of this bacterium in tryptic soya broth (TSB) was characterised over 24 h (Fig. 1). The preparation of one set ($n = 1$) of cultures is described. Each sample comprised three cultures in order to ensure that enough material was produced and to account for differences between populations. Thus for each biological replicate, 3 × 3 × 1 L cultures were grown in unmodified TSB that had been autoclaved. Mini-cultures (10 × 10 mL) were incubated (16 h, 37 °C, orbital incubator, 250 r.p.m.,) before inoculating 9 × 1 L to give cultures of OD_{620} ~0.03. After incubation (37 °C, 240 min, orbital, 250 r.p.m., average OD_{620} 0.4), three cultures were mixed together to make the 4 h control time point and cells harvested (fixed-angle rotor, 6k × *g*, 10 min, 4 °C). Three cultures were treated with RIF (50 mg/L final concentration, added as methanolic solution of 50 mg/mL). After 360 min h, the three remaining control cultures were mixed and harvested together (making the 6 h control time point which is equivalent to the point at which the cultures treated with RIF are arrested), and after 480 min the remaining three cultures treated with RIF were harvested together.

Fluorescence and light microscopy. Cells were photographed after harvesting and before the administration of lipase inhibitors. Cells were stained with Nile Red as previously described[73–75]. Briefly, cells were collected by centrifugation (fixed-angle rotor, 6 k × *g*, 10 min, 4 °C), washed once with PBS and resuspended in PBS at OD_{620} ~2.0. Nile Red (2 µg/mL, sample volume 1 mL, dye stock solution in DMSO) was added and the sample (1 mL) allowed to stand at room temperature (20 min). Cells (60–80 per picture, 180–200 per sample) were measured from at least three images for each culture/time point each from four independent cultivations (*i.e.* (~70 × 3) × 3 × 4). The mean and standard deviation were calculated for each and an independent student *t*-test was used to determine statistical significance ($p = < 0.01$). The null hypothesis was that the lengths of the bacteria are the same for each sample. Images were taken using a Leica DMI6000 B microscope equipped with a Leica DFC350 FX camera and processed with (the 3D deconvolution function in) Leica Application Suite, Advanced fluorescence 1.7.0 software with AF6000 configuration and open source ImageJ software.

Isolation of lipid fraction. Fresh cell pellets were resuspended immediately (PBS, 5 mL) and treated with PhosSTOP (1 tab/10 mL final concentration, 10 × stock dissolved in PBS), 2-butoxyphenylboronic acid (BPBA, 2 mg/mL final concentration, ethanolic stock solution 100 mg/mL) and a stored mixture of mutanolysin (50 µg), lysozyme (10 mg), RNAase (200 µg) (volume of aliquots 1 mL, glycerol/PBS 1:1, stored at 193 K). The total volume of the resulting solutions was 10 mL per sample and they were agitated gently in air tight falcon tubes (50 mL, gel staining table, 16–20 h) before being frozen (193 K) and freeze-dried. The freeze-dried material was stored at 253 K until isolation of the lipid fraction.

The free-flowing powdered cellular matter was mixed with dichloromethane/methanol (20 mL, 3:1, 0.5 mg/mL triethylammonium chloride, TEAC) and sonicated (sonication bath, 5 min) before being centrifuged (5 min, 5.25 k × *g*). The organic solution was decanted and retained. The pellet was mixed with more of the same dichloromethane/methanol mixture (20 mL, 3:1, 0.5 mg/mL TEAC), agitated, centrifuged and the solvent decanted. The pellet was then resuspended in a mixture of dichloromethane and water (20 mL, 1:1, separating funnel) and diluted with sufficient methanol to make a stable uniphasic solution (~40 mL), and agitated briefly. The mixture was then made biphasic by addition of dichloromethane (20 mL). The dichloromethane solution was removed and the aqueous solution washed (dichloromethane, 20 mL). TEAC was added to the remaining aqueous solution (final concentration of 2 mM, 2 M stock) and the aqueous solution washed with dichloromethane (2 × 20 mL).

The combined organic solutions (~130 mL) were filtered through filter paper and concentrated *in vacuo* before storage under nitrogen at 253 K.

Isolation of residual lipidic material. The aqueous phase and precipitate produced during the lipid isolation (above) were freeze-dried together and then treated with acid (H_2SO_4, 5%, 20 mL, gentle agitation, 24 h, r.t.p.). The reaction mixture was quenched ($NaHCO_3$) and freeze-dried. The free-flowing powder was washed twice with chloroform. The organic phases were combined and concentrated *in vacuo*. The remaining material (~8 mg/120 mg LF isolated) was dissolved in deuterated chloroform (650 µL) before commencing ^{1}H NMR. The integrals of each spectrum were calibrated according to the α-CH_2 signal (2.3–2.4 ppm) present (Fig. S4).

Solution phase ^{31}P NMR spectroscopy. Lipid films (10-15 mg) from cultures of *L. Innocua* were dissolved in the CUBO solvent system[15,35,76] (500 µL/sample). Data acquisition was similar to published work[15,35] but using a Bruker 400 MHz Avance III HD spectrometer equipped with a 5 mm BBO S1 (smart) probe operating at 298 K for all data except that shown in Fig. S5. ^{31}P spectra were acquired at 161.98 MHz using inverse gated proton decoupling, with 2048 scans per sample and a spectral width of 19.99 ppm. An overall recovery delay of 6.5 s was used which gave full relaxation. Data were processed using line broadening of 1.00 Hz prior to zero filling to 19428 points, Fourier transform and automatic baseline correction. The data for Fig. S5 were acquired on a Bruker Avance III 800 MHz spectrometer, equipped with a QCI cryoprobe probe. Acquisition used inverse gated proton decoupling. Spectra were averaged over 1312 transients with 3882 complex points with a spectral width of 14.98 ppm. An overall recovery delay of 8.4 s was used. Data were processed using an exponential line broadening window function of 1.5 Hz prior to zero filling to 32768 points, Fourier transform and automatic baseline correction. All spectra were processed and analysed using (the dcon function in) TopSpin 3.2.

Preparation of fatty acid isolates. Representative samples used for head group profiling were dried *in vacuo* (high-vac pump) before being diluted (H_2SO_4 97% in methanol, 1:20 *v/v* final concentration, 5 mL) and heated under intermittent agitation (4–6 h, 50 °C). The reaction mixture was quenched ($NaHCO_3$, 1 g) before being diluted (H_2O, 30 mL; diethyl ether, 20 mL). The mixture was shaken vigorously in a separating funnel before the organic fraction was collected. The aqueous solution was washed (diethyl ether, 20 mL). The organic solutions were combined and dried *in vacuo*. The resulting oil (5–10 mg) was dissolved ($CDCl_3$, 500–600 µL) and subjected to ^{1}H NMR spectroscopy. δ_H (500 MHz, 16 scans, $CDCl_3$, calibrated to 7.24 ppm) 3.6 (singlet, $RCH_2CH_2COOCH_3$), 2.3 (triplet, $J = 7.6$ Hz, $RCH_2CH_2COOCH_3$), 1.6-1.5 (m, $RCH_2CH_2COOCH_3$), 1.4-1.0 (m, methylenes), 0.9-0.8 (m, methyl groups) ppm.

Mass spectrometry. Samples were prepared and measurements taken according to published methods[15,35]. Accurate mass LC-MS and MS/MS was performed on an OrbiTrap Dionex 3000, (Waltham, MA, USA). Dry lipid mixtures were dissolved in dichloromethane/isopropanol 1:1 and an inject volume of 10 µL was used. Analytes were separated chromatographically on a UPLC C18 column (1.7 µm particle size, Waters) at 40 °C at a rate of 0.4 mL/min. Mobile phase A consisted of 0.1% formic acid in water at *p*H 6.0, and mobile phase B was 56% acetonitrile, 40% isopropanol and 5% water with 0.1% formic acid. Ions were monitored in positive mode (*m/z* range 300-2000, resolution 140,000). Selected peaks were fragmented (normalised collision energy set to 36) and MS2 collected with a resolution of 17,500.

Analyses consisted of searches for lipid isoforms in MS1 spectra, followed by fragmentation (MS2) for appropriate *m/z* values. Lipid isoform searches were restricted by head group (PG, PE, PA, PS and CL), FAR (chain length from 10 to 20 C, up to three double bonds) and adduct (H^+, Na^+, K^+, NH_4^+). The search was augmented to include lysyl and *lyso-* isoforms. Matches were compared (see Fig. S6 for example). The software-generated scores were checked manually. Analyses were performed using Thermo Xcalibur 3.0.63 and recently-developed software by Kochen *et al.*[77]. Original code for non-standard head groups was written by us in Matlab R2015b.

Broad line ^{31}P NMR sample preparation. Lipid mixtures were made in solution (dichloromethane, 10–15 mg/mL) and dried to a lipid film *in vacuo*. Dried lipid films were dispersed in aqueous buffer (NaCl 100 mM, tris 50 mM, $CaCl_2$ 2.5 mM, $MgCl_2$ 2.5 mM, *p*H 7.4; 30:1 *v/w*) with sonication and agitation. Deuterium oxide (10% *v/v* against buffer) was added and the mixture agitated and then freeze-thawed 8–10 times. Samples were then stored at 193 K, transported at ~295 K and were stored at 253 K before running.

Broad line ^{31}P NMR spectroscopy. A Bruker Avance III HD 400 MHz DRX spectrometer equipped with a Bruker BBO S1 (smart) probe was used for proton-decoupled broad line ^{31}P NMR experiments. Experiments were performed at 161.98 MHz with an inverse-gated pulse sequence with proton decoupling during acquisition, spectral width of 200.44 ppm, acquisition time of 0.299 s, pre-scan delay (DE) time of 20 µs, receiver gain of 203 with 19428 data points and 2048 scans per spectrum. The duration of each scan, acquisition time and relaxation delay, was 2.332 s. Spectra were processed using TopSpin 3.2 and 3.5 with line broadening of 50 Hz, phase correction and automatic baseline correction (abs).

Broad line ^{31}P NMR temperature scans. Samples were brought to and held at the desired temperature for 15 min before acquisition. Temperature scans consisted of acquisitions at the following temperatures: 298, 273, 293, 298, 310, 318, 273, 310 K. The latter two temperature points were used to assess the reliability of the equilibration time used (15 min). Acquisitions at 338 K were carried out separately with equilibration and acquisition at 310 K immediately beforehand. Stackplots of spectra were prepared manually from individual traces processed as above.

References

1. Bates, D. *et al*. The *Escherichia coli* baby cell column: a novel cell synchronization method provides new insight into the bacterial cell cycle. *Mol Microbiol* **57**, 380–391, doi:10.1111/j.1365-2958.2005.04693.x (2005).
2. Boye, E., Stokke, T., Kleckner, N. & Skarstad, K. Coordinating DNA replication initiation with cell growth: differential roles for DnaA and SeqA proteins. *Proc Natl Acad Sci USA* **93**, 12206–12211 (1996).
3. Ferullo, D. J. & Lovett, S. T. The Stringent Response and Cell Cycle Arrest in *Escherichia coli*. *PLoS Genet* **4**, e1000300, doi:10.1371/journal.pgen.1000300 (2008).
4. Haeusser, D. P. & Levin, P. A. The Great Divide: Coordinating cell cycle events during bacterial growth and division. *Current opinion in microbiology* **11**, 94–99, doi:10.1016/j.mib.2008.02.008 (2008).
5. Hartwell, L. H. Nobel Lecture: Yeast and Cancer. *Bioscience Reports* **22**, 373–394, doi:10.1023/a:1020918107706 (2002).
6. Hunt, T. Nobel Lecture: Protein Synthesis, Proteolysis, and Cell Cycle Transitions. *Bioscience Reports* **22**, 465–486 (2002).
7. Nurse, P. Cyclin Dependent Kinases and Cell Cycle Control (Nobel Lecture). *ChemBioChem* **3**, 596–603, doi:10.1002/1439-7633(20020703)3:7<596::AID-CBIC596>3.0.CO;2-U (2002).
8. Arends, S. J. R. & Weiss, D. S. Inhibiting Cell Division in *Escherichia coli* Has Little If Any Effect on Gene Expression. *Journal of Bacteriology* **186**, 880–884, doi:10.1128/jb.186.3.880-884.2004 (2004).
9. Rueda, S., Vicente, M. & Mingorance, J. Concentration and Assembly of the Division Ring Proteins FtsZ, FtsA, and ZipA during the *Escherichia coli* Cell Cycle. *Journal of Bacteriology* **185**, 3344–3351, doi:10.1128/jb.185.11.3344-3351.2003 (2003).
10. Si, F., Busiek, K., Margolin, W. & Sun Sean, X. Organization of FtsZ Filaments in the Bacterial Division Ring Measured from Polarized Fluorescence Microscopy. *Biophysical Journal* **105**, 1976–1986, doi:10.1016/j.bpj.2013.09.030 (2013).
11. Taheri-Araghi, S. *et al*. Cell-Size Control and Homeostasis in Bacteria. *Current Biology* **25**, 385–391, doi:10.1016/j.cub.2014.12.009 (2015).
12. Campos, M. *et al*. A Constant Size Extension Drives Bacterial Cell Size Homeostasis. *Cell* **159**, 1433–1446, doi:10.1016/j.cell.2014.11.022 (2014).
13. Ghusinga, K. R., Vargas-Garcia, C. A. & Singh, A. A mechanistic stochastic framework for regulating bacterial cell division. *Scientific Reports* **6**, 30229, doi:10.1038/srep30229 (2016).
14. Robert, L. Size sensors in bacteria, cell cycle control and size control. *Frontiers in Microbiology* **6**, 515, doi:10.3389/fmicb.2015.00515 (2015).
15. Furse, S., Wienk, H., Boelens, R., de Kroon, A. I. P. M. & Killian, J. A. *E. coli* MG1655 modulates its phospholipid composition through the cell cycle. *FEBS Letters* **589**, 2726–2730, doi:10.1016/j.febslet.2015.07.043 (2015).
16. Takada, H. *et al*. An essential enzyme for phospholipid synthesis associates with the Bacillus subtilis divisome. *Molecular Microbiology* **91**, 242–255, doi:10.1111/mmi.12457 (2014).
17. Seddon, J. M. & Templer, R. H. in *The Handbook of Biological Physics* Vol. I (eds R. Lipowsky & E. Sackman) (Elsevier Science, 1995).
18. Cullis, P. R. & De Kruijff, B. Lipid polymorphism and the functional roles of lipids in biological membranes. *##Biochimica et Biophysica Acta (BBA) - Reviews on Biomembranes* **559**, 399–420, doi:10.1016/0304-4157(79)90012-1 (1979).
19. Cullis, P. R. & De Kruijff, B. The polymorphic phase behaviour of phosphatidylethanolamines of natural and synthetic origin. A 31P NMR study. *Biochimica et Biophysica Acta (BBA) - Biomembranes* **513**, 31–42, doi:10.1016/0005-2736(78)90109-8 (1978).
20. Marsh, D. & Seddon, J. M. Gel-to-inverted hexagonal (L[beta]-HII) phase transitions in phosphatidylethanolamines and fatty acid-phosphatidylcholine mixtures, demonstrated by 31P-NMR spectroscopy and X-ray diffraction. *Biochimica et Biophysica Acta (BBA) - Biomembranes* **690**, 117–123 (1982).
21. Seddon, J. M. Structure of the Inverted Hexagonal (Hii) Phase, and Non-Lamellar Phase-Transitions of Lipids. *Biochim Biophys Acta* **1031**, 1–69 (1990).
22. Seddon, J. M., Kaye, R. D. & Marsh, D. Induction of the lamellar-inverted hexagonal phase transition in cardiolipin by protons and monovalent cations. *Biochimica et Biophysica Acta (BBA) - Biomembranes* **734**, 347–352 (1983).
23. Ortiz, A., Killian, J. A., Verkleij, A. J. & Wilschut, J. Membrane Fusion and the Lamellar-to-Inverted-Hexagonal Phase Transition in Cardiolipin Vesicle Systems Induced by Divalent Cations. *Biophysical Journal* **77**, 2003–2014, doi:10.1016/S0006-3495(99)77041-4 (1999).
24. Alley, S. H., Ces, O., Barahona, M. & Templer, R. H. X-ray diffraction measurement of the monolayer spontaneous curvature of dioleoylphosphatidylglycerol. *Chemistry and Physics of Lipids* **154**, 64–67 (2008).
25. Findlay, E. J. & Barton, P. G. Phase behavior of synthetic phosphatidylglycerols and binary mixtures with phosphatidylcholines in the presence and absence of calcium ions. *Biochemistry* **17**, 2400–2405, doi:10.1021/bi00605a023 (1978).
26. Pazos, M. *et al*. FtsZ Placement in Nucleoid-Free Bacteria. *PLOS ONE* **9**, e91984, doi:10.1371/journal.pone.0091984 (2014).
27. Sun, Q., Yu, X.-C. & Margolin, W. Assembly of the FtsZ ring at the central division site in the absence of the chromosome. *Molecular Microbiology* **29**, 491–503, doi:10.1046/j.1365-2958.1998.00942.x (1998).
28. Rowlett, V. W. & Margolin, W. The bacterial divisome: ready for its close-up. *Philosophical Transactions of the Royal Society B: Biological Sciences* **370**, doi:10.1098/rstb.2015.0028 (2015).
29. Perrin, M., Bemer, M. & Delamare, C. Fatal Case of *Listeria innocua* Bacteremia. *Journal of Clinical Microbiology* **41**, 5308–5309, doi:10.1128/JCM.41.11.5308-5309.2003 (2003).
30. Jemmi, T. & Stephan, R. Listeria monocytogenes: food-borne pathogen and hygiene indicator. *Rev Sci Tech* **25**, 571–580 (2006).
31. Chakraborty, T., Hain, T. & Domann, E. Genome organization and the evolution of the virulence gene locus in Listeria species. *International Journal of Medical Microbiology* **290**, 167–174, doi:10.1016/S1438-4221(00)80086-7 (2000).
32. Boye, E. & Løbner-Olesen, A. Bacterial growth control studied by flow cytometry. *Research in Microbiology* **142**, 131–135, doi:10.1016/0923-2508(91)90020-B (1991).
33. Boye, E., Løbner-Olesen, A. & Skarstad, K. Timing of chromosomal replication in *Escherichia coli*. *Biochimica et Biophysica Acta (BBA) - Gene Structure and Expression* **951**, 359–364, doi:10.1016/0167-4781(88)90107-8 (1988).
34. Skarstad, K., Boye, E. & Steen, H. B. Timing of initiation of chromosome-replication in individual *Escherichia coli* cells. *Embo Journal* **5**, 1711–1717 (1986).
35. Furse, S. *et al*. The lipidome and proteome of oil bodies from Helianthus annuus (common sunflower). *Journal of chemical biology* **6**, 63–76, doi:10.1007/s12154-012-0090-1 (2013).
36. Goldfine, H., Johnston, N. C. & Knob, C. Non-specific phospholipase C of Listeria monocytogenes: activity on phospholipids in Triton X-100-mixed micelles and in biological membranes. *Journal of Bacteriology* **175**, 4298–4306 (1993).
37. Netterling, S., Vaitkevicius, K., Nord, S. & Johansson, J. A Listeria monocytogenes RNA Helicase Essential for Growth and Ribosomal Maturation at Low Temperatures Uses Its C Terminus for Appropriate Interaction with the Ribosome. *Journal of Bacteriology* **194**, 4377–4385, doi:10.1128/jb.00348-12 (2012).
38. Filgueiras, M. H. & den Kamp, J. A. F. O. Cardiolipin, a major phospholipid of Gram positive bacteria that is not readily extractable. *Biochimica et Biophysica Acta (BBA) - Lipids and Lipid Metabolism* **620**, 332–337, doi:10.1016/0005-2760(80)90215-5 (1980).
39. Tatituri, R. V. V., Wolf, B. J., Brenner, M. B., Turk, J. & Hsu, F. F. Characterization of polar lipids of Listeria monocytogenes by HCD and low-energy CAD linear ion-trap mass spectrometry with electrospray ionization. *Anal Bioanal Chem* **407**, 2519–2528, doi:10.1007/s00216-015-8480-1 (2015).
40. Chihib, N.-E., Ribeiro da Silva, M., Delattre, G., Laroche, M. & Federighi, M. Different cellular fatty acid pattern behaviours of two strains of Listeria monocytogenes Scott A and CNL 895807 under different temperature and salinity conditions. *FEMS Microbiol. Lett.* **218**, 155–160, doi:10.1111/j.1574-6968.2003.tb11512.x (2003).

41. Püttmann, M., Ade, N. & Hof, H. Dependence of fatty acid composition of Listeria spp. on growth temperature. *Research in Microbiology* **144**, 279–283, doi:10.1016/0923-2508(93)90012-Q (1993).
42. Mastronicolis, S. K. *et al*. Alteration of the phospho- or neutral lipid content and fatty acid composition in Listeria monocytogenes due to acid adaptation mechanisms for hydrochloric, acetic and lactic acids at pH 5.5 or benzoic acid at neutral pH. *Antonie van Leeuwenhoek* **98**, 307–316, doi:10.1007/s10482-010-9439-z (2010).
43. Liu, T., Vora, H. & Khosla, C. Quantitative analysis and engineering of fatty acid biosynthesis in E. coli. *Metabolic Engineering* **12**, 378–386, doi:10.1016/j.ymben.2010.02.003 (2010).
44. Ingram, L. O. Adaptation of membrane lipids to alcohols. *Journal of Bacteriology* **125**, 670–678 (1976).
45. Grogan, D. W. & Cronan, J. E. Cyclopropane ring formation in membrane lipids of bacteria. *Microbiology and Molecular Biology Reviews* **61**, 429–441 (1997).
46. Chang, Y.-Y. & Cronan, J. E. Membrane cyclopropane fatty acid content is a major factor in acid resistance of *Escherichia coli*. *Molecular Microbiology* **33**, 249–259, doi:10.1046/j.1365-2958.1999.01456.x (1999).
47. Furse, S., Egmond, M. R. & Killian, J. A. Isolation of lipids from biological samples. *Molecular Membrane Biology* **32**, 55–64, doi:10.3109/09687688.2015.1050468 (2015).
48. Bligh, E. G. & Dyer, W. J. A Rapid Method of Total Lipid Extraction and Purification. *Canadian Journal of Biochemistry and Physiology* **37**, 911–917 (1959).
49. Murgia, S., Mele, S. & Monduzzi, M. Quantitative characterization of phospholipids in milk fat via P-31 NMR using a monophasic solvent mixture. *Lipids* **38**, 585–591, doi:10.1007/s11745-003-1500-3 (2003).
50. Ghosh, B. K. & Carroll, K. K. Isolation, Composition, and Structure of Membrane of Listeria monocytogenes. *Journal of Bacteriology* **95**, 688–699 (1968).
51. Fischer, W. & Leopold, K. Polar lipids of four listeria species containing L-lysylcardiolipin, a novel lipid structure, and other unique phospholipids. *International Journal of Systematic Bacteriology* **49**, 653–662, doi:10.1099/00207713-49-2-653 (1999).
52. Mastronicolis, S. K. *et al*. Coordinated Regulation of Cold-Induced Changes in Fatty Acids with Cardiolipin and Phosphatidylglycerol Composition among Phospholipid Species for the Food Pathogen Listeria monocytogenes. *Applied and Environmental Microbiology* **74**, 4543–4549, doi:10.1128/aem.02041-07 (2008).
53. Seelig, J. & Gally, H. U. Investigation of phosphatidylethanolamine bilayers by deuterium and phosphorus-31 nuclear magnetic resonance. *Biochemistry* **15**, 5199–5204, doi:10.1021/bi00669a001 (1976).
54. Hauser, H., Pascher, I., Pearson, R. H. & Sundell, S. Preferred conformation and molecular packing of phosphatidylethanolamine and phosphatidylcholine. *Biochimica et Biophysica Acta (BBA) - Reviews on Biomembranes* **650**, 21–51, doi:10.1016/0304-4157(81)90007-1 (1981).
55. Kollmitzer, B., Heftberger, P., Rappolt, M. & Pabst, G. Monolayer spontaneous curvature of raft-forming membrane lipids. *Soft Matter* **9**, 10877–10884, doi:10.1039/c3sm51829a (2013).
56. Killian, J. A. *et al*. Effect of divalent cations on lipid organization of cardiolipin isolated from *Escherichia coli* strain AH930. *Biochimica et Biophysica Acta* **1189**, 225–232, doi:10.1016/0005-2736(94)90069-8 (1994).
57. Rietveld, A. G., Killian, J. A., Dowhan, W. & Dekruijff, B. Polymorphic Regulation of Membrane Phospholipid composition in *Escherichia coli*. *Journal of Biological Chemistry* **268**, 12427–12433 (1993).
58. Krumova, S. B. *et al*. Phase behavior of phosphatidylglycerol in spinach thylakoid membranes as revealed by 31P-NMR. *Biochimica et Biophysica Acta (BBA) - Biomembranes* **1778**, 997–1003, doi:10.1016/j.bbamem.2008.01.004 (2008).
59. Murata, N. & Yamaya, J. Temperature-Dependent Phase Behavior of Phosphatidylglycerols from Chilling-Sensitive and Chilling-Resistant Plants. *Plant Physiology* **74**, 1016–1024, doi:10.1104/pp.74.4.1016 (1984).
60. Epand, R. M. *et al*. Formation of a new stable phase of phosphatidylglycerols. *Biophysical Journal* **63**, 327–332 (1992).
61. Koynova, R. & Caffrey, M. Phases and phase transitions of the hydrated phosphatidylethanolamines. *Chemistry and Physics of Lipids* **69**, 1–34 (1994).
62. Barák, I. & Muchová, K. The Role of Lipid Domains in Bacterial Cell Processes. *International Journal of Molecular Sciences* **14**, 4050 (2013).
63. Agasøster, A. V. *et al*. The Interaction of Peripheral Proteins and Membranes Studied with α-Lactalbumin and Phospholipid Bilayers of Various Compositions. *Journal of Biological Chemistry* **278**, 21790–21797, doi:10.1074/jbc.M211466200 (2003).
64. Bogdanov, M., Heacock, P., Guan, Z. & Dowhan, W. Plasticity of lipid-protein interactions in the function and topogenesis of the membrane protein lactose permease from *Escherichia coli*. *Proceedings of the National Academy of Sciences* **107**, 15057–15062, doi:10.1073/pnas.1006286107 (2010).
65. Halskau, Ø. *et al*. Large-scale modulation of thermodynamic protein folding barriers linked to electrostatics. *Proceedings of the National Academy of Sciences* **105**, 8625–8630, doi:10.1073/pnas.0709881105 (2008).
66. McDonald, C., Jovanovic, G., Ces, O. & Buck, M. Membrane Stored Curvature Elastic Stress Modulates Recruitment of Maintenance Proteins PspA and Vipp1. *mBio* **6**, doi:10.1128/mBio.01188-15 (2015).
67. Arduin, A., Gaffney, P. R. J. & Ces, O. Regulation of PLCβ2 by the electrostatic and mechanical properties of lipid bilayers. *Scientific Reports* **5**, 12628, doi:10.1038/srep12628 (2015).
68. Stöckl, M., Fischer, P., Wanker, E. & Herrmann, A. α-Synuclein Selectively Binds to Anionic Phospholipids Embedded in Liquid-Disordered Domains. *Journal of Molecular Biology* **375**, 1394–1404, doi:10.1016/j.jmb.2007.11.051 (2008).
69. Lokappa, S. B. *et al*. Sequence and Membrane Determinants of the Random Coil–Helix Transition of α-Synuclein. *Journal of Molecular Biology* **426**, 2130–2144, doi:10.1016/j.jmb.2014.02.024 (2014).
70. Ghio, S., Kamp, F., Cauchi, R., Giese, A. & Vassallo, N. Interaction of α-synuclein with biomembranes in Parkinson's disease —role of cardiolipin. *Progress in Lipid Research* **61**, 73–82, doi:10.1016/j.plipres.2015.10.005 (2016).
71. Di Scala, C. *et al*. Common molecular mechanism of amyloid pore formation by Alzheimer's β-amyloid peptide and α-synuclein. *Scientific Reports* **6**, 28781, doi:10.1038/srep28781 (2016).
72. Furse, S. & Scott, D. J. Three-Dimensional Distribution of Phospholipids in Gram Negative Bacteria. *Biochemistry* **55**, 4742–4747, doi:10.1021/acs.biochem.6b00541 (2016).
73. van Meer, G. & de Kroon, A. I. P. M. Lipid map of the mammalian cell. *Journal of Cell Science* **124**, 5–8 (2011).
74. Spiekermann, P., Rehm, B. H. A., Kalscheuer, R., Baumeister, D. & Steinbüchel, A. A sensitive, viable-colony staining method using Nile red for direct screening of bacteria that accumulate polyhydroxyalkanoic acids and other lipid storage compounds. *Archives of Microbiology* **171**, 73–80, doi:10.1007/s002030050681 (1999).
75. Donovan, C., Schwaiger, A., Krämer, R. & Bramkamp, M. Subcellular Localization and Characterization of the ParAB System from Corynebacterium glutamicum. *Journal of Bacteriology* **192**, 3441–3451, doi:10.1128/jb.00214-10 (2010).
76. Culeddu, N., Bosco, M., Toffanin, R. & Pollesello, P. P-31 NMR analysis of phospholipids in crude extracts from different sources: improved efficiency of the solvent system. *Magnetic Resonance in Chemistry* **36**, 907–912, doi:10.1002/(SICI)1097-458X(199812)36:12<907::AID-OMR394>3.0.CO;2-5 (1998).
77. Strahl, H., Bürmann, F. & Hamoen, L. W. The actin homologue MreB organizes the bacterial cell membrane. *Nature Communications* **5**, 3442, doi:10.1038/ncomms4442 (2014).
78. Kochen, M. A. *et al*. Greazy: Open-Source Software for Automated Phospholipid Tandem Mass Spectrometry Identification. *Analytical Chemistry* **88**, 5733–5741, doi:10.1021/acs.analchem.6b00021 (2016).

Acknowledgements

The Research Council of Norway is acknowledged for funding (grant application ES528542), and for financial support through the Norwegian NMR Platform, NNP (grant 226244 / F50). The authors wish to thank Drs Fedor Kryuchkov and Marc Niere for assistance with MS and microscopy, respectively, and SF would also like to thank Drs J. Loewe, S. Liddell and T. Allers for helpful discussions. The authors thank Drs Ø. Larsen and A.E. Lewis for critical review of the manuscript and acknowledge Dirk Petersen (NNP UiO node) and Olav-Audun Bjørkelund (NNP UiB node) for their help in facilitating the work.

Author Contributions

The laboratory work was carried out by S.F. and M.J., and supervised by S.F. and Ø.H. NMR data was collected by F.R. who also advised on acquisition parameters, and H.E.W. Data were analysed and interpreted by S.F., M.J., C.R. and Ø.H. C.R. supplied cultivation and handling protocols and *Listeria innocua* NCTC 11288 starting culture. S.F. and Ø.H. conceived the research questions and designed the experiments. The original grant proposal and the research programme were conceived, devised and written by Ø.H. The manuscript was written by S.F. and Ø.H., and figures prepared by S.F. and M.J. All authors commented on the manuscript and approved the final version.

Additional Information

Supplementary information accompanies this paper at doi:10.1038/s41598-017-06855-z

Competing Interests: The authors declare that they have no competing interests.

Publisher's note: Springer Nature remains neutral with regard to jurisdictional claims in published maps and institutional affiliations.

Open Access This article is licensed under a Creative Commons Attribution 4.0 International License, which permits use, sharing, adaptation, distribution and reproduction in any medium or format, as long as you give appropriate credit to the original author(s) and the source, provide a link to the Creative Commons license, and indicate if changes were made. The images or other third party material in this article are included in the article's Creative Commons license, unless indicated otherwise in a credit line to the material. If material is not included in the article's Creative Commons license and your intended use is not permitted by statutory regulation or exceeds the permitted use, you will need to obtain permission directly from the copyright holder. To view a copy of this license, visit http://creativecommons.org/licenses/by/4.0/.

© The Author(s) 2017

Supplementary Information

For: Evidence that *Listeria innocua* modulates its membrane's stored curvature elastic stress, but not fluidity, through the cell cycle

Samuel Furse[§], Martin Jakubec[§], Frode Rise‡, Huw E. Williams[†], Catherine E. D. Rees[◊], Øyvind Halskau[§,*]

[§]*Department of Molecular Biology, University of Bergen, Thormøhlensgate 55, NO-5006, Bergen, Norway.*

[†]*Centre for Biomolecular Sciences, University of Nottingham, University Park, Nottingham NG7 2RD, United Kingdom.*

[‡]*Department of Chemistry, University of Oslo, P. O. Box 1033, Blindern, NO-0315 Oslo, Norway.*

[◊]*School of Biosciences, University of Nottingham, Sutton Bonington Campus, Nottinghamshire, LE12 5RD, United Kingdom.*

**oyvind.halskau@uib.no. Tel. +47 55 58 45 63.*

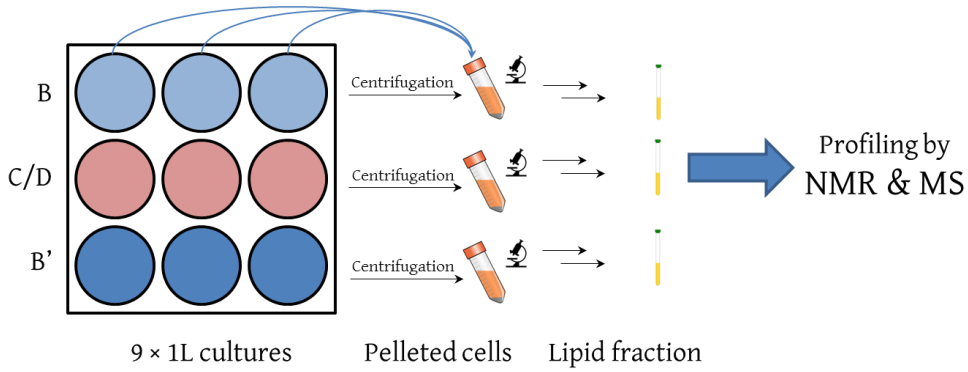

Figure S1. Experimental steps following preparation of the exponentially growing cultures. After harvesting, each culture was pelleted. Microscopy was performed to determine the morphology of the cells under study and for measurement of cell length and calculation of cell length distribution. Pelleting was followed by digestion of the cell wall in the presence of lipase inhibitors. The resulting material was then freeze-dried and the lipid fraction isolated. Finally, the lipid fraction was dispersed in CUBO solvent[15,35,49,76-78] for profiling using ^{31}P NMR and in isopropanol/dichloromethane (1:1 v/v) for profiling using MS.

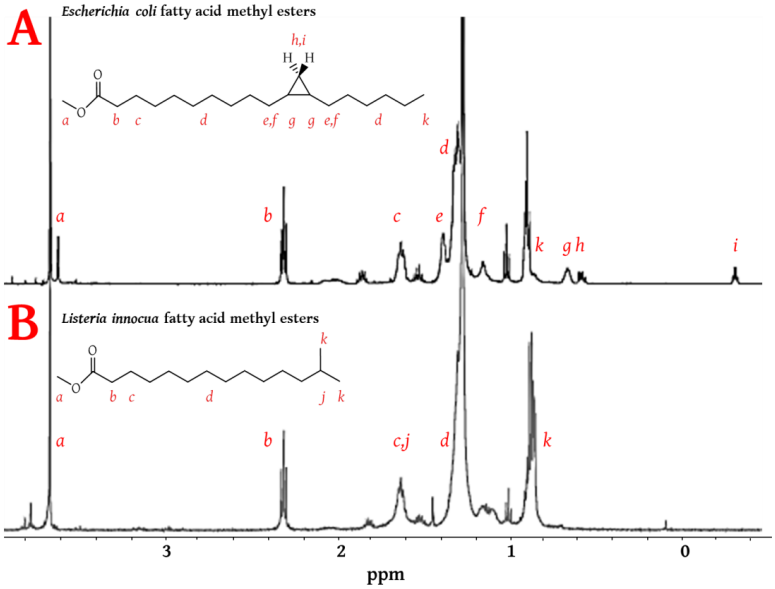

Figure S2. [1]H NMR traces of fatty acid methyl esters isolated from lipid fractions of E. coli *(trace A) and* L. innocua *(trace B), with example structures shown inset. The resonances corresponding to particular proton nuclei are marked (*a-k*), with a key on inset structures. The integrations of the appropriate signals indicate that around 40% of the FARs in the* E. coli *sample possess a cyclopropyl ring (*b *compared to* g,h,i*) and that the average number of methyl branches per FAR in* Listeria *is at least one (*b *compared to* k*).*

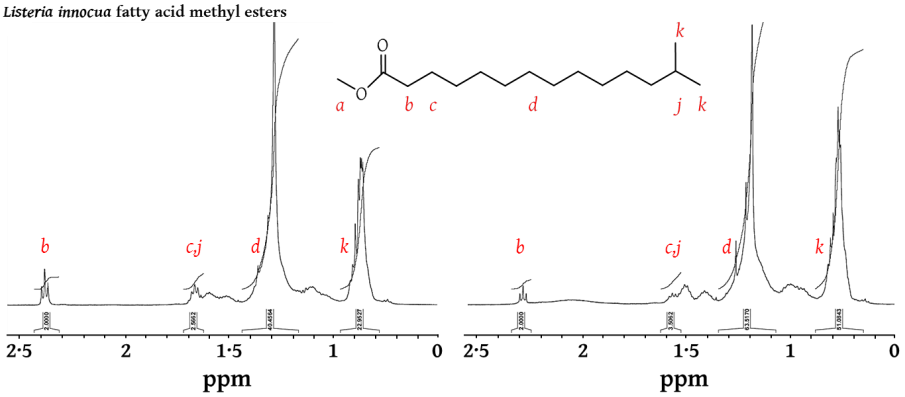

Figure S3. Two representative [1]H NMR spectra of chloroform-soluble material from the dried and acid-treated remaining (aqueous/precipitate) fraction of the lipid isolation. The effectiveness of the isolation procedure developed in this study was tested by an attempt to isolate remaining fatty acid residues. The aqueous solution and precipitate were dried together and then treated with strong acid in order to hydrolyse any ester bond present, before being dried and washed with chloroform. The dried oil was subject to [1]H NMR spectroscopy. The integrations of the signals are calibrated by the α-CH_2 signal (signal b*, 2.3-2.4 ppm). This indicates that the integration of other signals (*e.g. *methyl signals,* k*, 0.6-0.8 ppm) are much higher than can be ascribed to FAMEs alone (~25H. The integration of one methyl group is 3H, indicating that there was an average of 8 protons in this chemical environment per FAR present). The complexity of the methyl signal and others also suggests the presence of other (lipophilic) species. The fraction of FAs present (25H/8H) was therefore judged as ~30%* w/w *(mean* n *= 4 measurements).*

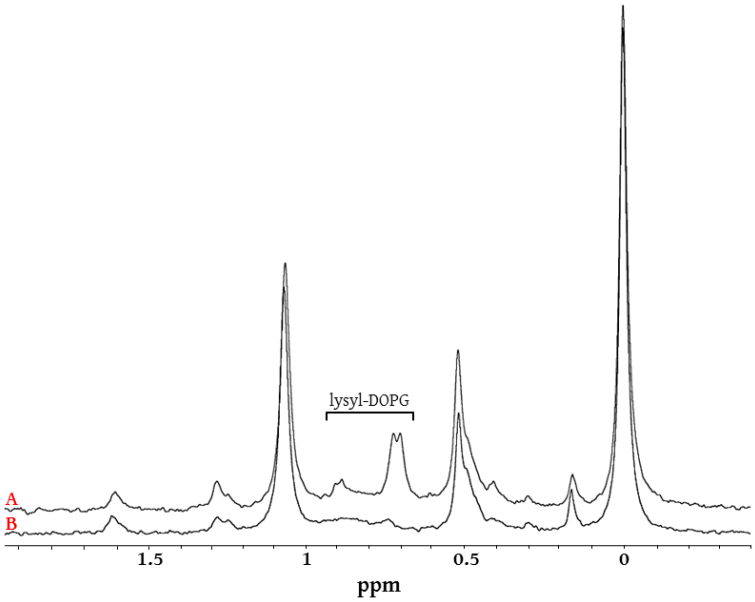

Figure S4. ^{31}P NMR (323.96 MHz) spectra for indicating lysyl-phosphatidylglycerol in lipid mixtures. Stacked traces of lecithin from Helianthus *mixed with lysyl-DOPG (A) and as supplied (B), indicating that the resonances for the two structural isomers of lysyl-DOPG are at ~0.7 and 0.9 ppm, representing the isomers with the lysyl groups on the primary and secondary hydroxyls of the head group's glyceryl moiety, respectively.*

	Cell cycle profile						*Phospholipid profiling*	
	B period ***(4h)***		*B′ period* *(6h)*		***C/D boundary***		*^{31}P NMR shift (ppm)*	*MS**
Cell length (µm, p = <0.001)	**1.24**	**± 0.29**	1.22	± 0.37	**1.92**	**± 0.44**	-	-
OD_{620} at harvest	**0.50**	**± 0.14**	1.57	± 0.18	**0.79**	**± 0.05**	-	-
PG	**32.7 %**	**± 8.4 %**	50.9 %	± 10.6 %	**43.3 %**	**± 14.4 %**	1.23-1.28	**637.4079** (C11:0/15:0); **665.4399** (C14:0/14:0); **679.4556** (C14:0/15:0); **693.4718** (C15:0/15:0); **705.4712** (C15:0/16:1); **707.4874** (C15:0/16:0); **721.5030** (C15:0/17:0; C16:0/16:0); **733.5025** (C15:0/18:1); **735.5187** (C16:0/17:0); **749.5338** (C17:0/17:0)
CL	**27.6 %**	**± 4.8 %**	20.1 %	± 5.1 %	**15.6 %**	**± 5.8 %**	0.77	**1098.7113** (C15:0/15:0/17:0/0:0); **1127.7504** (C17:0/15:0/17:0/0:0; C19:0/15:0/15:0/0:0). **1238.8314** (C13:0/15:0/13:0/15:0); **1294.8936** (C11:0/17:0/15:0/17:0; C13:0/18:0/14:0/15:0; C14:0/14:0/18:0/14:0; C15:0/15:0/15:0/15:0); **1308.9093** (C14:0/16:0/15:0/16:0; C15:0/15:0/16:0/15:0; C14:0/16:0/15:0/16:0); **1322.9252** (C14:0/16:0/17:0/15:0; C15:0/15:0/17:0/15:0; C14:0/16:0/16:0/16:0; C15:0/15:0/16:0/16:0); **1334.9249** (C16:1/15:0/17:0/15:0); **1336.9405** (14:0/17:0/16:0/16:0; 15:0/16:0/16:0/16:0; C15:0/16:0/17:0/15:0; C16:0/15:0/17:0/15:0); **1350.9564** (C14:0/18:0/17:0/15:0; C15:0/15:0/19:0/15:0; C15:0/15:0/17:0/17:0; C15:0/17:0/17:0/15:0; C16:0/16:0/16:0/16:0; C16:0/16:0/17:0/15:0; C17:0/15:0/17:0/15:0); **1362.9562** (C17:0/15:0/18:1/15:0); **1364.9719** (C16:0/16:0/17:0/16:0); **1378.9875** (C15:0/17:0/17:0/17:0);
PE	**19.6 %**	**± 6.2 %**	12.5 %	± 8.7 %	**7.8 %**	**± 4.3 %**	0.05, 0.10, 0.22, 0.31, 0.58[a]	**690.5084** (15:0/17:0); **704.5241** (C16:0/17:0); **718.5398** (C17:0/17:0; C15:/19:0)
lysyl-PG[†]	**2.8 %**	**± 3.1 %**	5.8 %	± 3.4 %	**4.3 %**	**± 4.1 %**	0.69	**807.5506** (C14:0/15:0); **821.5668** (15:0/15:0); **835.5824** (C15:0/16:0); **849.5980** (C15:0/17:0; C16:0/16:0); **877.6288** (C17:0/17:0)
lyso-PA	**0.6 %**	**± 0.7 %**	0.3 %	± 0.4 %	**1.8 %**	**± 1.0 %**	6.0-6.3[b]	**423.2510** (C17:0); 451.2823 (C19:0)
PA	**2.5 %**	**± 3.4 %**	3.5 %	± 2.0 %	**5.0 %**	**± 3.6 %**	4.8-5.3[b]	**647.4663** (C15:0/17:0); 661.4819 (C16:0/17:0); **675.4976** (C15:0/19:0; C17:0/17:0); **703.5283** (C17:0/19:0)
lysyl-CL[‡]	**4.4 %**	**± 2.9 %**	1.6 %	± 2.3 %	**13.1 %**	**± 12.7 %**	0.63[‡]	**1395.8457** (C58:0); **1409.8723** (C59:0); **1423.8990** (C60:0); **1437.9256** (C61:0)
PS	**0.7 %**	**± 1.4 %**	0.8 %	± 0.9 %	**0.4 %**	**± 0.3 %**	0.52	**706.0507** (C15:0/15:0); **721.4888** (C15:0/16:0; C14:0/17:0); **734.4937** (C15:0/17:0); **748.5093** (C16:0/17:0); **762.5250** (C17:0/17:0); **790.5604** (C17:0/19:0)
lyso-PG	**n/d**		3.5 %	± 3.2 %	**2.0 %**	**± 2.0 %**		**456.2488** (C14:0); **470.2644** (C15:0); **484.2801** (C16:0); **498.2957** (C17:0).
Others	**<5 %**		<5 %		**<5 %**		Var.	-

Table S1. Cell length and lipid head group profile of L. innocua *NCTC 11288. Cell length distributions determined through measurement of cells on micrographs (*Fig. *1, p = <0.01, independent samples students' t-test), lipid profile determined using ^{31}P NMR and MS from* n *= 5 isolates. *HRMS/MS performed in positive ion mode; masses given are the* m/z *less the adducts. Assignments in ^{31}P spectra were made using literature references[35,76-78] and [†]stacked 1D data from this study (Fig. S4). The FAs identified by MS are consistent with previous studies of* Listeria spp.[51,79,80]. *[‡]Tentative assignment. [a]PE exhibits several shifts* in vitro *due to interactions with the solvent and as a function of* p*H and concentration. [b]The shift of phosphate* mono-*ester-containing lipids is* p*H dependent.*

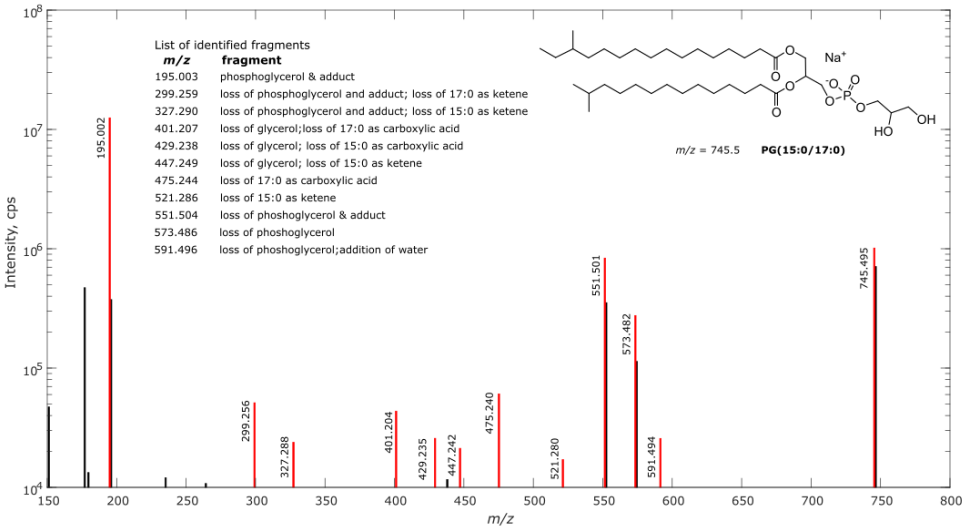

Figure S5. Representative fragmentation spectrum of a lipid (isoform PG(15:0, 17:0)) from Listeria innocua*. Only spectra in which fragmentation that described the lipid unambiguously were used to support identification. The data was acquired on an OrbiTrap Dionex 3000, (Waltham, MA, USA). Briefly, dry lipid mixtures were solubilized using a dichloromethane/isopropanol 1:1 mixture. The samples from this solution was injected (10 µL) and lipids separated by chromatography using a UPLC C18 column (1.7 µm particle size, Waters, 40°C, and flow rate of 0.4 mL/min). Ions were detected in positive mode, and MS data were analysed using software from Kochen* et al.[75], and Matlab code developed by authors. *Only spectra in which fragmentation that described the lipid unambiguously were used to support identification.*

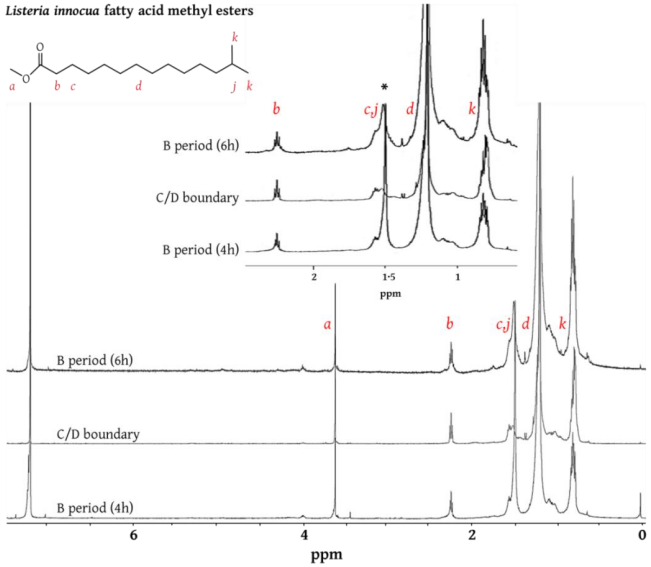

*Figure S6. Representative [1]H NMR spectra of fatty acid methyl ester preparations of lipid fractions isolated used for head group profiling. Resonances as described in the Experimental, with example labelled as inset structure. *resonance pertaining to grease (1.45 ppm), that overlaps with that of the β-CH_2 signal (c, 1.6 ppm). There was no evidence for the cyclopropyl groups typical of Gram-negative bacteria in any of the* Listeria *samples used.*

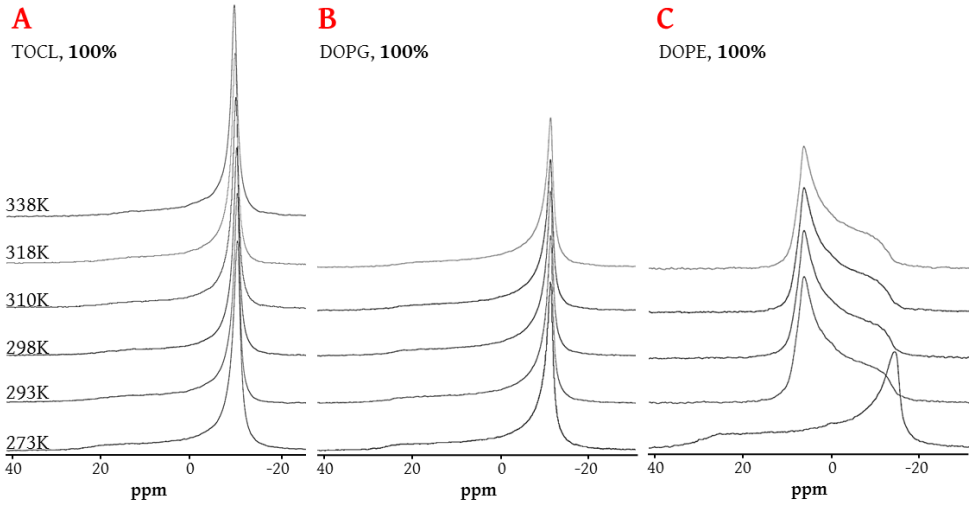

Figure S7. Broad line [31]P NMR temperature scans of hydrated single-lipid systems. A, TOCL; B, DOPG; C, DOPE.

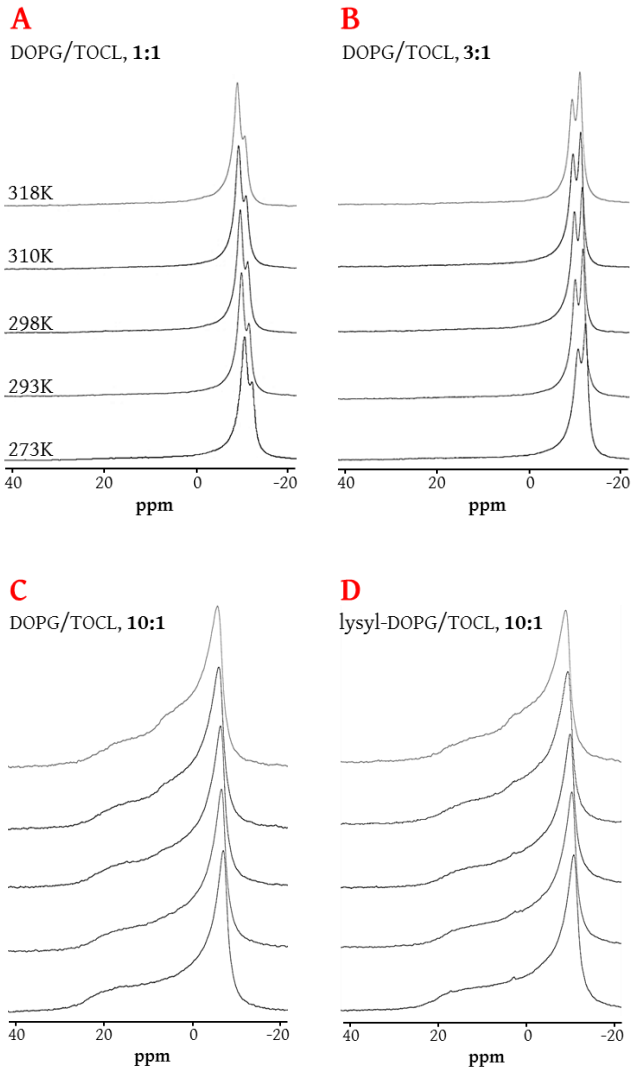

Figure S8. Broad line ^{31}P NMR (161.98 MHz) temperature scans of hydrated mixtures of DOPG and TOCL (A-C) and lysyl-DOPG and TOCL (D). A, 1:1 molar ratio of DOPG and TOCL; B, 3:1 molar ratio; C, 10:1 molar ratio; D, 10:1 molar ratio of TOCL and lysyl-DOPG.

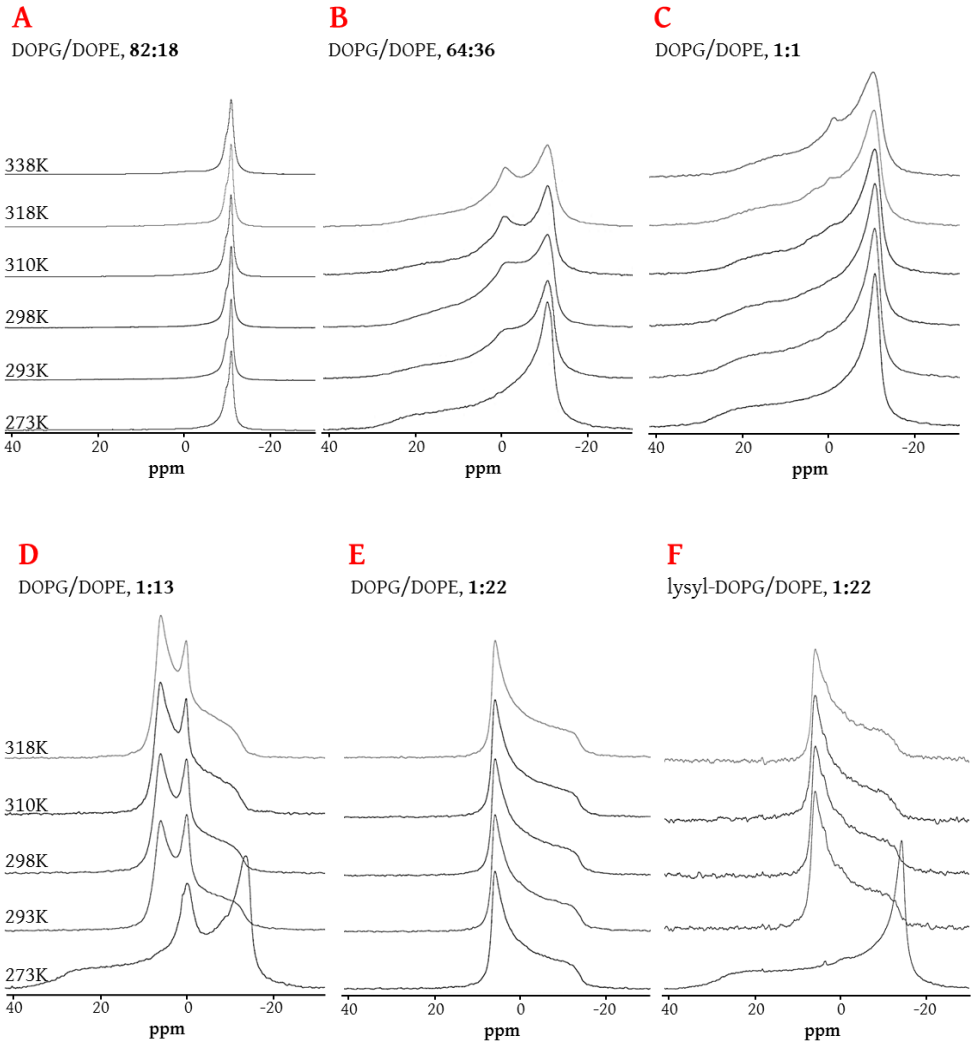

Figure S9. Broad line ^{31}P NMR (161.98 MHz) temperature scans of hydrated mixtures of DOPG and DOPE (A-E) and lysyl-DOPG and DOPE (F). A, 82:18 molar ratio of DOPG and DOPE; B, 36:64 molar ratio; C, 1:1 molar ratio; D, 1:13 molar ratio; E, 1:22 molar ratio; F, 1:22 molar ration of lysyl-DOPG and PE.

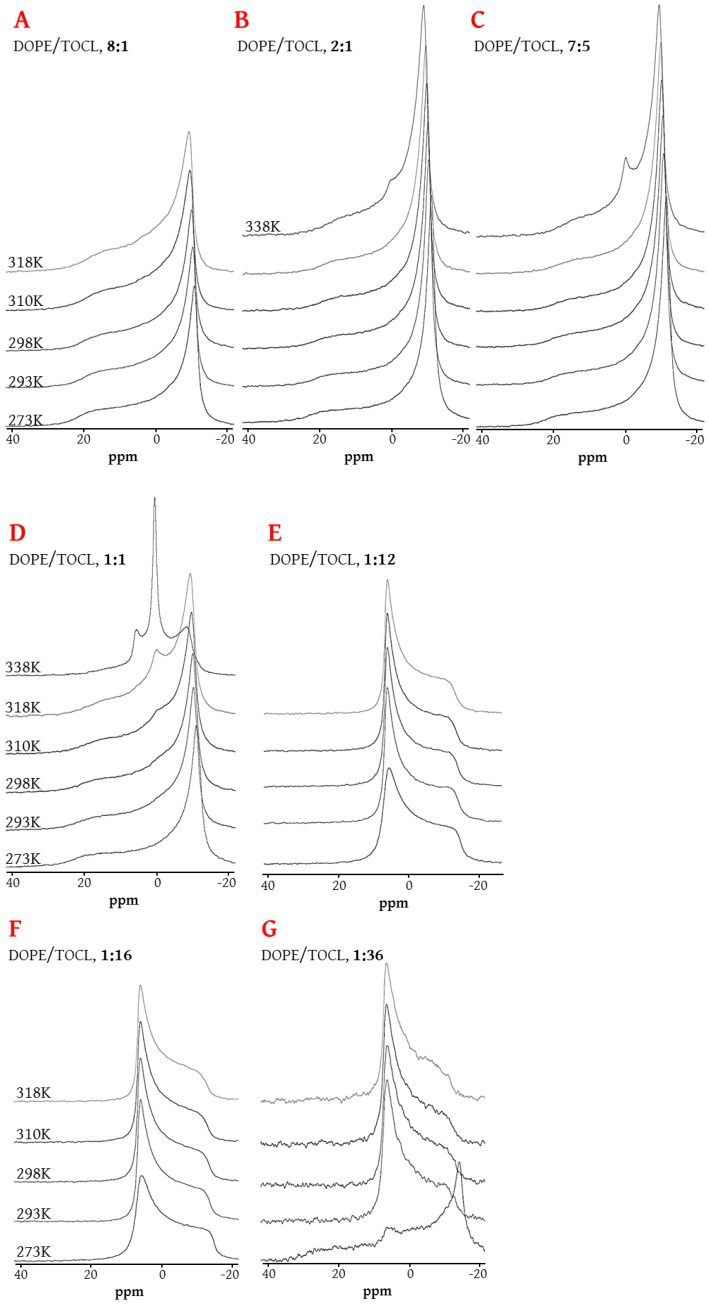

Figure S10. Broad line ^{31}P NMR (161.98 MHz) temperature scans of hydrated mixtures of TOCL and DOPE. A, 8:1 molar ratio of TOCL and DOPE; B, 2:1 molar ratio; C, 7:5 molar ratio; D, 1:1 molar ratio; E, 1:12; F, 1:16; G, 1:36.

III

Graphic design: Communication Division, UiB / Print: Skipnes Kommunikasjon AS

uib.no

ISBN: 978-82-308-3525-8